UNIVERSIDADE FEDERAL DE ALAGOAS
Instituto de Ciências Biológicas e da Saúde (ICBS)
Programa de Pós-Graduação em Ciências da Saúde

DIEGO DE SIQUEIRA FIGUEREDO

Estudo de microRNAs relacionados a ritmos circadianos: identificação e validação de candidatos, perfil transcriptômico e impacto na normalização de ensaios de expressão gênica

MACEIÓ
2018

DIEGO DE SIQUEIRA FIGUEREDO

Estudo de microRNAs relacionados a ritmos circadianos: identificação e validação de candidatos, perfil transcriptômico e impacto na normalização de ensaios de expressão gênica

Tese de Doutorado apresentada ao Programa de Pós-Graduação em Ciências da Saúde (PPGCS), do Centro de Ciências Biológicas e da Saúde (ICBS) da Universidade Federal de Alagoas, como parte dos requisitos para obtenção do título de Doutor em Ciências da Saúde.

Orientador:

Dr. TIAGO GOMES DE ANDRADE

MACEIÓ
2018

Catalogação na fonte
Universidade Federal de Alagoas
Biblioteca Central
Bibliotecária Responsável: Helena Cristina Pimentel do Vale – CRB4 661

F475e Figueredo, Diego de Siqueira.
Estudo de microRNAs relacionados a ritmos circadianos : identificação e validação de candidatos, perfil transcriptômico e microRNAs candidatos a modulação de ritmos circadianos : análise in silico e impacto na normalização de ensaios de expressão gênica / Diego de Siqueira Figueredo. – 2018.
104 f. : il.

Orientador: Tiago Gomes de Andrade.
Tese (doutorado em Ciências da Saúde) - Universidade Federal de Alagoas. Instituto de Ciências Biológicas e da Saúde. Maceió, 2018.

Inclui bibliografia.

1. Ritmos circadianos. 2. miRNAs. 3. Genes relógio. 4. Genes de referencia. 5. Bioinformática. I. Título.

CDU: 577.2:004

Universidade Federal de Alagoas
Instituto de Ciências Biológicas e da Saúde
Programa de Pós-graduação em Ciências da Saúde

ICBS - UFAL – *Campus* A. C. Simões
Av. Lourival Melo Mota, S/N
Cidade Universitária – Maceió-AL
CEP: 57072-900
E-mail: ppgcs9@gmail.com
Fone: 82 3214 1850

Folha de Aprovação

Diego de Siqueira Figueredo

Estudo de microRNAs relacionados a ritmos circadianos: identificação e validação de candidatos, perfil transcriptômico e impacto na normalização de ensaios de expressão gênica.

Tese submetida ao corpo docente do Programa de Pós-Graduação em Ciências da Saúde da Universidade Federal de Alagoas e aprovada em 25 de setembro de 2018.

Banca Examinadora

Prof. Dr. Felipe Sarmento – (UFAL)

Prof. Dr. Rodolfo Carneiro Cavalcante - (UFAL)

Prof.ª Dr.ª Aline Cristine Pereira – (UNIRB-Arapiraca)

Dedico este trabalho aos colegas da PPGCS, por toda experiência e colaboração, especialmente aos professores orientadores que tornam o sonho da pós-graduação pública possível. Ademais, dedico os resultados apresentados à toda sociedade brasileira, pois sem ela e sua crença no serviço público, o filho de caminhoneiro não teria se formado doutor. De maneira especial, dedico essa tese aos meus pais, irmãos, esposa e filho.

“A mente que se abre a uma nova ideia jamais

voltará ao seu tamanho original.”

(Albert Einstein).

“O tempo é relativo e não

pode ser medido exatamente

do mesmo modo e por toda a parte”

(Albert Einstein)

AGRADECIMENTOS

Ao Dr. Tiago Gomes de Andrade por uma orientação baseada na confiança e no estímulo ao que há de melhor, incluindo a autonomia de ideias.

Ao professor John Hogenesch (*Center for Chronobiolog, Cincinnati Children's Hospital Medical Center, Cincinnat, USA*) pelo experimentos realizados com seu modelo celular PER2:LUC e por todo suporte prestado nas análises dos dados de bioluminescência.

Aos pesquisadores americanos Dra. Lauren Francey e Dr. Gang Wu, e o professor Dr. Tiago Andrade pelos experimentos realizados em *Cincinnati,* USA;

Aos Amigos do laboratório LABMEG (Laboratório de Biologia Molecular e Expressão Gênica) pelos bons anos de convivência, em especial aos colegas do grupo de cronobiologia da UFAL (Daniel Coimbra, Mayara Rodrigues, Luiz Araújo, Aline Cristina, Maria Oliveira, Victor Menezes, Ellyda Fernanda e Tiago Andrade);

A Maria Graziela Gomes da Silva, minha esposa, por acreditar nos meus sonhos como se fossem seus;

Ao meu anjo, meu filho, meu Miguel! Fonte de força, de amor eterno, de inspiração e de vitória!

Aos meus pais, Erivaldo Alves e Maria Gorete, minha base, essência de todas as minhas conquistas.

A Professora Elaine Virgínia (coordenadora do LABMEG, e chefia imediata na UFAL Arapiraca) por compreender e estimular minhas atividades de pesquisa.

Aos animais, parte fundamental desse trabalho, obrigado por suas contribuições à ciência.

A FAPEAL pelos financiamentos de insumos usados nos ensaios experimentais.

Aos professores das bancas examinadoras de qualificação e defesa pela oportunidade de aprendizado, troca de experiências e considerações. Agradeço aos membros titulares e suplentes.

A sociedade brasileira por acreditar e financiar a educação pública, principal ferramenta de transformação da realidade social.

A Deus pela dádiva da vida.

RESUMO

Estima-se que 50% dos genes codificadores de proteínas possuem oscilação rítmica em diferentes tecidos de mamíferos. Curiosamente, metade das proteínas desses genes possuem seus RNAm correspondentes com expressão constitutiva (arrítmica), ressaltando a relevância de eventos pós-transcricionais para a oscilação de proteínas. Os "*High throughput Assays*" (HTA) circadianos são extremamente importantes, pois fornecem informações acerca da expressão de milhares de transcritos e de proteínas, uma rica coleção cronobiológica que pode ajudar na resolução de diferentes problemas científicos, não apenas os abordados nas pesquisas originais. Embora altamente reprodutivos e informativos, ensaios de biologia molecular circadiana apresentam algumas divergências em seus resultados, ressaltando a necessidade do aprimoramento de métodos de normalização e análise dos diferentes ensaios de expressão. Até o momento, não se conhecem os impactos da normalização do RNA em ensaios de expressão de pequenos RNAs, como miRNAs. Este estudo objetivou: (1) analisar a co-expressão de miRNAs e RNAm e proteínas de genes alvos; (2) identificar e validar miRNAs candidatos ao sistema molecular circadiano; (3) analisar o impacto da normalização do RNA total em estudos circadianos de miRNAs. Através da sistematização de diferentes dados circadianos de HTA (RNA-seq, small RNA-seq, Chip-seq e proteoma), de bioinformática e de interações miRNA:RNAm validadas, identificamos uma lista de 152 microRNAs (miRNAs) candidatos ao controle pós-transcricional dos ritmos moleculares. Desses, os dois mais relevantes, miR-29b-3p e miR-23b-3p, foram experimentalmente validados como importantes para a manutenção do período dos ritmos das células U2OS PER2:LUC. Análises de HTA também permitiram a identificação de diferenças nas fases de expressão de miRNAs 3p e 5p, com genes alvos divergentes. Interessantemente, a identificação de padrões de expressão de RNAm e proteínas de genes alvos de miRNAs, permite sugerir um mecanismo de ajuste das amplitudes dos ritmos das proteínas dependente da fase do RNAm. Por fim, através do controle de etapas experimentais, demonstramos oscilação circadiana na concentração do RNA total de diferentes regiões de cérebros de camundongos. A normalização desse ritmo, durante a síntese de cDNA, afeta o perfil de expressão de transcritos, incluindo os dos genes relógio *Per1-2* e *Bmal1*. Ademais, através de análises com RNA exógeno, ou *spike-ins*, demonstramos que o ajuste da concentração do RNA compromete a análise de miRNAs, possivelmente por interferências nos rendimentos de extração e nas reações de síntese de cDNA. Este estudo apresenta dois novos miRNAs importantes para a manutenção da ritmicidade circadiana e uma nova estratégia de análise de qPCR para estudos cronobiológicos de miRNAs.

***Palavras-chave**:* Ritmos circadianos, bioinformática, miRNAs, genes relógio, genes de referência.

APRESENTAÇÃO DA TESE

A tese está estruturada em formato de artigos científicos, contemplando os seguintes manuscritos:

PRIMEIRO ARTIGO:

Systematization of circadian high throughput assays: differences in miRNAs 3p/5p forms and potential miRNA-adjustment of protein amplitude dependent of mRNA-phase.

SEGUNDO ARTIGO:

miR 29b modulates the circadian period in human cells.

TERCEIRO ARTIGO:

Usual normalization strategies for gene expression studies impair the detection and analysis of circadian patterns (publicado no periódico “Chronobiology International”).

Sumário

LISTA DE SÍMBOLOS E SIGLAS

HTA - *High throughput Assays,* ou ensaio genéticos de larga escala
RNA - Ácido Ribonucleico
HKGs - *Housekeeping genes*
qPCR - Reação em cadeia da polimerase quantitativa
RNA-seq - Sequenciamento de RNA de última geração
Chip-seq - *Chromatin Immunoprecipitation Sequencing,* ou sequenciamento de sequência de DNA imunoprecipitadas
miRNA - microRNA
U2OS - Linhagem de células do osteosarcoma humano
LUC – Luciferase, enzimas que catalisam reações biológicas transformando energia química em energia luminosa.
cDNA - DNA complementar
PUBMED – Ferramenta do *National Center for Biotechnology Information* (NCBI) para busca de artigos científicos
NSQ - Núcleos supraquiasmáticos
E-box - *Enhancer box*
CCG - Genes controlados pelo relógio, ou *Clock-controlled genes*
RNAPII - RNA polimerase II
CT - *Circadian Time*
ZT – *Zeitgeber Time*
Ct – *Cycle Threshold*
RNAm – RNA mensageiro
Pri-miRNA – miRNA primário
Pre-miRNA – miRNA precursor
RISC – *RNA induced silencing complex*
3'UTR - *3' untranslated region*
G1 – *Gap 1* ou intervalo 1
S – Síntese
miRnoma – Conjunto de todos os miRNA de um determinado tecido ou célula
Small-RNA-seq – Sequenciamento de última geração de pequenos RNA, incluindo miRNAs
CTF - Circadian transcription factors
HITS-CLIP – High throughput sequencing of RNA isolated by crosslinking immunoprecipitation;
NAFLD - *Non-alcoholic fatty liver disease*
HTLV-1 - *Human T-cell leukemia vírus type 1*
P/T - *Peak to trough ratio*

1. INTRODUÇÃO GERAL

Aspectos gerais de ritmos biológicos

A cronobiologia é definida como a ciência que estuda as características temporais da matéria viva, em seus diferentes níveis de organização (molecular, celular, etc). Os ritmos biológicos são o cerne do estudo cronobiológico. A saber, um "*ritmo*" é definido como qualquer evento que se repete regularmente. Por sua vez, o "*ritmo biológico*" é conceituado como um evento, ou fenômeno de ordem biológica, com repetição regular. Alguns estudiosos, ou cronobiólogos, defendem o uso do termo (ritmos biológicos) aos ritmos gerados por mecanismos inerentes aos seres vivos, ou seja, ritmos não induzidos por fatores dos ambientes (como luz e temperatura) (Nelson Marques; Luiz Menna-Barreto., 2003; Sehgal, 2003).

A associação entre "tempo e os eventos naturais" já era relatada na bíblia, ou mesmo por grandes filósofos, como Hipócrates e Aristóteles. Embora os ritmos biológicos sejam observados em sociedades antigas, a Cronobiologia, como disciplina e ciência, é recente. Não é difícil acreditar que mesmo sociedades primitivas, com pouca tecnologia, tenham notado processos biológicos que variam em um dado tempo (horas, dias ou anos). Em verdade, hoje sabemos que os ritmos biológicos são fundamentais a vida, dada a associação com processos indispensáveis à mesma, incluindo sua evolução. De fato, a vida surgiu em um ambiente instável, ou "*cíclico*", cujos diferentes eventos repetem em um dado intervalo de tempo. O "*ciclo*" é definido como o intervalo de tempo em que a sequência, ou a repetição de eventos (o ritmo) ocorre. Tais variações decorrem da organização do sistema solar, especialmente, das interações existentes entre o Sol, a Terra e a Lua, que resultam em ciclos ambientais, como dia e a noite, estações do ano, fases da lua e as marés (Nelson Marques; Luiz Menna-Barreto., 2003; Sehgal, 2003).

A depender do período de ocorrência, a cronobiologia moderna classifica os ritmos biológicos em três categorias principais: circadianos, ultradianos e infradianos. Entende-se "*período*" como a duração de um evento, mais precisamente a duração de um ciclo. Os ritmos circadianos são aqueles com período de 24 ± 4h (h: horas). Os ritmos ultradianos e infradianos possuem período de ocorrência menor que 20h e maior que 28h, respectivamente. Como exemplos de ritmos circadianos, temos o estado de repouso e alerta de animis ou ciclo vigília e sono de humanos, além de variações na pressão sanguínea e na temperatura corporal. A hibernação e o batimento cardíaco são exemplos de ritmos infradianos e ultradianos (Nelson Marques; Luiz Menna-Barreto., 2003; Sehgal, 2003).

Os ritmos biológicos podem ser gerados pelas células dos diferentes organismos e sincronizados/ou induzidos por diversos fatores ambientais cíclicos (como a luz, marés, etc). Para os cronobiologistas, as variáveis do ambiente que alteram os ritmos biológicos são caracterizadas como "*agentes arrastadores*", pois promovem mudanças nos ritmos biológicos dos diferentes seres vivos. O termo alemão *Zeitgeber* é empregado para os agentes arrastadores. *Zeitgeber* literalmente significa "doador de tempo". Os *Zeitgeber*s estão presentes no ambiente ao qual o organismo se encontra e impactam na fisiologia e no comportamento dos indivíduos, como horários para despertar, dormir ou predar. O entendimento dos *Zeitgeber*s é importante não apenas para o estudo da adaptação dos seres vivos aos ritmos do seu ecossistema, mas também para a identificação do "*caráter endógeno"* dos ritmos biológicos.

Entende-se "*caráter endógeno"* a capacidade intrínseca do organismo de gênese dos seus ritmos biológicos, mesmo quando alocados em condições laboratoriais (experimentais) controladas (constantes), ou seja, sem *Zeitgeber*s. Tal condição (sem *Zeitgeber*s) é conhecida como "*livre-curso*" (no inglês: *free-running*), em que são eliminadas oscilações externas, por exemplo, como ocorre quando camundongos são mantidos em laboratório com temperatura e escuro constantes durante os dias de estudo. No ambiente natural, variações de temperatura e de luz ao longo do dia e da noite poderiam ajustar o *período*, a *fase* e/ou *amplitude* dos ritmos biológicos do camundongo. Por essa razão, para estudar o caráter endógenos dos ritmos biológicos, como a identificação de órgãos associados com sua gênese, faz-se necessário o estudo em *livre-curso.* É importante diferenciar "*Circadian Time"* (CT) e "*Zeitgeber*s *Time"* (ZT). O CT refere-se a "*hora circadiana*", que é a fase de um ritmo circadiano em condição de *livre-curso.* Já o ZT indica a fase do ritmo circadiano quando na presença de um "*agente arrastador"* (ou um *Zeitgeber*) (Nelson Marques; Luiz Menna-Barreto., 2003; Sehgal, 2003).

O *período*, a *fase* e a *amplitude* são características importantes para os ritmos biológicos e geralmente são obtidos através da análise de dados biológicos coletados em diferentes momentos do dia ou do ano. O "*período"* é definido como a duração de um evento, ou de um ciclo. A *"fase"* conceituada como um momento do ciclo, podendo se referir a um intervalo do ciclo (por exemplo, a fase clara do dia) ou a um momento específico, como o horário em que a variável em estudo apresenta seu valor máximo. O momento, ou fase, em que é maior a probabilidade de se encontrar o valor mais elevado da variável é chamado de *"acrofase"*. Por fim, a "*amplitude"* é definida como a diferença entre os valores máximos (ou mínimos) e o valor médio (chamado "*mesor*") dos dados do ritmo em estudo (Nelson Marques; Luiz Menna-Barreto., 2003; Sehgal, 2003). A figura 1 ilustra as diferenças entre as três principais

classificações dos ritmos biológicos, bem como das características importantes em seu estudo, como período e amplitude.

Os ritmos circadianos estão dentre os mais estudados, dado o impacto nas atividades diárias dos seres humanos e sua associação com diferentes patologias (Nelson Marques; Luiz Menna-Barreto., 2003; Sehgal, 2003). Os ritmos circadianos são inerentes aos diversos organismos (desde bactérias ao homem) ajustando-os às condições ambientais importantes à sobrevivência, como luz, temperatura, disponibilidade de alimentos, outros (Nelson Marques; Luiz Menna-Barreto., 2003). A descoberta do mecanismo molecular dos ritmos circadianos em Drosófila, em meados dos anos 80, rendeu o último Prêmio Nobel de Fisiologia e Medicina (em 2017), ressaltando sua importância para as diferentes áreas das ciências da vida, incluindo a medicina. Após 38 anos de estudos, a cronobiologia tornou-se uma área promissora ao demonstrar o aspecto temporal dos diferentes processos vivos. Atualmente, o PUBMED possui 73865 artigos relacionados com o termo "*circadian rhythm*" (a busca no PUBMED foi realizada em agosto de 2018). Importantemente, muitos trabalhos foram publicados em revistas de alto impacto (como *Nature*, *Cell* e *PNAS*) e em diferentes linhas de pesquisa, como ciência básica ou estudos que associam alterações em ritmos biológicos com doenças.

Como em outros campos da ciência, os avanços tecnológicos permitiram a melhor compreensão das estruturas associadas com a gênese da ritmicidade biológica. Hoje, sabemos que os ritmos circadianos estão presentes em diferentes tecidos de mamíferos, sendo sincronizados pelos neurônios dos núcleos supraquiasmáticos (NSQ). Conhecidos como marca-passo circadiano, os NSQ sincronizam sua atividade elétrica à variação diária de luminosidade ambiental, gerando um sinal que modula os ritmos dos tecidos periféricos (fígado, rins, intestino, outros) (Figura 2) (Hastings, Maywood e Brancaccio, 2018; Pilorz, Helfrich-Förster e Oster, 2018).

Entretanto, os NSQ não são fundamentais para gerar os ritmos desses diferentes órgãos, apenas atuam ajustando-os ao ambiente (Husse *et al.*, 2014; Izumo *et al.*, 2014). Como nos NSQ, as células dos diferentes tecidos possuem um ritmo autônomo, mantendo a oscilação circadiana mesmo quando isoladas em cultura, ou seja, sem pistas temporais ambientais ou sistêmicas (Moore *et al.*, 2014; Ruan *et al.*, 2008; Welsh, Takahashi e Kay, 2010). A autonomia celular dos NSQ e dos tecidos periféricos é o resultado da ação de um mecanismo genético comum, o relógio molecular, que é composto por um conjunto de genes chamados "genes relógio" (Figura 3) (Schibler *et al.*, 2016).

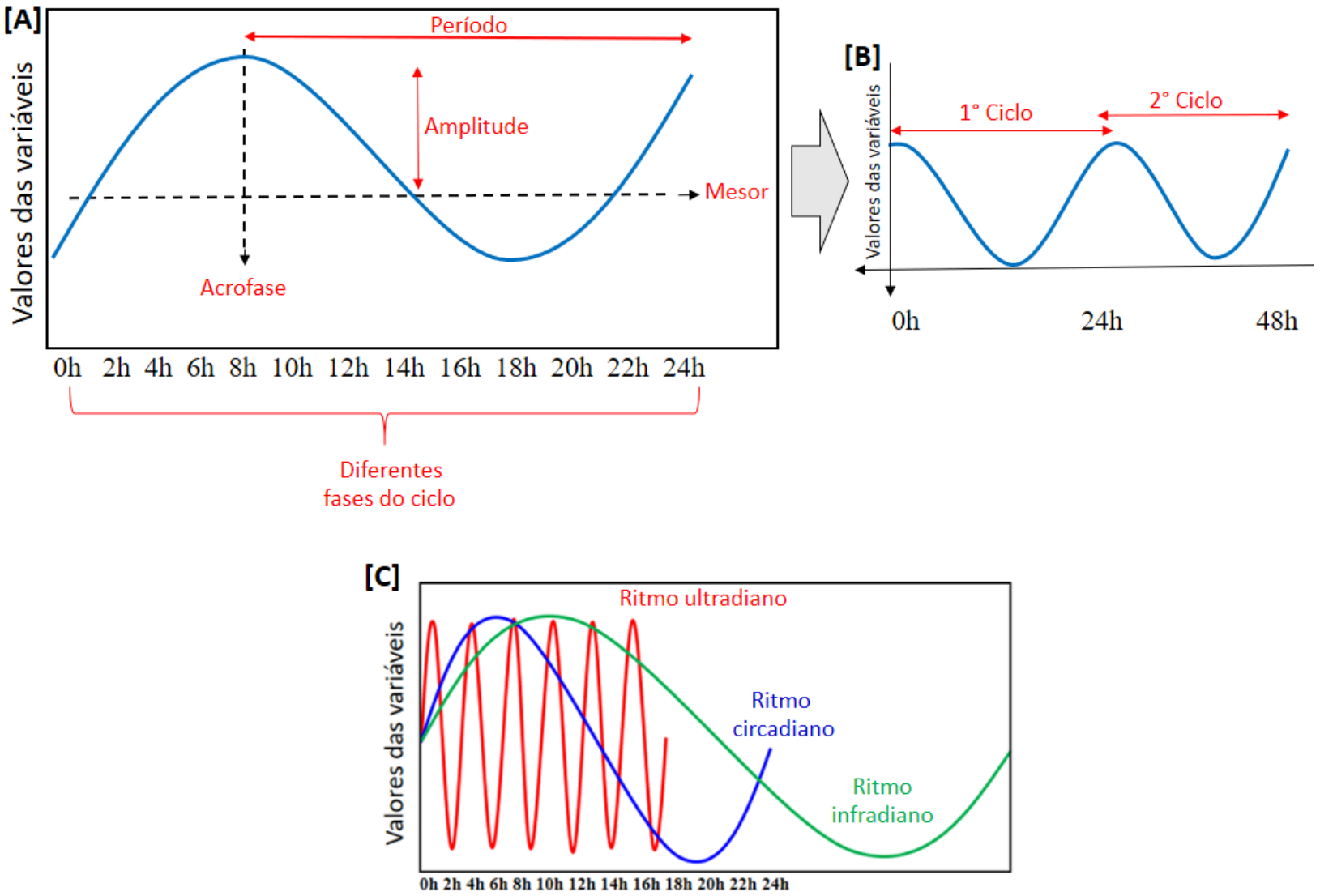

Figure 1. Ilustração das diferentes classificações dos ritmos biológicos e dos principais parâmetros analisados em ensaios cronobiológicos. [A] Representação do período, fases, acrofase, amplitude e mesor. [B] Ilustração de dois ciclos consecutivos do ritmo biológico de uma variável hipotética. [C] Representação dos três diferentes ritmos: circadiano, ultradiano e infradiano [Figura do próprio autor, 2018].

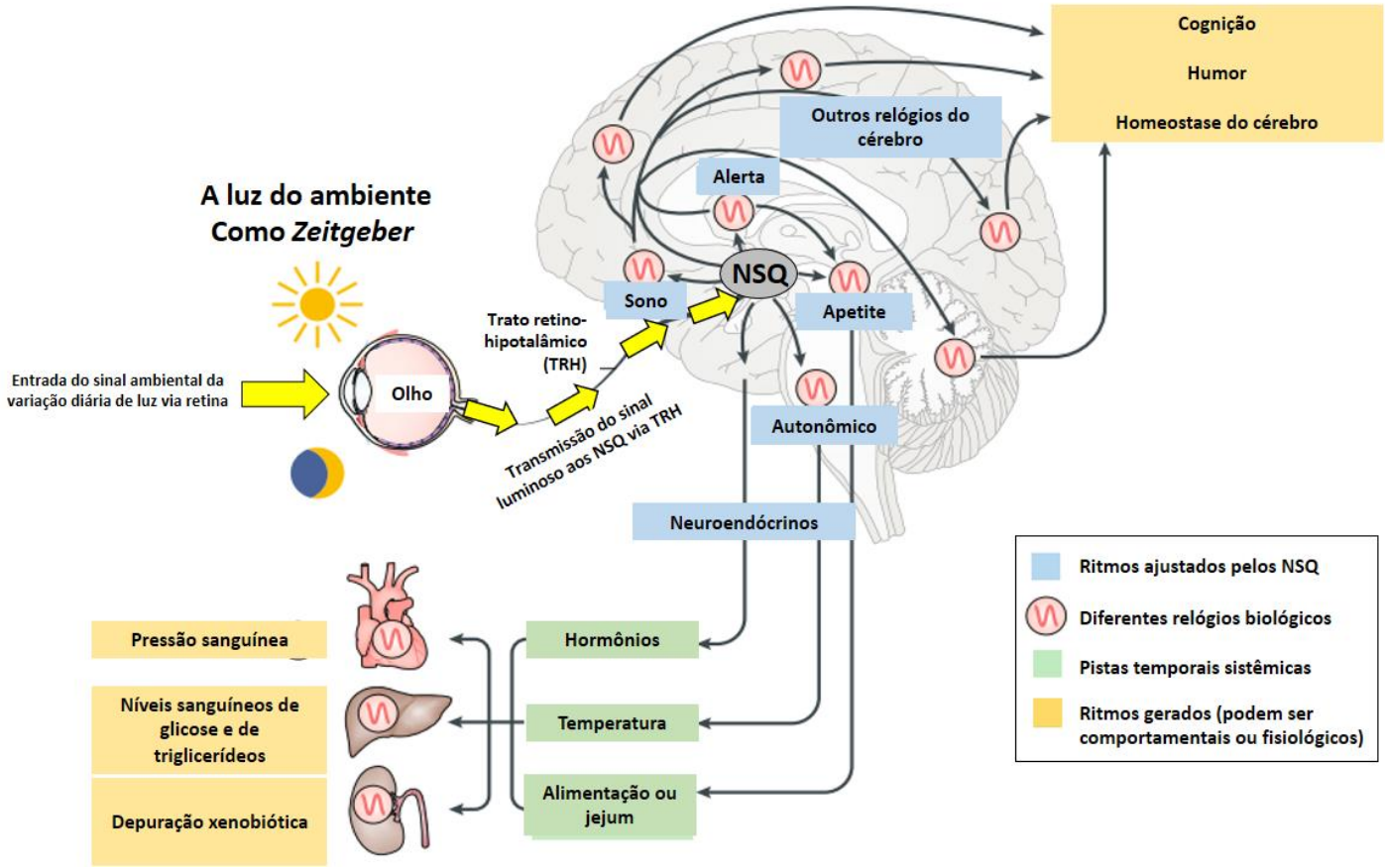

Figura 2. Organização circadiana de mamíferos. O marca-passo circadiano, NSQ, é localizado no cérebro de mamíferos, mais precisamente na base do hipotálamo. Os NSQ recebem inervações da retina via TRH. As retinas captam as variações diárias da luminosidade ambiental. Um sinal é gerado, sendo transmitido aos NSQ via TRH. Ao receber o sinal, os neurônios dos NSQ ajustam sua atividade elétrica ao ritmo ambiental (variações diárias dos de luminosidade). Por sua vez, os NSQ, ajustados ao ambiente, transmitem sinais para os diferentes relógios localizados em outras regiões do cérebro ou mesmo em órgãos periféricos (como coração, fígado, rins, e muitos outros). Assim, os NSQ atuam como um "maestro", "orquestrando" ou ajustando, os diferentes ritmos do organismo (como sono, estado de alerta, humor, pressão sanguínea, outros). Os NSQ podem interferir nas fases, períodos ou amplitudes desses ritmos. Entretanto, é importante destacar que a gênese dos ritmos das diferentes estruturas é independente dos NSQ, ou que as células dos órgãos possuem a capacidade de gerar seus ritmos circadianos, mesmo quando isoladas em condições laboratoriais constantes. Essa figura destaca a ação de um Zeitgeber (a luz) nos diferentes ritmos circadianos de mamíferos; o importante papel dos NSQ na adaptação do organismo aos ritmos ambientais; e a existência de diferentes relógios biológicos no cérebro e em órgãos periféricos. Fonte da figura: Hastings et al. 2018. [Figura adaptada pelo autor da tese].

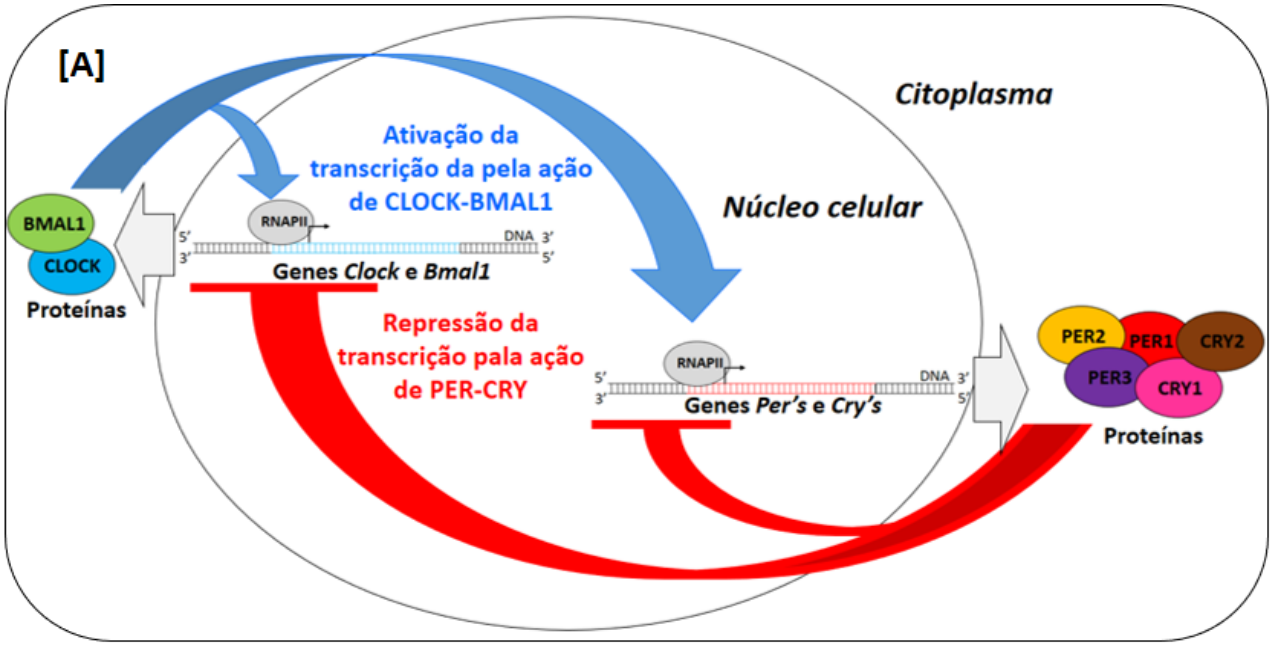
[A]
Citoplasma
Ativação da transcrição da pela ação de CLOCK-BMAL1
Núcleo celular
BMAL1
CLOCK
Proteínas
RNAPII
DNA
Genes Clock e Bmal1
Repressão da transcrição pala ação de PER-CRY
RNAPII
DNA
Genes Per's e Cry's
PER2
PER1
CRY2
PER3
CRY1
Proteínas

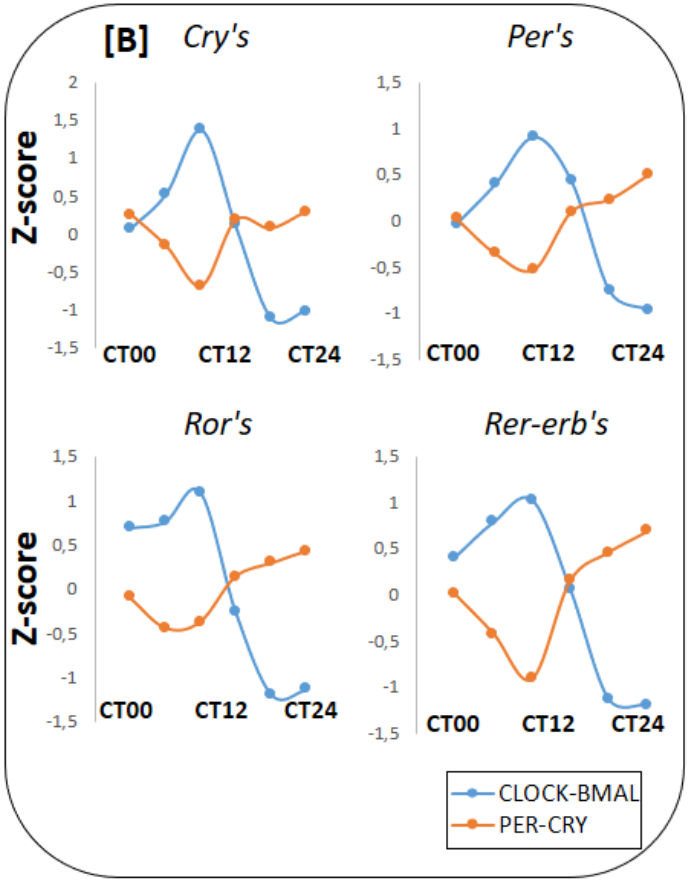
[B]
Cry's
Per's
Ror's
Rer-erb's
Z-score
CT00
CT12
CT24
CLOCK-BMAL
PER-CRY

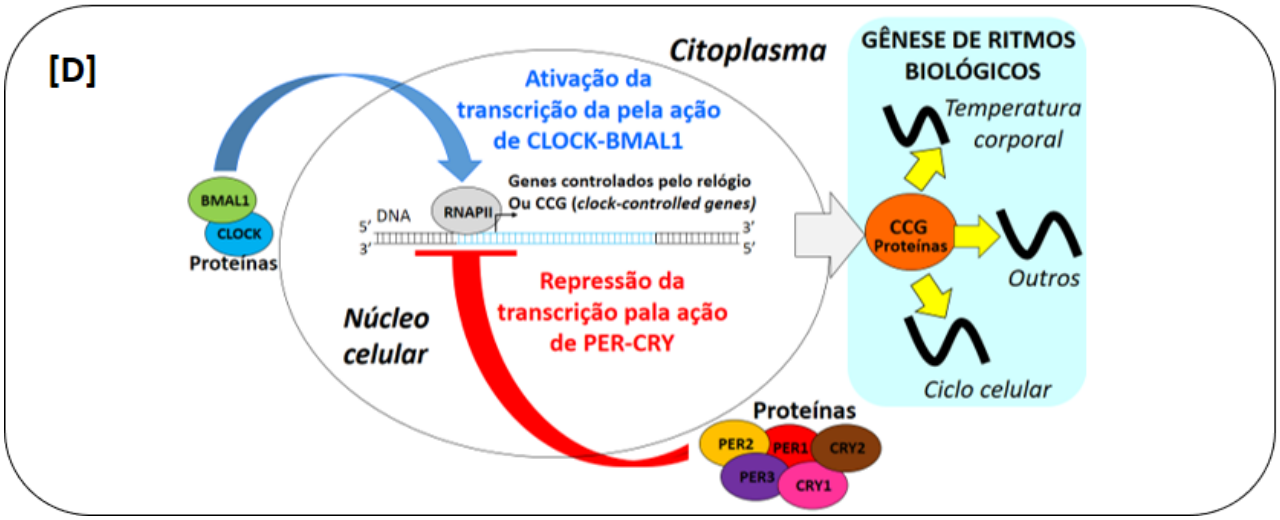
[D]
Citoplasma
Ativação da transcrição da pela ação de CLOCK-BMAL1
Genes controlados pelo relógio
Ou CCG (clock-controlled genes)
BMAL1
CLOCK
Proteínas
DNA
RNAPII
Núcleo celular
Repressão da transcrição pala ação de PER-CRY
GÊNESE DE RITMOS BIOLÓGICOS
Temperatura corporal
CCG
Proteínas
Outros
Ciclo celular
Proteínas
PER2
PER1
CRY2
PER3
CRY1

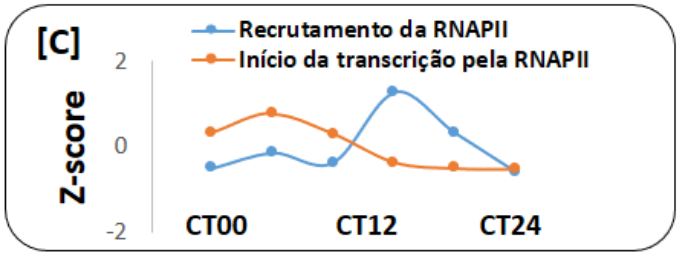
[C]
Recrutamento da RNAPII
Início da transcrição pela RNAPII
Z-score
CT00
CT12
CT24

Figura 3- Alça de retroalimentação circadiana e a gênese da oscilação temporal do transcriptoma. [A] Alças de retroalimentação em modelo simplificado, ressaltando os principais genes do sistema (*Clock, Bmal1, Per1, Per2, Per3, Cry1* e *Cry2*). Os heterodímeros de proteínas CLOCK-BMAL1 e PER-CRY ativam e reprimem a RNAPII, respectivamente. [B] Adaptação dos dados de Chip-seq obtidos em Koike et al. 2012. Em [B] apresentamos a ligação rítmica dos fatores de transcrição circadianos (CLOCK-BMAL1 e PER-CRY) nas sequências regulatórias dos promotores dos próprios genes relógio (*Per's:* Média de *Per1, Per2* e *Per3*; *Cry's:* Média de *Cry1* e *Cry2*; *Rorc* e Rev-erb's: Média de *Rev-erbα* e *Rev-erbβ*). Esses dados demonstram a auto-regulação do sistema, ou a alça de retroalimentação. É importante observar que CLOCK-BMAL1 (ativador) e PER-CRY (repressor) possuem níveis de ligação ao DNA em fases opostas. [C] Atividade rítmica da RNAPII em promotores dos genes relógio. Adaptação dos dados de Chip-seq obtidos em Koike et al. 2012. [D] Importância do sistema em alça de retroalimentação na gênese dos ritmos circadianos de mamíferos. Indução de vários ritmos via controle de CCG. Nota: CT (Circadian Time): tempo quando na ausência de fatores ambientais que alteram ritmos biológicos, como a luz. Geralmente os animais são mantidos durante dias em escuro e temperatura constantes, condição conhecida como livre-curso ou *free-running*. Para animais noturnos, como camundongos, o CT12 refere-se ao momento de início de atividade, geralmente inferido pela movimentação do animal [Figura do próprio autor, 2018].

Ativadores ou repressores transcricionais, os genes relógio estão no cerne da gênese da oscilação circadiana do transcriptoma (Chaix, Zarrinpar e Panda, 2016; Koike *et al.*, 2012) (Figura 3). As proteínas dos genes relógio *Clock* e *Bmal1* formam o heterodímero CLOCK-BMAL1 que ocupa, de maneira rítmica, várias regiões, ou sequências E-box (*enhancer box*) dos promotores de vários genes, ativando sua transcrição (Chaix, Zarrinpar e Panda, 2016; Koike *et al.*, 2012) (Figura 3). *Per1, Per2, Per3, Cry1 e Cry2* são genes relógio com transcrição rítmica induzida por CLOCK-BMAL1 (Figura 3A-B). As proteínas desses genes também se ligam e formam o complexo PER-CRY que inibe a ação do seu próprio ativador transcricional, o heterodímero CLOCK-BMAL1 (Chaix, Zarrinpar e Panda, 2016; Koike *et al.*, 2012) (Figura 3A-B). Milhares de genes, conhecidos como genes controlados pelo relógio (ou CCG, do inglês: *Clock-controlled genes*), têm seus ritmos gerados através da oscilação da atividade (ligação ao DNA) dos elementos das vias de ativação eferentes (CLOCK-BMAL1) e inibição (PER-CRY) circadiana (Chaix, Zarrinpar e Panda, 2016; Koike *et al.*, 2012) (Figura 3C).

Embora com genes diferentes, eucariontes e procariontes possuem ritmos induzidos por um sistema em alça de retroalimentação de semelhante ação (Chaix, Zarrinpar e Panda, 2016; Mendoza-Viveros *et al.*, 2017). Interessantemente, a própria RNA polimerase II (RNAPII), enzima fundamental ao processo de transcrição, possui atividade circadiana, com ritmicidade em seu recrutamento e atividade transcricional nos promotores de vários genes (Koike *et al.*, 2012), incluindo dos genes relógio (Figura 3D).

Modelo experimental usado em pesquisas cronobiológicas

O conhecimento da autonomia celular de gênese circadiana, em conjunto com os avanços em biotecnologia, permitiram o deselvolvimento de modelos celulares voltados ao estudo de ritmos circadianos, que permitem analisar, em condições controladas, o ritmo endógeno de um determinado tecido, ou mesmo de uma única célula (Guenthner *et al.*, 2014;

Hamada *et al.*, 2016; Moore *et al.*, 2014; Saini *et al.*, 2013). Dentre esses modelos, as células imortalizadas de osteossarcoma humano (células U2OS), *knock-in* para o gene lucifesase (LUC), são amplamente usadas para a análise, em tempo real, de ritmos circadianos humanos (Zhang *et al.*, 2009). Luciferases são enzimas que transformam energia química em energia luminosa, quando na presença do seu substrato (luciferina). O gene da proteína Luciferase (LUC) é predominante em organismos marinhos, podendo ser encontrado em insetos terrestre, como vagalumes (Kaskova, Tsarkova e Yampolsky, 2016).

Como demonstrado na figura 4, através de engenharia genética, em células U2OS, a sequência codificante do gene LUC foi inserida antes do códon de terminação (stop códon) e da sequência 3’ não traduzida (do inglês: 3’UTR, ou *3' untransleted region*) do gene *Per2* (Figura 4)(Zhang *et al.*, 2009). Dessa forma, o RNAm e a proteína de Luciferase são ritmicamente produzidos, já que luciferase passa a ser transcricionalmente controlada pelo promotor do gene *Per2* (como demonstrado na figura 4). Na presença do substrato luciferina, mantido em concentrações constantes no meio de cultura celular, a luciferase produz luminescência no mesmo padrão de oscilação circadiana da proteína do gene *Per2*. Esse modelo de estudo circadiano é conhecido como U2OS PER2:LUC (Zhang *et al.*, 2009). As células U2OS PER2:LUC são cultivadas em equipamentos (como Lumicycle) que além de permitir o cultivo das células, também é capaz de detectar, em tempo real, os dados do o ritmo de luminescência de luciferase em minutos e durante dias consecutivos. Importantemente, a combinação de U2OS PER2:LUC e Lumicycle permite analisar ritmos circadianos endógenos e em nível molecular na ausência de zeitgebers como temperatura, luminosidade, variação de nutrientes, outros (Figura 4).

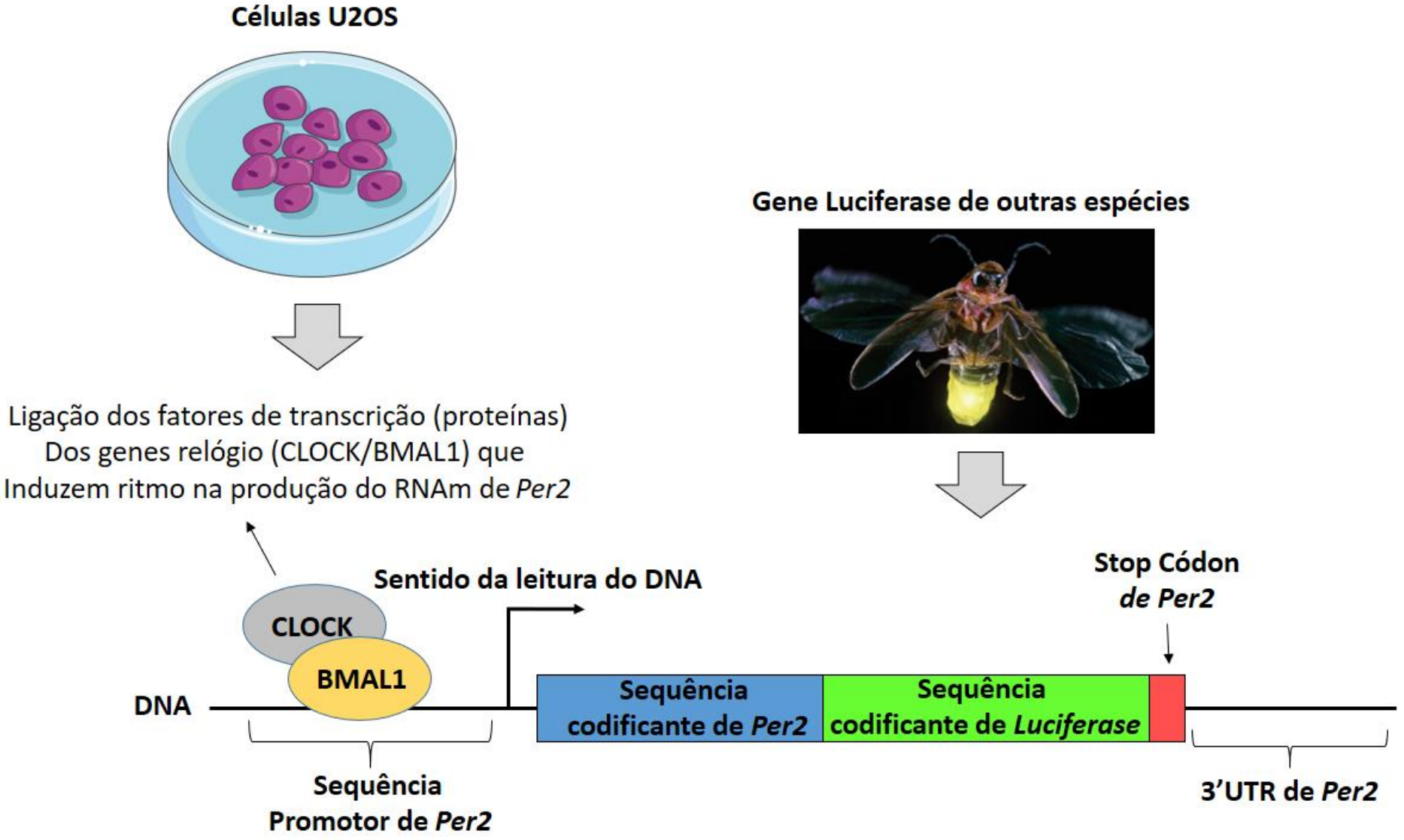
Células U2OS
Gene Luciferase de outras espécies
Ligação dos fatores de transcrição (proteínas)
Dos genes relógio (CLOCK/BMAL1) que
Induzem ritmo na produção do RNAm de *Per2*
Sentido da leitura do DNA
Stop Códon
de Per2
CLOCK
BMAL1
DNA
Sequência
codificante de *Per2*
Sequência
codificante de *Luciferase*
Sequência
Promotor de *Per2*
3'UTR de *Per2*

Figura 4. Modelo celular comumente usado em estudos circadiano. [A] Representação simplificada da sequência do gene relógio *Per2*, cujos produtos (RNAm e proteína) apresentam oscilação circadiana em seus níveis. [B] Representação simplificada da sequência do gene Luciferase, responsável pela produção de enzima LUCIFESASE (LUC) capaz de transformar energia química em luminosidade. [C] Representação do modelo *knock-in* U2OS PER2:LUC. [D] Inserida dentro da sequência do gene relógio *Per2*, a sequência codificante da proteína LUC permite a produção de bioluminescência no mesmo padrão rítmico da proteína PER2. Isso é possível, uma vez que o RNAm de LUC passa a ser ritmicamente produzido, dada a ação do promotor do gene *Per2* e dos fatores de transcrição circadianos (como CLOCK e BMAL1). [E] Foto do equipamento Lumicycle, que permite, simultaneamente, a cultura das células U2OS e a detecção do ritmo da bioluminescência. As células podem ser mantidas no equipamento durante dias, ou semanas [Figura do próprio autor, 2018].

A relevância de miRNAs para a modulação de ritmos circadianos

Estudos circadianos de larga escala (RNA-seq e proteoma) têm apresentado ritmos moleculares independentes dos genes relógio (Mauvoisin *et al.*, 2014; Robles, Cox e Mann, 2014). Em fígado, metade das proteínas com oscilação circadiana possuem RNAm arrítmico, demonstrando que os ritmos podem ser induzidos independentemente da transcrição (Mauvoisin *et al.*, 2014). Além disso, em relação ao RNAm, muitas proteínas possuem um atraso de 6h de suas acrofases, ou seja, um ajuste da fase em nível traducional (Mauvoisin *et al.*, 2014; Robles, Cox e Mann, 2014).

miRNAs são pequenos transcritos (20-22 pares de base, pb), não codificantes, que controlam a expressão gênica ao induzir degradação do RNAm e/ou inibir a tradução em proteínas (Chen, Alessandro e Lee, 2013; Du *et al.*, 2014)(Figura 5). miRNAs possuem genes conservados em diferentes espécies (Ha e Kim, 2014). Esses pequenos RNAs são inicialmente transcritos em moléculas primárias de RNA (os pri-miRNAs) através da ação da RNAPII (Ha e Kim, 2014) (Figura 5). O pri-miRNA é longo (tipicamente acima de 1 kb) e contém uma estrutura em forma de alça, ou *stem–loop*, na qual as seqüências de miRNAs maduras (funcionais) são incorporadas (Ha e Kim, 2014) (Figura 5). Ainda no núcleo celular, os pri-miRNAs são modificados através de clivagens de suas extremidades, pela ação da enzima DROSHA, gerando o miRNA precursor (pre-miRNA) (Ha e Kim, 2014) (Figura 5).

Após a exportação para o citoplasma, através da exportin 5 (EXP5), o pre-miRNA é clivado pela enzima DICER, próximo da alça terminal, liberando um pequeno *miRNA-duplex*, composto pelas formas funcionais miRNA-5p e miRNA-3p, oriundas dos braços 5’ e 3’ do pre-miRNA, respectivamente (Ha e Kim, 2014) (Figura 5). O *miRNA-duplex* gerado pela DICER é subseqüentemente carregado em uma proteína AGO (Argonauta) para formar o complexo de silenciamento induzido por RNA, ou RISC (do inglês: *RNA-induced silencing complex*) (Ha e Kim, 2014) (Figura 5). As proteínas AGO guiam os miRNAs (miRNA-5p ou miRNA-3p) para as sequências-alvos específicas, através da complementaridade entre os nucleotídeos dos miRNAs e os da região não traduzida 3’UTR (*3′ untranslated region*) do mRNA (Figura 5). A

junção miRNA-AGO-RISC-3'UTR desencadeia a clivagem do mRNA ou a inibição da tradução, ambas reduzem os níveis das proteínas dos genes alvos (Ha e Kim, 2014) (Figura 5).

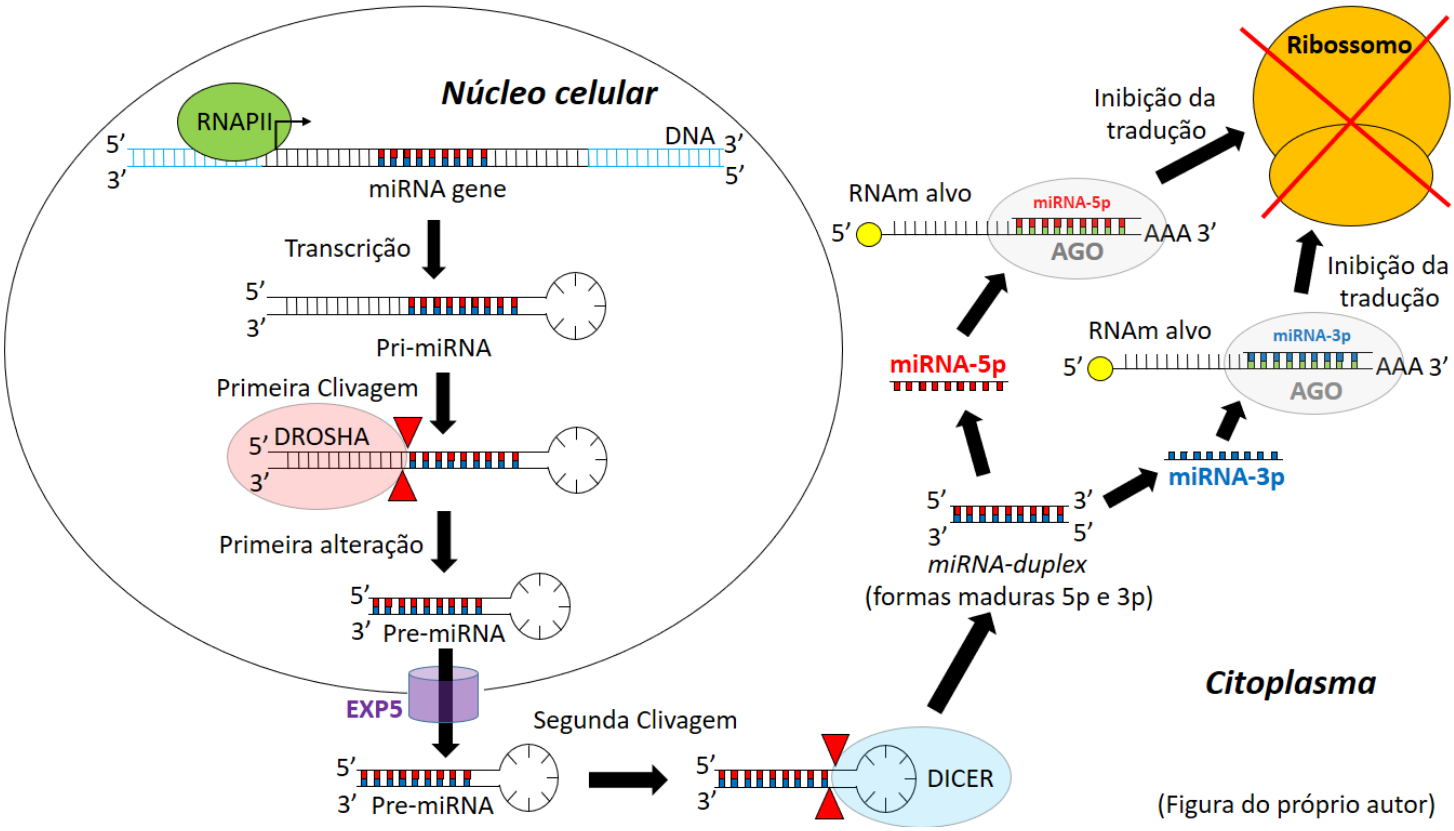

Figura 5. Transcrição, maturação e função de mRNAs. Representação esquemática da transcrição de genes de miRNAs em pri-miRNAs e de sua maturação em miRNA-3p e miRNA-5p através das enzimas DROSHA e DICER. Também é apresentada a inibição da tradução via complexo miRNA-AGO-RISC. Os triângulos vermelhos representam o ponto de clivagem da dupla fita de RNA durante a ação de DROSHA e DICER. [Figura do próprio autor, 2018].

Estima-se que miRNAs controlam a expressão de mais de 60% de genes humanos codificadores de proteínas (Friedman *et al.*, 2009). Curiosamente, o atlas circadiano da expressão gênica de ZHANG, R. et al., 2014 mostra que 43% de todos os genes codificadores de proteínas possuem transcrição circadiana em algum tecido de mamífero (Zhang *et al.*, 2014). miRNAs possuem um papel basal no controle dos ritmos biológicos (Chen, Alessandro e Lee, 2013; Du *et al.*, 2014; Umemura *et al.*, 2017;Umemura *et al.*, 2017)(Figura 6).

miRNAs são importantes para a gênese circadiana durante a gestação de camundongos (Umemura *et al.*, 2017)(Figura 6). Estudos com modelos animais com depleção do miRnoma confirmam a relevância dos miRNAs para o controle da ritmicidade circadiana (Chen, Alessandro e Lee, 2013; Du *et al.*, 2014; Umemura *et al.*, 2017)(Figura 6). miRNAs ajustam as fases e amplitudes de 30% dos mRNAs ritmicamente transcritos (Du *et al.*, 2014) e controlam

a velocidade da tradução de PER1 e PER2, cuja a alteração foi associada com o encurtamento do período (-2h) tanto de ritmos moleculares, quanto do comportamento de atividade e repouso de camundongos (Chen, Alessandro e Lee, 2013)(Figura 6). Além disso, como demonstrado em dois estudos de small-RNA-seq, uma porção do miRnoma de fígado possui ritmicidade circadiana em sua expressão (Vollmers *et al.*, 2013; Yoshitane *et al.*, 2014). Embora esses dois estudos não identifiquem alvos para os miRNAs, é possível que a oscilação destes miRNAs module os ritmos de diferentes transcritos e/ou proteínas (Figura 6).

Alguns estudos demonstram que a oscilação circadiana de miRNAs pode ser induzida pelos genes relógio (Gao, Zhou, Yang, S. Y., *et al.*, 2016; Tan *et al.*, 2012). Como ocorre na alça de retroalimentação circadiana (Figura 3), ao mesmo tempo, miRNAs podem ajustar os níveis dos RNAm e proteínas dos genes relógio, seus moduladores.

Estudos têm identificado essa relação entre miRNAs e genes relógio (Gao, Zhou, Yang, S., *et al.*, 2016; Tan *et al.*, 2012). GAO et al., 2016 demonstram que miR-17-5p inibe a tradução de CLOCK e que CLOCK ativa a transcrição do miRNA (Gao, Zhou, Yang, S., *et al.*, 2016). TAN et al., 2012 identificaram miR-142-3p como regulador, dos níveis do mRNA e proteína, do gene *Bmal1*, que ativa a transcrição do miR-142-3p (Tan *et al.*, 2012). Embora extremamente informativos, estes dois estudos realizaram ensaios de ocupação dos fatores de transcrição CLOCK e BMAL1 em apenas um momento do dia (Gao, Zhou, Yang, S., *et al.*, 2016; Tan *et al.*, 2012). Além dessas evidências de possível controle circadiano por CLOCK e BMAL1, um estudo apresenta oscilação circadiana na expressão do RNAm de *Dicer* em diferentes tecidos, um gene importante para a maturação dos miRNAs (Yan *et al.*, 2013).

Em conjunto, essas informações destacam ser possível que, assim como outros genes (Koike *et al.*, 2012), miRNA possuem ligação rítmica dos fatores de transcrição circadianos em suas sequências promotoras. Además, miRNAs podem ter ritmos pós-transcricionalmente modulados pela ação de enzimas importantes para a sua maturação, como a DICER.

Perturbações dos ritmos circadianos dos miRNAs poderiam induzir mudanças da oscilação de diferentes genes alvos, desencadeando patologias. De fato, autores têm destacado a importância de miRNAs circadianos para o campo da medicina (Hansen, Sakamoto e Obrietan, 2011). Diferentes estudos demonstram relevância de miRNAs para o câncer, uma patologia sabidamente associada a alterações no ciclo circadiano normal.

Em câncer colorretal, miR-103 inibe a ação apoptótica do gene relógio *Per3* (Hong *et al.*, 2014). Em jejuno de ratos, miR-16 apresenta um ritmo de expressão oposto aos das proteínas ciclinas CCND1, CCND2, CCND3, CCNE1 e CDK6, indispensáveis à regulação das

fases G1/S do ciclo celular (Balakrishnan *et al.*, 2010). O aumento da expressão do miR-16 reduz os níveis das ciclinas, causando um arrastamento da fase G1 (Balakrishnan *et al.*, 2010). As exposições a hábitos de atividades incomuns à espécie humana também têm sido associadas ao desenvolvimento do câncer (Erren *et al.*, 2010; Samulin Erdem *et al.*, 2017).

Trabalhos por turnos são comuns na sociedade moderna, sendo exigidos aos mais diferentes profissionais. Por exemplo, na saúde, enfermeiros e médicos trabalham em regimes de plantão noturno e diurno, que muitas vezes se alternam ao longo do mês, induzindo constante mudanças na ritmicidade circadiana do organismo e impedindo sua sincronização a um ritmo ambiental (Erren *et al.*, 2010; Samulin Erdem *et al.*, 2017). Em 2007 a agência internacional de pesquisa em câncer e a organização internacional de saúde classificaram os trabalhos por turnos como disruptores dos ciclos circadianos, ou como cronoperturbadores, sendo o trabalho noturno destacado como potencialmente carcinogênico (Erren *et al.*, 2010; Samulin Erdem *et al.*, 2017). Esses diferentes regimes podem induzir alterações genéticas importantes (Samulin Erdem *et al.*, 2017; Shi *et al.*, 2013).

Um estudo demonstrou que enfermeiras norueguesas que trabalhavam durante seis noites consecutivas por mais de 5 anos apresentam o encurtamento do telômero, aumentando consideravelmente o risco de câncer de mama (Samulin Erdem *et al.*, 2017). Interessantemente, Shi et al. 2013 identificaram alterações epigenéticas em 31 miRNAs de trabalhadoras noturnas, também associadas ao maior risco de desenvolvimento de neoplasia de mama (Shi *et al.*, 2013). Disfunções circadianas semelhantes às dos trabalhos em turno também induzem alteração na expressão em nível de miRnoma (conjunto de miRNAs do organismo) de glândulas mamárias de ratos (Kochan *et al.*, 2015). Curiosamente, com exceção de um miRNA, todos os miRNAs alterados são associados com a progressão do câncer (Kochan *et al.*, 2015).

Em suma, os dados apresentados ressaltam a importância dos miRNAs na gênese da ritmicidade biológica, bem como a conexão entre miRNAs, ritmos circadianos e patologias. Acreditamos que o estudo circadiano de miRNAs pode ser promissor para a medicina, especialmente no entendimento e diagnóstico de doenças, como o câncer. Entretanto, são necessários mais esforços para a identificação de miRNAs relevantes a gênese circadiana, especialmente ao se considerar o número elevado de miRNAs de mamíferos (1978 miRNAs para camundongos e 2656 para humanos; fonte: miRbase.org) e o potencial de um único miRNA controlar diferentes genes alvos. Além disso, poucos estudos demonstram a relevância de miRNAs para a manutenção da ritmicidade, seja pelo ajuste do período ou da amplitude de

ritmos circadianos (Chen, Alessandro e Lee, 2013; Cheng *et al.*, 2007; Curtis *et al.*, 2015; Gao, Zhou, Yang, S. Y., *et al.*, 2016; Smith *et al.*, 2016).

Neste estudo, objetivamos analisar os perfis de oscilação de miRNAs e de genes alvos (em nível de RNAm e proteína), bem como da ocupação rítmica de fatores de transcrição circadianos (CLOCK-BMAL1, PER-CRY, outros), como forma de identificar o possível papel dos miRNAs na modulação de ritmos proteicos. Além disso, objetivou-se identificar miRNAs candidatos ao sistema circadiano através de uma nova abordagem de sistematização de dados de experimentos circadianos de larga escala (Small-RNA-seq, RNA-seq, Chip-seq e proteoma) e validação experimental em modelo cronobiológico humano, PER2:LUC. Por fim, através de ensaios controlados, objetivamos demonstrar os impactos do ajuste da concentração do RNA total nas análises de expressão gênica circadiana, incluindo de pequenos RNAs, como microRNAs.

Os ensaios de validação funcional foram possíveis mediante colaboração com o grupo de pesquisa do professor John Hogenesch (*Cincinnati*, USA). O professor John Hogenesch é um importante cronobiologista. Foi um dos descobridores do gene relógio *Bmal1* e participou do desenvolvimento do modelo sinérgico PER2:LUC U2OS, usado nessa pesquisa. Os experimentos com miRNAs foram realizados no *Center for Chronobiology*, do *Cincinnati Children's Hospital Medical Center*, USA, pelos pesquisadores Dra Lauren Francey, Dr. Gang Wu e Dr. Tiago Gomes de Andrade.

Representações gráficas de dados circadianos

Estudos de ritmos biológicos costumam apresentar seus dados em gráficos específicos, que possibilitam melhor análise das séries temporais. Como exemplificado na figura 7, os gráficos em formato *polar plot* representam as acrofases dos ritmos circadianos. Por sua vez, ilustrações em formato *radial plot* apresentam os dados em suas diferentes fases (não apenas a acrofase) do ritmo, permitindo o estudo do perfil de oscilação e das amplitudes (figura 7).

Diferentes estudos

Expressão circadiana da enzima Dicer

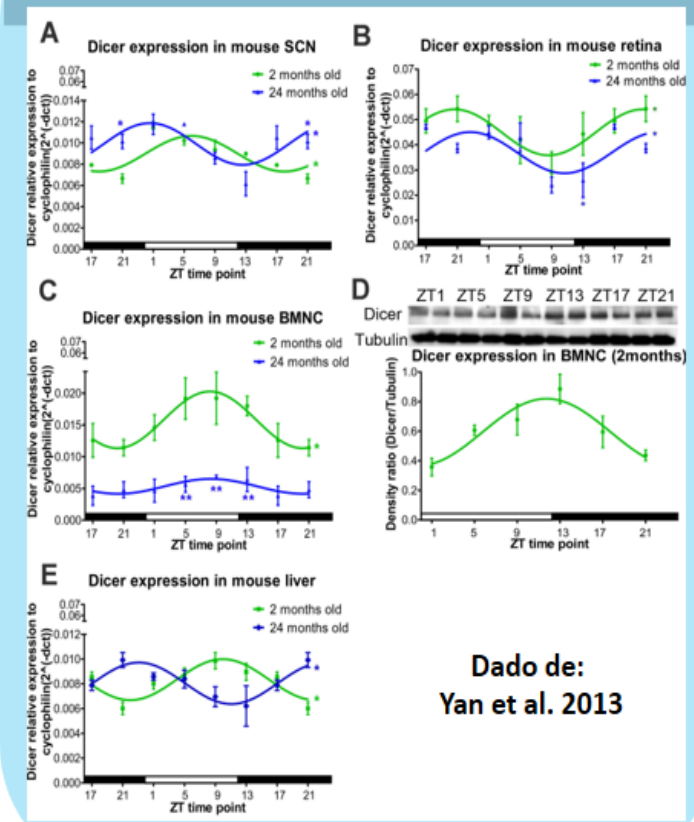

Dado de:
Yan et al. 2013

Expressão circadiana de miRNAs

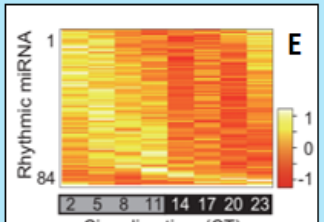

Dado de:
Yoshitane et al. 2014

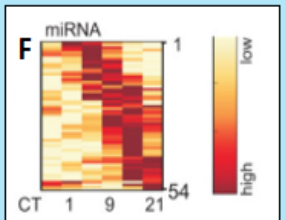

Dado de:
Vollmers et al. 2012

Modelos *Dicer* $^{-/-}$ e *Dgcr8* $^{-/-}$ *knockouts*, ou ensaio com ausência de 3'UTR

G

1. Ritmo encurtado (em - 2h) em células e animais, com tradução mais rápida das proteínas PER1 e PER2 (Chen, et al. 2013).
2. Alteração nas fases e amplitudes de 30% dos RNAm de fígado (Du et al. 2014).
3. 2% dos RNAm de fígado possuem ritmo que pode ser induzido por miRNAs (Du et al. 2014).
4. Camundongos sem a 3'UTR do gene *Per2* apresentam ritmo com amplitude 3x maior e aumento período (Yoo, et al. 2017).
5. Animais respondem aos estímulos ambientais (luz e temperatura) de maneira diferente (Yoo, et al. 2017).
6. Arritmia em células tronco (Umemura, et al. 2017).
7. miRNAs são importantes para a gênese circadiana durante a gestação de camundongos (Umemura, et al. 2017).

Demonstram a importância dos miRNAs para a ritmicidade Circadiana

Figura 6. Diferentes estudos associam miRNAs e ritmos circadianos. [A-E] Perfil de oscilação diária do gene *Dicer* (importante para a maturação/produção de miRNAs) em diferentes tecidos de camundongo. Variação do RNAm de *Dicer* em [A] NSQ (SCN), [B] retina, [C] células mononucleares da medula óssea (BMNC) e [E] fígado. E em nível de proteína, *Dicer* apresenta oscilação diária em células mononucleares da medula óssea (BMNC) [D]. Dados/gráficos obtidos em Yan, et al. 2013. Para mais informações ver o artigo original (Yan, et al. 2013). [E-F] Expressão circadiana de vários miRNAs de fígado de camundongo representada em mapa-quente, ou Heat map (Vollmers et al. 2012; Yoshitane et al. 2014). Dados/gráficos obtidos nos dois estudos circadianos de small-RNA-Seq, Vollmers et al. 2012 e Yoshitane et al. 2014. Em [E] foram identificados 84 e em [F] 54 miRNAs maduros com oscilação circadiana de seus níveis. Legenda, ZT (*Zeitgeber Timer*): referenciação de tempo quando na presença do fator ambiental luminosidade. A luz age como um *Zeitgeber* (termo alemão que significa doador de tempo. Muito usado por cronobiologistas para referir às variáveis ambientais que ajustam os ritmos biológicos dos organismos). ZT0: luz ligada. ZT12: luz desligada. Já CT (Circadian Time): referenciação de tempo quando na ausência do fator ambiental ou *Zeitgeber*. Geralmente os animais são mantidos em escuro e temperatura constantes, condição conhecida como livre-curso ou *free-running*. Para animais noturnos, como camundongos, o CT12 refere-se ao momento de início de atividade, geralmente inferido pela movimentação do animal. [G] Importância dos miRNAs para a os ritmos de RNAm e proteínas. Principais achados de diferentes estudos funcionais [Figura do próprio autor, 2018].

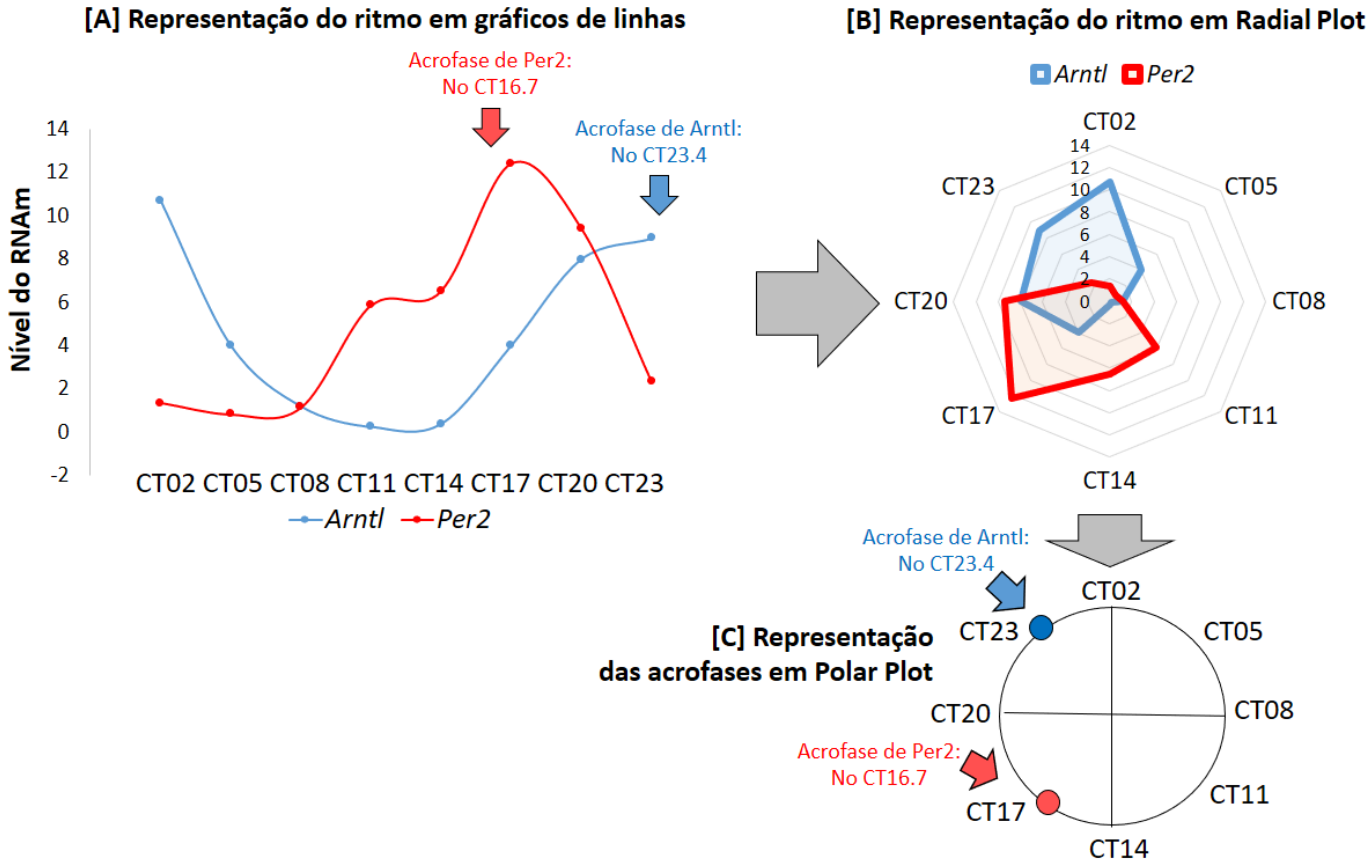

Figura 7. Radial plot e polar plot, duas representações gráficas típicas de estudos cronobiológicos. [A] Representação em simples gráfico de linhas dos dados de expressão rítmica circadiana dos genes relógio *Arntl* e *Per2*. Adaptação dos dados de RNA-seq de YOSHITANE et. al 2014. Apresentação dos mesmos dados de [A] nas formas gráficas de radial plote [B] e radial plot [C]. A ilustração em formato radial plot apresenta os dados em suas diferentes fases (não apenas a acrofase) do ritmo, permitindo o estudo do perfil de oscilação e das amplitudes. Em polar plot são representadas apenas as acrofases (valor máximo da variável) dos ritmos circadianos [Figura do próprio autor, 2018].

2. METODOLOGIA

2.1. Metodologia empregada no capítulo 1

Análise da oscilação circadiana e do controle transcricional de miRNAs em fígado de camundongo.

Dois estudos circadianos de small RNA-seq de fígado de camundongo (YOSHITANE et al. 2014 e VOLLMERS et al. 2013) foram selecionados com o intuito de analisar o padrão de oscilação do miRnoma e a co-expressão com os produtos de genes alvos (RNAm e Proteínas). Os dados de Chip-seq obtidos em KOKE et al. 2012 foram usados para a investigação dos possíveis mecanismos moleculares responsáveis pela gênese da ritmicidade na expressão dos miRNAs. Em KOKE et al. 2012 foram obtidos dados da ligação rítmica dos principais fatores de transcrição circadiano (as proteínas dos genes relógio: *Clock, Bmal1, Npas2, Per1, Per2, Cry1* e *Cry2*), bem como da RNAPII, em sequências de DNA regulatórias de miRNAs. A base de dados miRIAD (*intragenic microRNA database*) foi empregada para identificar analisar possíveis diferenças no controle transcricional de miRNAs localilzados em diferentes regiões do genoma. miRIAD permitiu a identificação de miRNAs intragênicos (dentro de outros genes, como genes codificadores de proteínas, chamados *host genes*) e intergênicos (entre genes). miRNAs intragênicos e intergênicos foram identificados no dado de expressão de small RNA-seq de YOSHITANE et al. 2014. Os padrões das oscilações circadianas dessas duas classes de miRNAs foram comparados para a análise de possíveis diferenças no controle transcricional de miRNAs genes localizados em diferentes regiões do genoma.

Através de miRIAD também identificamos *host genes* com expressão circadiana no RNA-seq de YOSHITANE et al. 2014. Consideramos *host genes* como pre-miRNAs (RNAs precursores de miRNAs). As oscilações circadianas de miRNAs maduros e pre-miRNAs (formas precursoras de miRNAs maduros) foram comparadas com o intuito de investigar possíveis diferenças entre vias transcricionais e pós-transcricionais do controle da ritmicidade de miRNAs. Ademais, com o intuído de investigar possíveis diferenças nos sistemas pós-transcricionais de maturação de miRNAs, comparamos os ritmos das formas maduras miRNA-3p e miRNA-5p. Para analisar ação de miRNA-3p e miRNA-5p, usamos a ferramenta de bioinformática mirPath v.3. para identificar vias moduladas por esses miRNAs.

Os dados de RNA-seq e de small RNA-seq de YOSHITANE et al. 2014 foram usados nas análises da expressão circadiana de RNAm e miRNAs por apresentar melhor amostragem temporal. YOSHITANE et al. 2014 realizaram ensaios com amostras de fígado coletadas de

animais eutanasiados em oito momentos de coletas, ou horas circadianas (*Circadian Time* – CT). O RNA-seq e o small RNA-seq de YOSHITANE et al. 2014 foram feitos a partir das mesmas amostras/animais, o que possibilitou a análise de co-expressão de RNAm e miRNAs. A figura 8 sumariza o pipeline dessa etapa do estudo.

Análise de genes alvos de miRNAs circadianos.

Os dados das bibliotecas de RNA-seq (total de 1126 transcritos) de YOSHITANE et. al. 2014 e de proteoma (total de 186 proteínas) de ROBLES et. al. 2014 foram empregados na identificação de genes que apresentam oscilação circadiana nos níveis de ambos, RNAm e proteínas. As amplitudes dos ritmos dos RNAm e das proteínas foram comparadas e os genes separados em dois grupos: (1) genes que reduzem ou (2) que aumentam as amplitudes das proteínas em relação ao seu RNAm. Para identificar miRNAs candidatos ao controle dos ritmos dos genes dos dois grupos [(1) e (2)], selecionamos genes alvos que apresentam maior redução (cutoff: fold de 0.5 - 0.12, em reação ao RNAm, com valor de referência 1) e maior aumento (cutoff: fold de 1.5 - 1.8, em reação ao RNAm, com valor de referência 1) das amplitudes. A ferramenta ChemiRs (*a web application for microRNAs and chemicals*) foi usada para identificar miRNAs candidatos. ChemiRs identifica interações miRNAs-RNAm através de 10 diferentes algoritmos (DIANA-microT, miRanda, miRDB, RNAhybrid, pictar(4way), pictar(5way), PITA, RNA22, TargetScan e miRWalk) e de ensaios experimentais publicados previamente. O estudo de co-expressão de miRNAs candidatos e RNAm alvos foi realizado com o objetivo de comparar a relação entre as fases dos ritmos dessas duas classes de transcritos. Para isso, foram usados os dados de small RNA-seq (miRNAs) e RNA-seq (RNAm) de YOSHITANE et. al. 2014.

Para investigar se os ritmos dos RNAm dos genes dos grupos (1) e (2) são modulado pelos miRNAs candidatos, realizamos análise comparativas de dados de Chip-seq e da expressão (RNA-seq) dos RNAm e pre-RNAm (formar precursora do RNAm). Esses dados, de Chip-seq e RNA-seq, foram obtidos em KOKE et al. 2012. A figura 8 sumariza o pipeline do estudo.

Cálculo das amplitudes, representação gráfica e análise estatística.

As amplitudes dos ritmos dos miRNAs, RNAm e das proteínas foram calculadas através do *peak to trough ratio* (P/T), ou pela razão do máximo e mínimo valor das variáveis (para expressão dos miRNAs, de RNAm ou proteínas): P/T (amplitude) = *máximo valor da expressão* / *menor valor da expressão*. Os valores de acrofases foram obtidos nas análises originais dos estudos. Os dados de expressão (RNA e proteínas) e de Chip-seq foram convertidos para a

escala Z-score para possibilitar a ilustração e análise gráfica de ritmos com diferentes amplitudes. Para cada amostra, o Z-score foi calculado através da equação: Z-score = ([*valor da variável na escala original* $_{\text{no CTx}}$] – [*média de todos os dados* $_{\text{conjunto dos 8 CTs}}$]) / (*desvio padrão de todos os dados* $_{\text{conjunto dos 8 CTs}}$). As representações gráficas em formato de barras foram realizadas através do programa Graphpad Prism. O diagrama de Venn foi feito com o auxílio da ferramenta da web Venny 2.1.0 (http://bioinfogp.cnb.csic.es/tools/venny/). Os gráficos em formato *polar plot* e *radial plot* foram gerados com em funções do R. O Teste t de Student foi usado para comparar as acrofases e amplitudes dos diferentes ritmos.

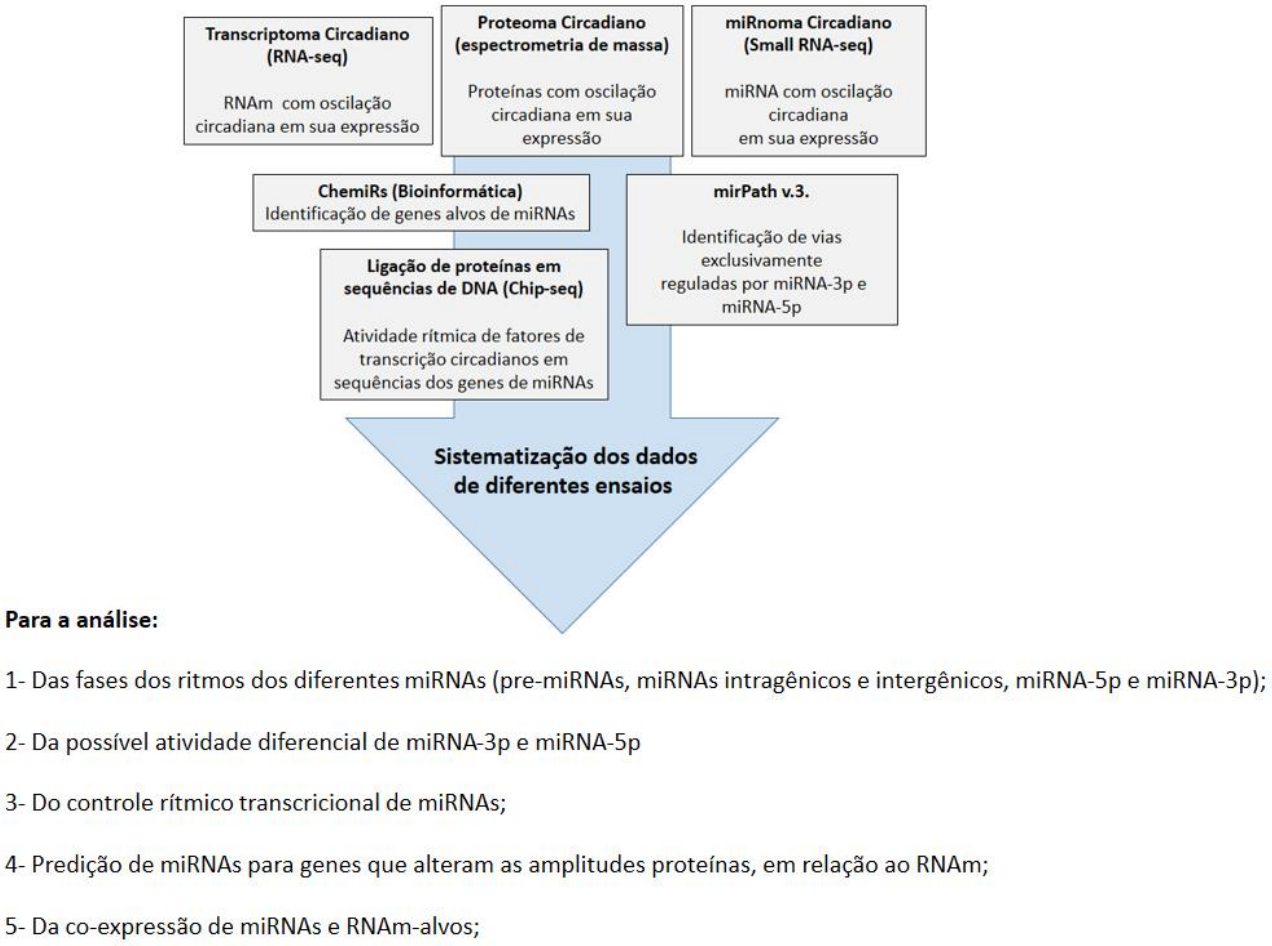

Figura 8. Resumo do pipeline do estudo. Uso de diferentes dados experimentais de estudos circadianos de larga escala e de bioinformática para análise de miRNAs [Figura do próprio autor, 2018].

2.2. Metodologia empregada no capítulo 2

Sistematização de dados de estudos circadianos de HTA e identificação de miRNAs relevantes ao sistema circadiano

Para identificar miRNAs candidatos ao controle dos genes relógio foi realizada a sistematização dos dados de 3 estudos circadianos de Chip-seq para proteínas dos genes relógio (KOIKE et al., 2012; WANG, H. et al., 2016b; YOSHITANE et al., 2014), 4 estudos de RNA-seq[25-28], e interações miRNA-RNAm (ligações químicas tipo pontes de hidrogênio entre essas duas classes de RNAs) experimentalmente suportadas (dados obtidos em: DIANA TarBase v7.0) e preditas (dados obtidos no estudo de bioinformática de: FIGUEREDO et al., 2013). Com a sistematização, foi criado um escore para cada miRNA identificado, que resulta da soma de: (1) expressão circadiana confirmada em diferentes estudos, computando o escore "de valor 1" por estudo e para cada host gene, o pre-miRNA e forma madura de miRNA de um miRNA gene. (2) modulação circadiana pelas proteínas do relógio (computando por fator de transcrição/proteínas do relógio que se ligam em sequências regulatórias do miRNA gene. Computando também o número de estudos); (3) número de genes relógio que são alvos preditos para o miRNA (computando pelo número de genes relógio alvos e número de programas de predição); (4) número de genes relógio que são alvos experimentalmente confirmados para o miRNA (computando pelo número de genes relógio alvos, com maior peso para validação experimental de interação direta entre miRNA-RNAm). Além disso, foi considerado um escore extra para genes relógio alvos de miRNAs que são igualmente preditos e validados. Os miRNAs foram ranqueados com base no escore total (do maior para o menor). Esse estudo infere que quanto maior escore, maior probabilidade do miRNA desempenhar importância no controle de ritmos circadianos endógenos. Os miRNAs com maior escore foram selecionados para o estudo experimental de validação funcional.

Análise da função dos dois miRNAs mais relevantes em modelo celular U2OS PER2:LUC

Cultura de U2OS PER2:LUC

O modelo U2OS PER2:LUC usado nesse estudo foi disponibilizado pelo colaborador Dr. John B. Hogenesch, importante pesquisador de ritmos circadianos e um dos principais descobridores do genes relógio *Bmal1*. Os ensaios funcionais de U2OS PER2:LUC foram realizados no laboratório do Dr. John B. Hogenesch, localizado no *Children's Hospital Medical Center*, em Cincinnati, nos Estados Unidos da América. As células foram cultivadas em meio DMEM (Gibco 11995-065), 1x L-Glutamine, 1x NEAA, 0.25% Trypsin e

enriquecido com 10% de soro bovino fetal e o antibiótico dexametasona (em concentração 0.1 uM). O crescimento celular ocorreu em estufa com temperatura de 37ºC e 5% do CO2 (dióxido de carbono). No equipamento Lumicycle, as células foram mantidas em placas de cultura com diâmetro de 35 milímetros e a luminescência de Lucicerase recordada com o auxílio de d-Luciferin (em concentração de 0.1mM) (Promega).

Nesse estudo, a combinação do modelo U2OS PER2:LUC e sistema Mimic (Invitrogen, USA) foi empregada para a avaliação da função dos miR-29b-3p e miR-23b-3p. O sistema mirVana™ Mimic system (Invitrogen, USA) possibilitou o aumento dos níveis celulares dos miRNAs. 15 nM (nanomolar) mirVana™ Mimic de miR-29b-3p e miR-23b-3p foram

Como controles dos ensaios funcionais, selecionamos um Scramble, o miR-450b-5p, miR-132-3p e miR-219a-1-3p. Essas quatro moléculas também tiveram seus níveis aumentados com o sistema Mimic na mesma concentração que miR-29b-3p e miR-23b-3p, 15 nM. O Scramble é uma molécula com sequência semelhante às dos miRNAs (em tamanho e constituição química), sendo desenhada e testada para não induzir alterações na expressão de genes humanos. miR-450b-5p foi o miRNA identificado nas análises de sistematização desse estudo, com pior posição e menor escore (valor: 0). O Scramble e o miR-450b-5p foram selecionados como controles negativos das transfecções e do método de identificação de miRNAs candidatos, respectivamente. miR-132-3p e miR-219a-1-3p são os dois miRNAs com maior citação na literatura circadiana. Estudos funcionais *in vivo* (em camundongos) confirmam a função de miR-219a-1-3p no ajusto do período do ritmo circadiano da atividade locomotora dos animais e de miR-132-3p na sincronização desse ritmo via estímulos luminosos. Aqui, miR-132-3p e miR-219a-1-3p foram selecionados como controles positivos dos ensaios com Mimics. Após as transfecções dos Mimics as células U2OS PER2:LUC foram incubadas por 24h antes da coleta do ritmo de luminescência.

PCR quantitativa em tempo real (qPCR)

Ensaios de qPCR foram realizados para a analisar o possível papel de miR-29b-3p na modulação expressão de outros genes relógio (*Per1, Per2, Per3, Cry1, Cry2, Arntl, Arntl2, Tef, Rora, Bhlhe40 e Nr1d1*) e de um gene de referência (usado para normalizar os dados de qPCR), o *Gapdh*. As células U2OS foram transfectadas com 15nM de Mimics de miR-29b-3p e após 24h o RNA total (com todos as classes de RNA da célula) foi extraído com Direct-zol RNA kit (Zymo research) em apenas um momento do ciclo circadiano. Em seguida, a concentração do RNA total foi quantificada em equipamento NanoDrop (ThermoFisher). 250ng RNA total foram usados para a conversão de RNA em cDNA (DNA complementar). Os cDNA foram

sintetizados em reações de transcrição reversa (realizadas com o kit qScript cDNA MasterMix, Quantabio) que converteram RNA em cDNA. Ao final das reações, 20uL de cDNA foram diluídos (1:10) e usados nas reações de qPCR para a quantificação dos RNAm dos 11 genes relógio e de *Gapdh*. As reações de qPCR foram realizadas através do sistema de sondas TaqMan (Thermo Fisher) e em equipamento QuantStudio Real-Time PCR (Thermo Fisher). As reações de qPCR foram feitas em triplicatas, ou seja, três grupos de células, para os grupos scramble e três para Mimic miR-29b-3p. Os dados brutos de *Cicle Threshold* (Ct) obtidos no equipamento QuantStudio Real-Time PCR foram normalizados (com *Gapdh*) e apresentados em $2^{-\Delta\Delta Ct}$. O grupo controle (Scramble), foi usado como calibrador (referência) na equação $2^{-\Delta\Delta Ct}$. Assim, nas representações gráficas Scramble possui valor médio setado para 1.

Identificação de genes alvos, de vias e análises de redes de interação miRNA-genes alvos

Análises de bioinformática, em conjunto com buscas de informações experimentais, foram empregadas para identificar genes relógio que possuem sequências com sítios alvos de miR-29b-3p. Os sítios alvos de miRNAs são sequências nucleotídicas que possuem complementaridade (ligação tipo ponte de hidrogênio) com a cadeia de nucleotídeos de miR-29b-3p. A ferramenta ChemiRs foi usada para predições de sequências alvo de miR-29b-3p nas 3'UTRs dos 11 genes relógio. Dados de análises de bioinformática também foram obtidos em publicação de nosso grupo pesquisa (FIGUEREDO et. al. 2013). Já indícios experimentais de interações miR-29b-3p:RNAm (de genes relógio) foram obtidas na base de dados DIANA TOOLS - TarBase v7.0, em ChemiRs e em publicações que associam miR-29b-3p com genes relógio. A ferramenta da web miRNet foi usada para análise o compartilhamento de miRNAs por genes relógio e o número de miRNAs exclusivos por gene. Por fim, a ferramenta Metascape foi usada para a identificação de vias celulares moduladas por miR-29b-3p. É importante ressaltar que as análises em miRNet e Metascape foram feitas com genes alvos identificados com informações experimentais de interações miR-29b-3p:RNAm.

Análise estatística e representação gráfica

O Graphpad Prism foi usado para gerar as ilustrações em barras dos dados de qPCR da expressão dos genes relógio e gráficos em linhas do ritmo de U2OS PER2:LUC. Os resultados das análises em miRNet são apresentados em uma figura de redes de interações (em inglês: *network*) gerada pelo próprio programa miRNet. Da mesma forma, as figuras relacionadas com os dados obtidos em Metascape resultam do próprio programa. O diagrama de Venn foi obtido com o auxílio da ferramenta da web Venny 2.1.0 (http://bioinfogp.cnb.csic.es/tools/venny/). Os

gráficos em formato *radial plot* foram gerados em funções do R. A figura que ilustra a hipótese, ou idéia final do trabalho, foi criada pelo próprio autor, no corel draw x7. O Teste t de Student foi usado para comparar os períodos e as amplitudes dos diferentes ritmos ($p<0.05$).

2.3. Metodologia empregada no capítulo 3

Animais e coleta de tecidos

Camundongos C57BL/6 (total: 24), machos e com idade de 8-12 semanas, foram inicialmente adaptados (em laboratório) ao regime de 12 h de luz e 12 h de escuro. Entretanto, para a análise do ritmo endógeno dos animais, foi necessária a exclusão dos Zeitgebers. Por essa razão, após essa adaptação inicial, os camundongos foram transferidos para as condições ambientais de escuro e temperatura constantes durante dois dias. Após esse período, os animais foram eutanasiados e o estriado e o tronco cerebral foram coletados nos CTs: CT00, CT04, CT08, CT12, CT16 e CT20. Em outro grupo de animais, o estriado e o córtex pré-frontal foram isolados quando na presença de Zeitgebers. Nesse segundo grupo os animais foram mantidos no regime de 12 h de luz e 12 h de escuro, simulando as variações diárias de luminosidade. Os tecidos foram isolados em seis Zeitgebers Times: ZT02, ZT06, ZT10, ZT14, ZT20 e ZT22. Esse último grupo teve o intuito de estudar o ritmo do RNA total na presença de pistas ambientais. Ressaltamos que os animais foram eutanasiados através de método aprovado pelo comitê de ética da UFAL (Protocolo de aprovação: CEUA56/2015).

Normalização de tecidos, isolamento e análise da concentração do RNA total

As diferentes etapas experimentais foram equalizadas para ajustar a quantidade de tecido usada para extração de RNA de tecidos coletados em diferentes fases (CTs ou ZTs) do ciclo circadiano. Tal ajuste foi realizado como tentativa de manter a ritmicidade do RNA total de cada tecido estudado. Os tecidos foram isolados pelo mesmo pesquisador para evitar possíveis variações metodológicas. Antes da dissecção dos tecidos, tubos de 1.5mL contendo 1,5 mL de Trizol LS Reagent (Thermofisher, USA) foram pesados em balança analítica de precisão. Em seguida, os pesos de cada tubo (com 1,5 mL de Trizol) foram setados (na balança) para 0 antes da adição dos tecidos. Em seguida, os tecidos foram pesados diretamente nos tubos de 1,5mL e a concentração (em ng/uL) das amostras foram calculadas. Os tecidos foram dissolvidos no Trizol com o auxílio de seringa estéril de 5mL. Subsequentemente, as amostras foram ajustadas (diluídas com Trizol) para a concentração de menor valor. Um volume fixo de Trizol (com a mesma concentração de RNA) foi usado nas demais etapas da extração. Ainda na tentativa de manter o ritmo endógeno do RNA, o protocolo original do Trizol LS Reagent (Thermofisher, USA) foi adaptado para garantir homogeneidade na extração do RNA das

diferentes amostras: (1) uso do mesmo volume de clorofórmio, de glicogênio (20 ng/uL), Isopropanol e etanol 75%; (2) transferir o mesmo volume de fase aquosa (com RNA) para um novo tubo; (3) diluir o RNA no mesmo volume de água livre de nuclease (50 uL). Nas extrações do RNA de tronco cerebral dois RNAs exógenos (Spike-ins) foram adicionados ao Trizol, em mesma concentração (0,26 fmol) e antes do isolamento do RNA total. Os Spike-ins são dois miRNAs de *Caenorhabditis elegans*, Cel-miR-39 e Cel-miR-54, comprados da Qiagen (Alemanha). Esses pequenos transcritos não possuem homologia em mamíferos e podem ser facilmente detectados no método de qPCR. Spike-ins foram usados tanto como estratégia para a análise da eficiência do isolamento de miRNAs em amostras com diferentes concentrações de RNA, como possíveis normalizadores dos dados da qPCR. A concentração do RNA total foi quantificada em triplicatas (por amostra) em equipamento de espectrofotômetro BioPhotometer plus (Eppendorf, USA). A figura 10 representa as etapas e os diferentes ajustes realizados durantes dos procedimentos de extração do RNA.

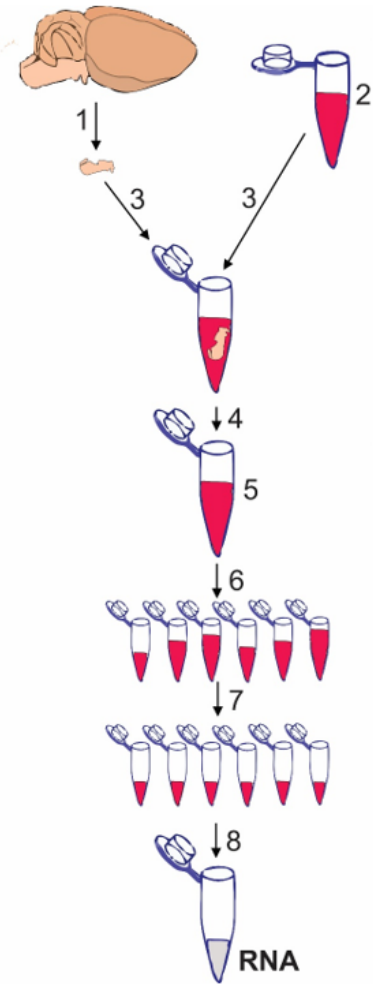

1. Dissecção de tronco cerebral e análise do preso do tecido em balança de precisão.
2. Análises do pesos dos tubos de 1.5mL + 750uL de Trizol.
3. Homogeneização dos tecidos em 750uL de Trizol.
4. Cálculo das concentrações dos tecidos (ng de tecido por volume de Trizol).
5. Análises do pesos dos tecidos homogeneizados em Trizol.
6. Normalização da concentração do tecido (ng/uL) em relação a amostra de menor concentração. As concentrações foram normalizadas pela diluição com novos volumes de Trizol.
6. Uso de um mesmo volume de Tecido normalizado em Trizol nas demais etapas do protocolo de extração. Agora as amostras possuem a mesma concentração de tecido, em ng/uL.
7. Adaptação do protocolo original de Trizol para igualar todas as condições, evitando variações experimentais.

Figura 9. Ajustes realizados durante a etapa de extração do RNA como tentativa de minimizar variações decorrentes de procedimentos e de manter o ritmo biológico do RNA. A figura destaca a extração de tronco cerebral, o tecido usado nas análises de expressão gênica. Entretanto, o método foi empregado para a extração dos demais tecidos. O RNA resultante foi usado para as análises do ritmo do RNA total (mensurado em espectrofotômetro) [Figura do próprio autor, 2018].

Síntese de cDNA

Duas abordagens foram usadas para a síntese dos cDNAs. No Grupo 1 (G1) os cDNAs foram sintetizados a partir do mesmo volume de RNA total (2.75uL), mantendo os ritmos endógenos dos RNAs. Já no grupo 2 (G2), sem considerar o ritmo endógeno, ajustamos o RNA total para a mesma concentração, 500 ng/amostra. As reações de síntese de cDNA foram realizadas através do kit miScript Reverse Transcription Kit (Qiagen, Alemanha), com volume final de 20uL. Seguindo orientações do fabricante, foram adicionados, em cada reação 4uL do miScrip Hiflex Buffer, 2uL de 10x miScrip Nucleics Mix e 2 uL de miScript Reverse Transcriptase Mix nas duas condições (G1 e G2). As reações foram inicialmente incubadas em 37°C/60 minutos para a conversão de RNA em cDNA pela ação da de miScript Reverse Transcriptase. Em seguida, a enzima foi inativada em 95°C por 5 minutos. Antes das reações de qPCR o cDNA foi diluído na razão de 1:10.

PCR em tempo Real quantitativa (qPCR)

Reações de qPCR foram realizadas para analisar a expressão dos RNAm dos genes *Actb, Gapdh, Ppib, Hprt1, Rplp1,* e *Eif2a*, *Bmal1, Clock, Per1* e *Per2*. Os genes *Actb, Gapdh, Ppib, Hprt1, Rplp1* e *Eif2a* são geralmente usados como normalizadores (ou housekeeping genes, HKG) de dados de reações de qPCR. Esses genes geralmente compõem vias basais às células e acredita-se que por essa razão apresentam estabilidade (sem variação da expressão) nas diferentes condições experimentais. Entretanto, para confirmar a estabilidade de HKG faz-se necessário o estudo dos genes nas diferentes condições, ou grupos experimentais. Nesse estudo, os 6 HKG foram selecionados a análise da estabilidade ao longo de um ciclo circadiano. Os genes relógio, *Bmal1, Clock, Per1* e *Per2,* com expressão circadiana confirmada em diferentes tecidos e espécies, foram selecionados para a análise da normalização com diferentes HKG e Spike-ins, além do estudo das possíveis alterações nos ritmos de genes individuais em decorrência do ajuste da concentração do RNA total na etapa de síntese de cDNA dos grupos G2. As reações de qPCR foram realizadas no equipamento StepOne Plus (Applied Biosystems, USA), com 0.35uL (3.5uM) de cada primer (forward e reverse), 5 uL de Sybr Select Master Mix (Thermofisher, USA), 2.15uL de água livre de nuclease (Amresco, USA) e 2.5 uL de cDNA (de G1 ou G2). O modo *fast* de ciclagem de temperatura do equipamento StepOne Plus foi usado. Todas as reações de qPCR foram realizadas em duplicatas, como réplicas técnicas. Apenas reações com réplicas técnicas com desvio padrão de Ct (Cycle Threshold) < 0.5 foram consideradas. As eficiências dos primers foram checadas através de cinco diluições seriadas do cDNA (em proporção 1:2). Foram considerados no estudo apenas os primers com eficiência

entre 90-110% e com apenas uma curva de melting. Os primers foram desenhados pelos próprios autores, ou obtidos em outros estudos (Ver tabela 1 do artigo). Para a análise dos níveis dos spike-ins, fi usado o sistema miScript PCR (Qiagen, Alemanha). As reações foram feitas com 2uL do miScript Primer Assays, 10uL do 2x Quantitec SYBR green PCR Master Mix, 2uL do 10x miScript universal primer, e 4uL de água livre de RNAse. Nas reações de qPCR de spike-ins foram consideradas as condições de ciclagem 95°C/15 minutos (Ativação da enzima HotStartTaq DNA polimerase), 94°C/15 segundos para a desnaturação do DNA, 55°C/30 segundos para o anelamentos dos primers e 70°C/30 segundos para a extensão. Foram usados 40 ciclos.

Análise dos dados

Os métodos de Cosinor e Fourier, que ajustam a série temporal de dados a cujas cosseno, são comumente usados em estudos de ritmos biológicos (Refinetti et al., 2007), sendo também empregados em nossas análises. No estudo de expressão gênica consideramos ambos, o Ct (Cycle threshold) convertido em valor absoluto (10^{10}) x 2^{-Ct} (or 2^{-Ct}), como previamente destacado (Kamphuis et al., 2005) e o dado normalizado com HKG (ou spike-ins) na equação do delta Ct comparativo ($2^{-\Delta\Delta Ct}$; ΔΔCt: {Ct[do Gene de interesse] - Ct [HKG]Amostra-A} - {Ct [do Gene de interesse] - Ct [HKG]Amostra referência ou calibrador}). Para comparar variações nas amplitudes dos ritmos dos diferentes genes os dados de expressão foram convertidos em *fold change* em relação ao *nadir* (hora circadiana, Circadian Time [CT] com menor expressão, com valor de referência ajustado para 1). Nas análises comparativas de dados em escalas diferentes (como concentração do RNA total e níveis dos Spike-ins) os dados foram convertidos em Z-score, o que possibilitou a plotagem desses diferentes ritmos em um mesmo gráfico. Os métodos estatísticos One way ANOVA (com correção de Bonferroni) e o t-test (com correção de Sidak Bonferroni) foram empregados para a comparação dos dados. Em conjunto com os métodos de Cosinor e Fourier, o programa geNorm foi usado para a análise da estabilidade dos HKG. Nessas análises foram usados os dados de 2^{-Ct}. Os gráficos e cálculos estatísticos foram realizados nos programas GraphPad Prism 6, IBM SPSS 20, Cosinor (http://www.circadian.org/softwar.html) e CircWave V1.4 (http://www.euclock.org/results/item/circ-wave.html). Os parâmetros rítmicos de robustez, amplitude e acrofase foram calculados no método cosinor, com período ajustado para 24h. O teste de correlação cruzada foi usado para comparar as fases de expressão dos genes nas diferentes condições (G1 e G2). O programa IBM SPSS 20 foi usado para calcular o teste de correlação cruzada. O *peak-to-trough ratio* (P/T), ou a razão entre os valores máximo e o

mínimo de expressão foi empregada como um método de análise complementar da amplitude dos ritmos dos genes.

3. RESULTADOS E DISCUSSÃO

ARTIGO 1: Systematization of circadian high throughput assays: differences in miRNAs 3p/5p forms and potential miRNA-adjustment of protein amplitude dependent of mRNA-phase.

Abstract

Circadian rhythms are fundamental properties of organisms in which clock genes control different cellular pathways by modulating the transcriptome. High throughput assays (HTA)(RNA-seq, Chip-seq and proteome) have helped to understand the circadian cellular mechanisms, demonstrate large differences between mRNAs and protein rhythms, and emphasize the importance of post-transcriptional pathways (such as miRNAs) in circadian control. In this study, we aimed to analyze the relationship between circadian transcription factors (CTF) and rhythm oscillation of miRNAs, the circadian differences of 3p and 5p miRNAs, as well as to identify miRNA that targeted genes that present alterations in protein rhythms (in relation to mRNA), and to show the possible role of miRNAs in gene translation. For this, we perform the systematization analysis of different circadian HTA studies. When crossing the results of two circadian small RNA-seq, we identified that 6.4% of miRNAs have circadian expression in mouse liver, with elevated levels during the phase of subjective day and less dispersion than those observed for mRNAs. The miRNA-genes sequences possess rhythmic occupancy of CTF and RNA polymerase II (RNAPII), suggesting a rhythmic transcriptional control of pri-miRNAs. Interestingly, the mature forms of the miRNAs (-3p and -5p) have different phases and exclusive target genes. These two classes of mature miRNAs have distincts maturation pathways, and it is possible that the differences observed in the phases result of miRNA post-transcriptional adjustments. In addition, only 6 genes oscillate in both miRNAs (3p and 5p), indicating a circadian selectivity for the functional form of miRNAs. In conjunction with differences in acrophases, the existence of genes that are exclusively target show a differential role of 3p and 5p forms. Curiously, the clock mRNAs are preferentially targeted by miRNA-3p forms, highlighting these elements are more impacting to the clock. miRNAs were also identified for targeting genes that alter their protein amplitudes relative to mRNA. miRNAs that exclusively modulate genes that reduce or that increase protein amplitudes have the similar expression phases. However, these miRNAs have different phase relationships with mRNA-targets. Proteins that reduce amplitude have mRNA in anti-phase with the miRNAs. For those who increase its amplitude, closer phases are observed. The similarities in pre-mRNAs e mRNAs indicates that phase differences at the mRNA level result from transcriptional regulation, non by mRNA degradation induced by miRNA. In this study, we demonstrated for the first time the circadian divergences of miRNA-3p and miRNA-5p matures forms. And that, the adjustment of the amplitudes of proteins rhythms by miRNAs can be mRNA-phase dependent. Future studies are needed to validate and better understand these results.

Key words: amplitude, miRNA, protein, mRNA, 3p, 5p, circadian

Introduction

In recent years the number of circadian HTA have expanded exponentially, with approximately 120 publications registered in 2015 and in 2016 [1]. These studies made available a circadian "big data", a rich chronobiological collection that can be used for different purposes, not just those of the original publications. In fact, studies have used data free-available from HTA circadian assays to identify genes or pathways important to the clock [2,3]. Using the systematization from publicly-available data, Bhargava et al. 2015 identified 11 novel robust candidate clock genes [2]. The web portals "CircadiOmics" and "CircaDB" integrate data from circadian HTA studies, that allows quick and easy identification of genes circadian expression in different tissues and organisms [4,5]. These different authors show that systematization of previous HTA studies is promising, and can help different chronobiology research groups. Unfortunately, methods such as RNA-seq and Chip-seq are still costly, having little accessibility in some countries, especially in chronobiological studies that require large sampling (collections at intervals of 2h for 48h, for example). The data systematization can answer different questions, reducing the need for funding, study time, and euthanized animals.

In liver, HTA circadian studies (RNA-seq and proteome) have shown that many rhythms are independent of CTF or that posttranscriptional/translational events impact in phases of proteins with mRNA transcribed by the CTF [6,7]. It has been demonstrated that half of the cyclic proteins have corresponding arrhythmic mRNA [6]. And many cyclic proteins have a delay in acrophases of 6 hours in relation to the rhythm of mRNA [6,7].

miRNAs control the levels of gene expression by inducing mRNA degradation and/or inhibiting of protein translation [8,9]. It is estimated that more than 60% of human protein-coding genes are modulated by miRNAs [10]. Interestingly, in a circadian gene expression atlas ZHANG, R. et al., 2014 show that 43% of all protein coding genes showed circadian rhythms in mRNA in some mammalian tissue [11]. Together these data reinforce the importance of miRNAs in the circadian control of protein rhythms.

In fact, models with depletion of mRnome show alterations in the rhythm of gene expression [8,9]. miRNAs adjust the phases and amplitudes of 30% mRNAs rhythmically transcribed [9] and the speed of PER1 and PER2 translation, associated with the shortening of the period (~2 hours) observed in molecular rhythm from cells and in the rest-activity behavior of mice [8]. In addition, miRNAs are importantly associated with the genesis of circadian rhythms at the molecular level during gestation[42] and with changes in rhythms during the aging process [43].

To date, only two small RNA-seq studies show the circadian oscillation of several miRNAs [12,13]. 84 circadian miRNAs were identified in YOSHITANE et al., 2014 e 53 em VOLLMERS et al., 2013, with high levels predominantly during the subjective day (interval between CT0 and CT12, CT= *circadian time*), which is equivalent to the resting phase of the animals [12,13].

These small RNA-seq studies do not demonstrate why miRNAs exhibit clustered oscillation during the day. Based on *chromatin immunoprecipitation sequencing* (ChIP-Seq) at a single CT, VOLLMERS et al., 2013 suggest a key role of CLOCK-BMAL1 in the biogenesis of miRNAs [12]. In a more complete study, KOIKE et al., 2012 presents details of the transcriptional architecture of the core circadian clock in mammals [14]. The authors performed Chip-seq (for CTF: BMAL1, CLOCK, NPAS2, PER1, PER2, CRY1 and CRY2) from mice livers collected in six different CT [14]. The inspection of the data generated by Koike (supplemental material of Chip-seq) allows to identify that several classes of transcripts are rhythmically modulated by CTF, including miRNA genes (see supplemental material of KOIKE et al., 2012). However, the authors do not highlight the transcriptional control of miRNAs in the article [14]. KOIKE et al., 2012 also performed two different RNA-seq for rhythms detection of pre-mRNA (intron RNA-seq) and mRNA (exon RNA-seq). Many miRNAs are intragenic, and the analysis of the miRNAs host genes (from RNA-seq intron) could be used to infer the miRNA nascent oscillation.

YOSHITANE et al., 2014 and VOLLMERS et al., 2013 did not analyze the phase relation of the miRNAs and different cyclic targets (at mRNA and proteins levels), or if there are differential expression by miRNA class (miRNA-3p and miRNA-5p, or intragenic and intergenic miRNAs).

By microarray hybridization, Na et al. 2009 analyzed the microRNA-mRNA co-expression rhythm in mouse liver for 48h, and demonstrate that the clock genes of positive (*Clock* and *Bmal1*) and negative (*Per* and *Cry*) transcriptional regulation have different phase relationship with their predicted miRNAs. [15]. To our knowledge, this is the only study that analyses the circadian co-expression of miRNAs and target genes. However, Na et al. 2009 focused their study on just some target genes, and at RNA level [15]. In comparison to VOLLMERS et al., 2013, YOSHITANE et al., 2014 have small RNA-seq experiment performed in better temporal resolution (8 CT groups, sampled at 3 CT intervals). In addition, mRNA data (from RNA-seq) has the same resolution as the small RNA-seq. Therefore it is possible to use the YOSHITANE et al., 2014 data to better compare the oscillation of miRNAs

and mRNA-targets. Assays of circadian proteomes have grown in recent years and may add the proteins analysis of in co-expression analyses [6,7]. By mass spectrometry Robles et al. 2014 identified 186 proteins that showed rhythmic profiles in mouse liver from free-running condition [7].

The circadian studies commonly use prediction algorithms for identification of miRNA-target genes [16]. Methods that combine large-scale sequencing and immunoprecipitation of Argonaute (Ago) to isolate native Ago-miRNA-mRNA complexes in living cells, such as HITS-CLIP (*High throughput sequencing of RNA isolated by crosslinking immunoprecipitation*), have been applied in identification of experimental miRNA:mRNA interaction [17–19]. However, to our knowledge, to date, HITS-CLIP, or similar methods, have not been used to identify miRNAs interacting with circadian genes.

By the systematization analysis of important circadian HTA studies, the present study aimed to analyze the circadian transcriptional control of miRNAs and the differential expression of the different classes of mature miRNAs (3p and 5p). In addition, by identification of experimental miRNA:mRNA interaction and expression data from circadian HTA studies, we aimed to study the co-expression of miRNAs and mRNA/proteins from target genes that have different alterations in your translations. Based on these analyzes we propose different circadian functions for 3p and 5p miRNAs, and an miRNA-adjustment of protein amplitude dependent of mRNA phase.

Materials and methods

HTA circadian data

For a general analysis of miRNAs oscillations, we used the data from two circadian studies of small RNA-seq [12,13]. For the identification and analysis of target gene with circadian oscillation in both mRNA and proteins, we used Poly (A)-tailed RNA-seq data from YOSHITANE et al., 2014 and mass spectrometry from ROBLES; COX; MANN, 2014 [7,13]. For co-expression analysis we selected mRNA and miRNA data from YOSHITANE et al., 2014 because they correspond to the same biological sample (allowing better comparison) and have good sampling (8 samples collected every 3 CTs). KOIKE et al., 2012 RNA-seq data were considered in pre-mRNA and mRNA analyzes, and also in the study of the occupation of CTF and RNA polymerase II (RNAPII) in sequences of target genes and miRNAs [14]. Cyclic miRNAs were classified into intragenic and intergenic by the use of the miRAD tool (an intragenic microRNA database)[20]. Cyclic host genes for intragenic miRNAs (also identified in miRAD) were obtained in Yoshitane's RNA-seq. The oscillation of the mRNA hoste gene was

considered to be the precursor-miRNAs (pre-miRNA). All selected studies performed analyzes on samples in free-running condition and in C57BL/6 mouse liver [7,12–14]. We consider the original circadian statistical analyzes of the studies. In the proteome study, proteins with expression profile adjusted to cosine waves and false discovery rate (q-value) $q<0.33$ were considered rhythmic [7]. In Yoshitane et al. 2014, the mRNAs e miRNAs were defined as rhythmically expressed if it maximal and minimal expression values were significantly different ($q<0.1$), and its expression profile was fitted with cosine curves ($P<0.01$)[13]. In Vollmers's small RNA-seq, to determinations of miRNAs oscillations was calculated the pMMC-beta in COSOPT algorithm [12]. In Koike et al 2012 the pre-mRNA and mRNA cycling were assessed by COSOPT, JTK cycle and ARSER programs [14]. A cycling gene was considered if two out of three programs detected cycling with threshold of $p<0.05$[14]. For ChIP-seq analysis, cycling was analyzed with ARSER ($p<0.05$)[14].

Target genes identification.

We use the web application ChemiRs (http://omics.biol.ntnu.edu.tw/ChemiRs/)[21] to identify miRNAs that modulate genes with variations in protein amplitudes. ChemiRs simultaneously identifies target genes through 10 prediction algorithms, as well as experimentally supported miRNA:mRNA interactions [21]. We considered only targets with miRNA-mRNA interaction reported in the literature. The pathway analysis were performed with DIANA-miRPath v3.0 from a list of -3p and -5p miRNAs [22]. In this DIANA-miRPath v3.0 analyses we searched targets that present experimentally validated miRNA:mRNA interactions from DIANA-TarBase v7.0, the first database that indexing more than half a million experimentally supported miRNA:mRNA interactions [22,23].

Statistical analysis and graphical representations

The t-test were used to compare the different groups, with $p<0.05$. Graphpad Prism was used to generate bar illustrations. Polar plot and radial graphs were generated in R functions. The Venn diagram was made in the Venny 2.1.0 web tool (http://bioinfogp.cnb.csic.es/tools/venny).

Results and discussion

Oscillation of miRNAs is modulated by the circadian occupation of RNAPII and CTF

When comparing the results of two small RNA-seq studies in mouse liver [12,13], we identified 126 (6.4% from 1978 mature forms described) mature miRNAs with rhythmic variation (Figure 1A).

These miRNAs can modulate the post-transcriptional levels (mRNA and/or protein) of clock genes, as well as clock-controlled genes (CCGs), both important for the control of cyclical events[24]. On the other hand, circadian transcription factors (CTF), which are products of the clock genes, may control the transcription of the miRNA precursors (pre-miRNAs) of intragenic or intergenic miRNAs. This reciprocal interaction would include the miRNAs in the molecular clock's feedback loop system. In fact, when analyzing data from Chip-Seq [14] , we identified 104 miRNAs with rhythmic CTF binding in the sequences of their genes, as well as the recruitment of RNA polymerase II (RNAPII) (Figure-1B-C). As shown in KOIKE et al., 2012 the RNAPII has global circadian oscillation in its recruitment and activity, mediated by rhythmic changes in the chromatin structure, by binding of CTF and coactivators (p300 and CBP)[14]. In KOIKE et al., 2012, two antibodies were used to identify (via Chip-seq) the recruitment of RNAPII into the pre-initiation complex (8WG16) of transcription and the initiation of transcription (Ser5P)[14]. For miRNAs, similar to that described by KOIKE et al., 2012, in its transcription analysis, CRY1 has cyclic activity in phase with the start of transcription (Ser5P) (Figure 1B-C), a stage of transcription preparation, wherein the action of CLOCK / BMAL1 / NPAS2 / RNAPII is momentarily inhibited by the proximal binding of CRY1 (Figure 1B-C).

Transcription of the primary miRNA transcripts (pri-miRNAs) would be activated at the time of maximum binding of CLOCK, BMAL1 and NPAS2, more precisely in CT9.8, CT6.3 and CT7.7, respectively (Figure 1B-C). The transcription step itself would occur during the increase of 8WG16 (close to CT12). In fact, WANG et al., 2016 identified 52 pri-miRNAs with oscillation in mouse liver, with mean in CT12.19 [25]. Later this transcription is repressed by the action of PER1-2 / CRY2 (Figure 1B-C). Finally, at the end of the cycle, between the CT16-20, Ser5P and CRY1 increase their levels by restarting the cycle (Figure 1B-C).

Using the miRIAD (*microRNA intragenic database*, http://bmi.ana.med.uni-muenchen.de/miriad/), we identified, from the list of the 84 cyclic miRNAs in YOSHITANE et al., 2014, 36 intragenic miRNAs (and their host genes) and 34 intergenic, with no difference

in their acrophases (Figure 1D). Possibly the similarities result from the same transcriptional circadian control of the different types of miRNAs genes.

When analyzing the circadian miRNAs (from YOSHITANE et al., 2014) by the mature forms, we identified 49 mature miRNAs type -3p and 35 type -5p, originating from the 3 'and 5' ends of the stem loop structure of the pri-miRNA, respectively. Curiously, only 6 miRNAs genes (from 81 miRNA genes identified YOSHITANE et al., 2014 presented both mature miRNAs with circadian oscillation (miR-let-7d, miR-193b, miR-21, miR-24-1, miR-26b and miR-28). We did not identify differences between the amplitudes of oscillation, however, the acrophases are different, with the mean in CT5.59 for miRNA-3p and CT7.61 for miRNA-5p (Figure 1E).

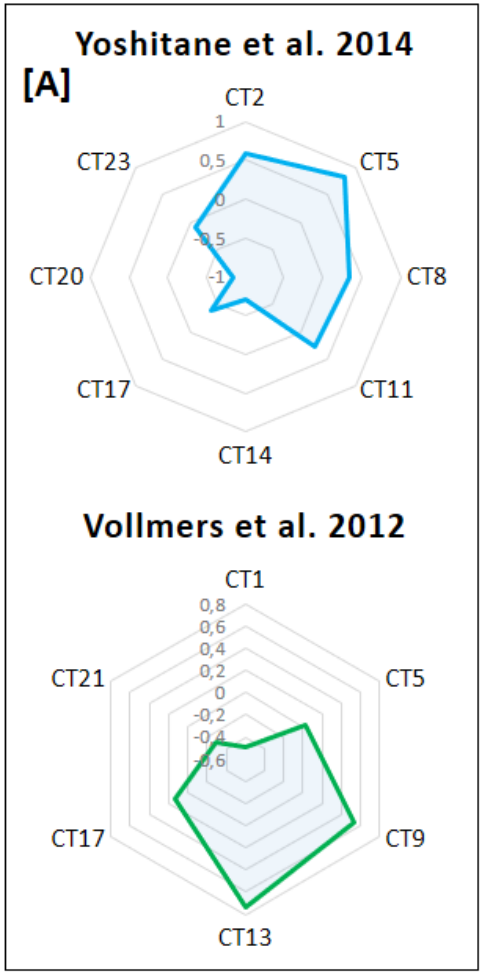
Yoshitane et al. 2014
[A]
CT2
CT5
CT8
CT11
CT14
CT17
CT20
CT23
Vollmers et al. 2012
CT1
CT5
CT9
CT13
CT17
CT21

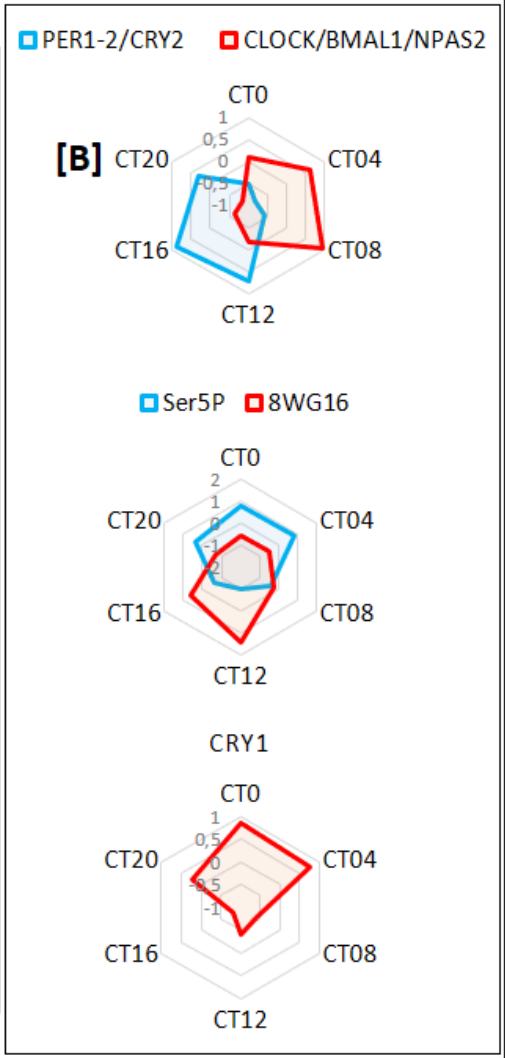
PER1-2/CRY2
CLOCK/BMAL1/NPAS2
[B]
CT0
CT04
CT08
CT12
CT16
CT20
Ser5P
8WG16
CRY1

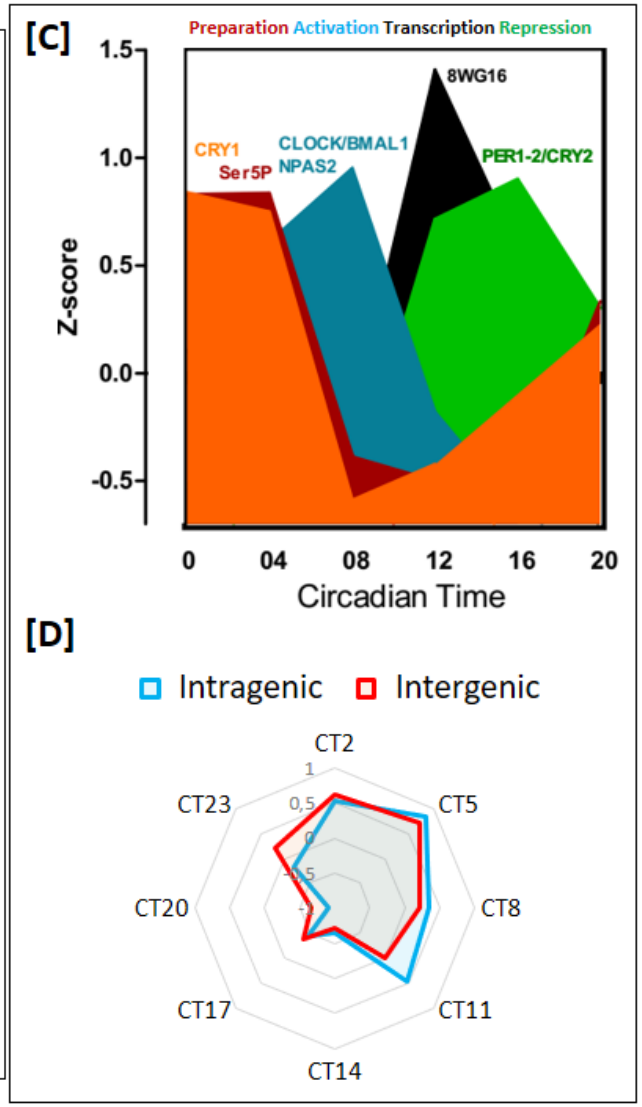
[C]
Preparation Activation Transcription Repression
8WG16
CRY1
Ser5P
CLOCK/BMAL1
NPAS2
PER1-2/CRY2
Z-score
Circadian Time
[D]
Intragenic
Intergenic
CT2
CT5
CT8
CT11
CT14
CT17
CT20
CT23

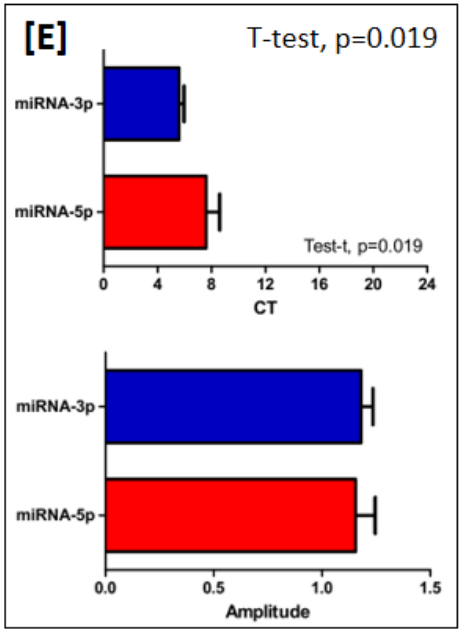
[E]
T-test, p=0.019
miRNA-3p
miRNA-5p
Test-t, p=0.019
CT
Amplitude

Figure 1. Circadian expression profile and rhythmic control of miRNAs in liver. [A] Circadian profile of the miRNAs identified in the studies of VOLLMERS et al., 2013 and YOSHITANE et al., 2014 [B] Identification of circadian transcriptional regulators of miRNAs. [C] Circadian landscape of transcriptional modulators of miRNAs. The analyzes in [B] and [C] were performed with Chip-seq data obtained from KOIKE et al., 2012. [D] Comparison of miRNA expression with gene locus within the structure of other genes (intragenic miRNAs) or between genes (intergenic). The miRNAs were classified (in intragenic and intergenic) from a list obtained in the database miRIAD (http://bmi.ana.med.uni-muenchen.de/miriad/). [E] Statistical analysis of the phases and amplitudes of miRNA-3p and miRNA-5p, was considered the T-test $p<0.05$. The data presented in [D] and [E] were obtained in YOSHITANE et al., 2014. Data were converted to Z-score to enable the visual comparison of rhythms of different intensities and amplitudes.

miRNA-3p and miRNA-5p are functional, with similar numbers of target genes [26]. miRNA-3p and miRNA-5p are matured in different pathways [27–30] and these phase differences may result from circadian variations in maturation genes (Supplementary Figure 1). miRNA-5p strand maturation is processed by *Drosha*, *DGCR8*, *p68*, p72, *Smads*, *p53* and *Erα* [27,28]. *Dicer*, *TRBP* and *PACT* produce the miRNA-3p [27,29]. The selection of the functional form of miRNA is highly refined, dependent on the tissue and cell type, or cell stage and pathology [26–28]. It is possible that the frequencies of -5p and -3p rhythmically expressed are tissue-specific, increasing the complexity of miRNAs function in oscillatory adjustment at the protein level. In fact, Dicer, the main enzyme related to the maturation of miRNA-3p, exhibits a tissue-specific daily variations in mice[31]. In liver, *Dicer* has peak expression in ZT9 (zeitgeber 9)[31]. The analysis in CircadiOmics (http://circadiomics.ics.uci.edu) shows that 3 genes involved in the maturation of miRNA-5p have daily variations statistically confirmed in liver (Supplementary Figure 1). It is possible that the divergence in the rhythms of 3p and 5p maturation genes induces the different acrophases observed for the two functional groups. However, there are no studies that confirm this hypothesis, and future studies are necessary.

Through the analysis performed in mirPath v.3 (http://snf-515788.vm.okeanos.grnet.gr), that is based on validated interactions between miRNAs: mRNAs, we identified 15 miRNA-3p-enriched pathways (Figure 2A-B) and 11 for miRNA-5b (Figure 2A-C). Non-alcoholic fatty liver disease (NAFLD) and human T-cell leukemia virus type 1 (HTLV-1) infection are the most enriched pathways for miRNA-3p and miRNA-5p, respectively. NAFLD has 66 target mRNAs and 23 cyclic miRNA-3p (Figure 2A-C) and HTLV-1 presents a higher amount of cyclic targets (n = 115) and only 15 miRNA-5p (Figure 2A-C). These two pathways are associated with progression of different types of cancer [32,33] and with alterations in the expression of the miRNAs [34,35]. NAFLD is also correlated with circadian disruptions [36], which also cause changes in miRnoma [37]. It is possible that changes in the circadian oscillation of specific miRNAs forms may predispose to NAFLD and HTLV-1,

and its complications, such as the development of cancer. Interestingly, the circadian pathway rhythm (with 16 target genes) was enriched for miRNA-3p (Figure 2B).

Together, the data demonstrate that liver miRNAs have circadian expression induced by the action of CTF, as observed for other classes of genes [14]. In addition, the phase differences observed in the two mature forms of miRNA indicate the action of circadian post-transcriptional mechanisms in their oscillations, since 3p and 5p transcripts have the same precursor molecules (pri-miRNA and pre-miRNA). Interestingly, 16 genes associated with rhythm control are preferentially modulated by miRNA-3p types (Figure 2), indicating that these miRNAs may be of greater relevance to the molecular timing system. Finally, only 6 miRNAs genes have the two mature cyclic forms, indicating the existence of cycling predominance in only one of the two functional molecules. As the miRNA-3p and miRNA-5p of a same miRNA-gene may exhibit different 3'UTR-targets, it is possible that the diferente frequencies of 3p and 5p cyclic miRNAs may vary in different tissues, increasing the complexity of post-transcriptional time adjustments by miRNAs.

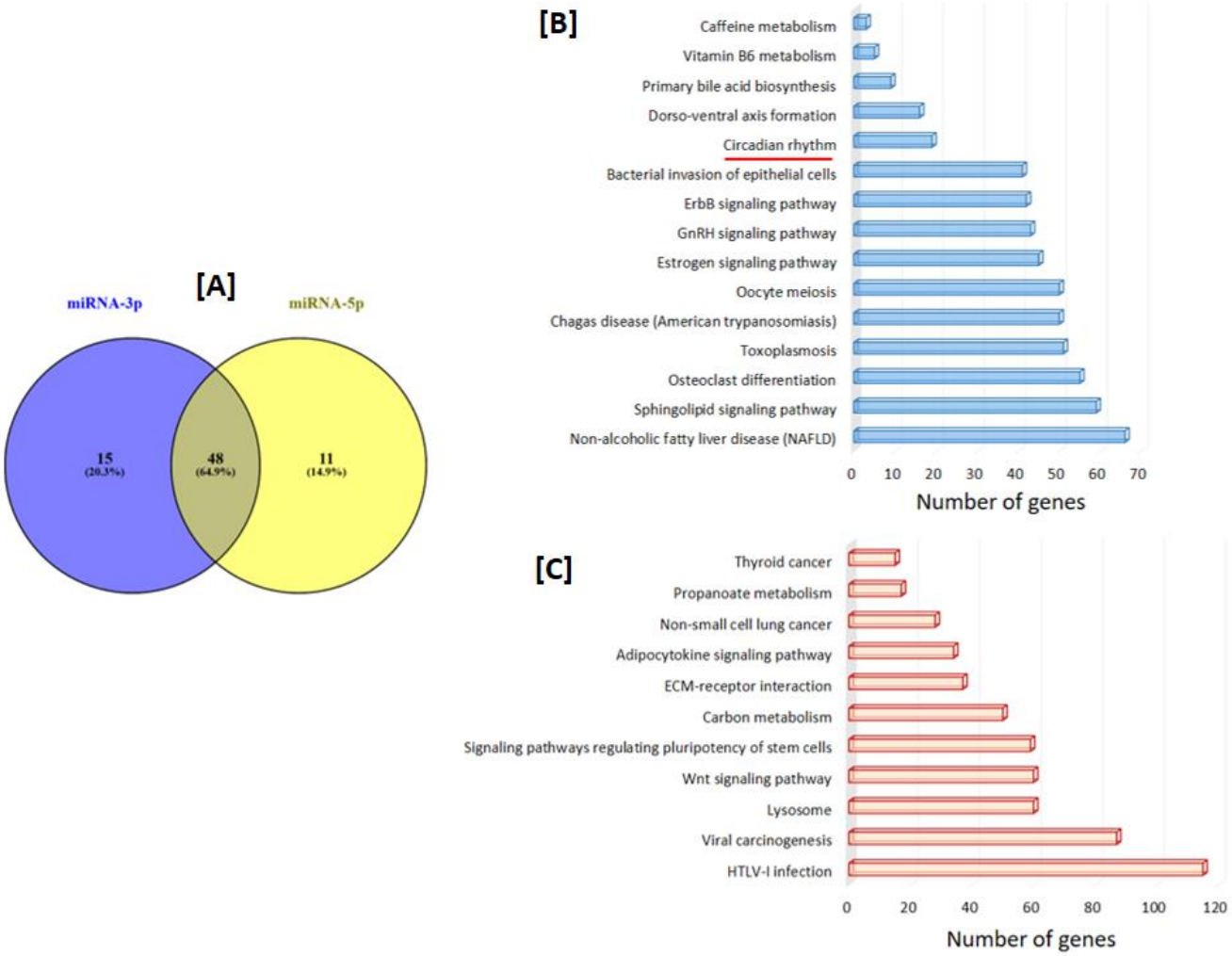

Figure 2. Identification of specific KEGG pathways for the different mature forms of circadian miRNAs. [A] Venn diagram showing the total of unique and shared pathways identified in mirPath v.3. Total target genes in enriched pathways of [B] miRNAs-3p and [C] miRNAs-5p. In [B] the circadian rhythms pathway is highlighted in red.

Different from mRNAs, pre-miRNAs and miRNAs are expressed during the subjective day

As mRNA, mature miRNAs are processed forms of a precursor RNA (pri-miRNAs and pre-miRNAs)[38]. As suggested in the above analysis, rhythmic pri-miRNAs are the result of nascent circadian transcription, whose oscillation is induced by the circadian system described in KOIKE et al., 2012. As discussed in KOIKE et al., 2012, by the post-transcriptional pathways of maturation and degradation, when compared to pre-mRNA, mRNAs have greater variation in their expression phases [14]. However, in comparison with mRNA, mature miRNAs show less dispersion of their acrophases, with greater abundance in the subjective day (Figura 3A-B). We believe that the greater clustering of the miRNAs phases is the result of a smaller number of post-transcriptional events. In addition, as observed for coding genes that oscillate in both pre-mRNA and mRNA [14], miRNAs and corresponding pri-miRNAs have similar phases, suggesting that transcriptional cycles primarily modulate mature miRNA rhythms (Figure 3C).

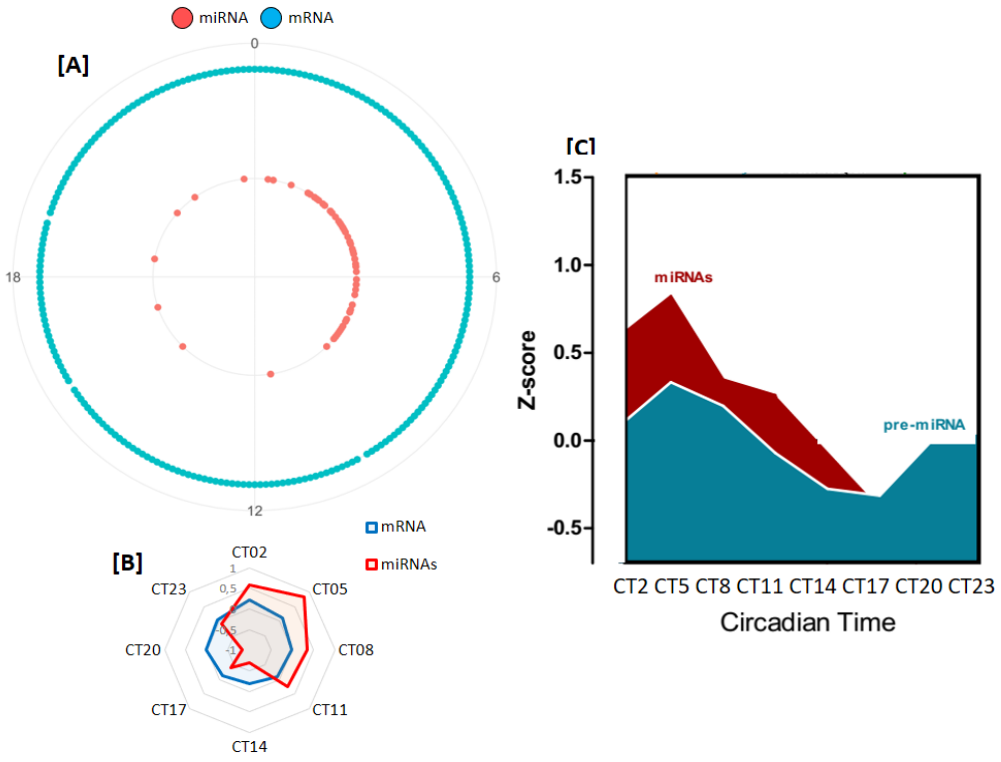

Figure 3 - Pre-miRNAs and miRNAs have elevated levels in the subjective day phase, with less dispersion of acrophases in mature forms, relative to mRNA. Polar plot of acrophases [A] and radial plot of levels in

different CT [B] of cyclic transcripts (84 miRNAs and 1126 mRNA) identified in Yoshitane et al, 2014. [C] Comparison of the oscillation profiles of pre-miRNAs and mature miRNAs. The host mRNA cyclic genes identified in Yoshitane et al, 2014 were considered to be rhythmic pre-miRNAs. The host genes were identified from a list obtained in the miRIAD database (http://bmi.ana.med.uni-muenchen.de/miriad/). The expression data were obtained from RNA-seq (RNAm) and Small RNA-seq (miRNAs) assays performed in YOSHITANE et al., 2014. The data were converted to Z-score to enable visual comparison of different rhythms intensities and amplitudes.

Genes that increase or decrease the amplitudes of their proteins in relation to the mRNA have unique miRNAs, with amplitude adjustment mRNA-phase dependente

Studies of circadian proteomics are recent and have led many advances in the knowledge of oscillation in the different levels of gene expression [7]. Using mass spectrometry ROBLES et al. 2014 quantified 3000 proteins every 3 hours during two circadian cycles [7]. Of these, 186 (6%) presented rhythmic expression [7]. Comparing with RNA-seq data from YOSHITANE et al., 2014, we identified a list of 34 genes with variation also present in the protein (Figure 4). As observed in ROBLES et al. 2014, in relation to the corresponding mRNA, the proteins present a delay of the phases (Figure 4), which for the 34 genes identified has the average of 4.5h (Figure 4). Only 3 proteins show progress of their acrophases in relation to the mRNA (Figure 4C). Interestingly, different from dispersion observed for the total mRNAs set (Figure 3A and 3B), the transcripts of these 34 genes show predominant expression at some stage of the cycle, between CT12-16 (Figure 4). As previously described, it is possible that the differences between mRNA and its proteins result from post-transcriptional events[7]. Interestingly, the expression phase of the 84 miRNAs anticipates those observed for the mRNAs (Figure 4A), suggesting the possible importance of these small molecules for the rhythms of the genes, such as the adjustment of the phases or amplitudes of mRNAs and/or proteins.

As shown in figure 5, in relation to their mRNAs, most proteins show variations in amplitudes, 21 with reduction and only 13 with increase, with fold variation (relative to mRNAs amplitude) between 0.12 to 1.86. (Figure 5A-C). We considered, for comparative analysis, only the following gene groups: (1) with the 10 genes with the greatest reduction in the amplitude of proteins *Mtss1, Acbd5, Dnaja1, Pah, Fkbp4, Hsp90ab1, Hspa8, Crot, Eif5* and *Hsph1* (cutoff 0.5 to 0.12 fold); and (2) 6 genes that have major increase, *Amdhd1, Thrap3, Cgn, Anp32e, Cyp2a5* and *Slc7a2* (with cutoff 1.5 to 1.86 fold).

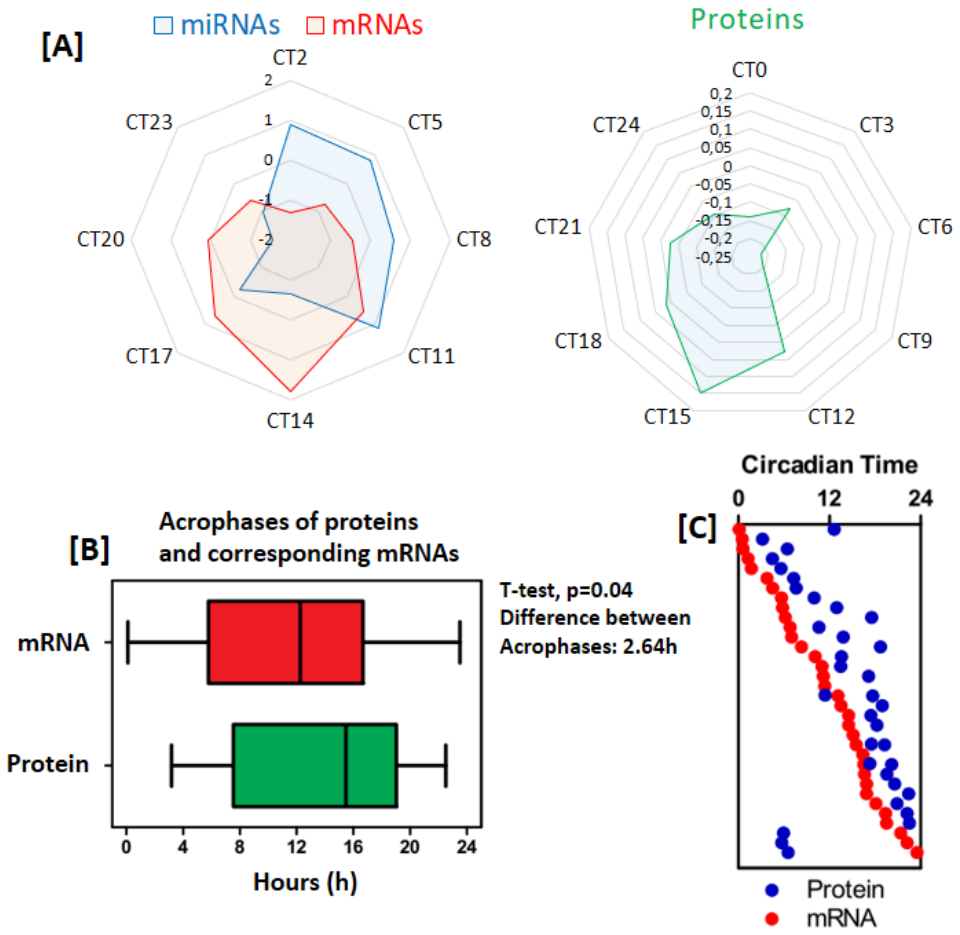

Figure 4- Differences in mRNA and protein phases of genes that oscillate at both expression levels. [A] comparison of the oscillation profiles of all 84 cyclic miRNAs, 34 mRNAs, and 34 proteins. [B] Statistical difference between mRNA and protein acrophases, T-test p <0.05. [C] The acrophase dispersion of mRNA and protein. The transcript expression data were obtained of RNA-seq (RNAm) and Small RNA-seq (miRNAs) assays from the same study (YOSHITANE et al., 2014), and the proteins from ROBLES et al. 2014 mass spectrometry assays. The expression values were converted to Z-score to enable the visual comparison of rhythms of different intensities and amplitudes.

Interestingly, the mRNAs of proteins that reduce the amplitude have greater amplitude than the mRNAs of the group of genes with increase in amplitudes (amplitudes of mRNA (1) vs mRNA (2), T-test, p = 0.0016, figure 5 B-C). Besides that, both mRNAs and proteins possess expression at opposite phases, with phase advancement for the group that increases the protein amplitude (Figure D and E). These data demonstrate that for this set of genes post-transcriptional events adjust the amplitudes of the proteins in relation to the mRNAs.

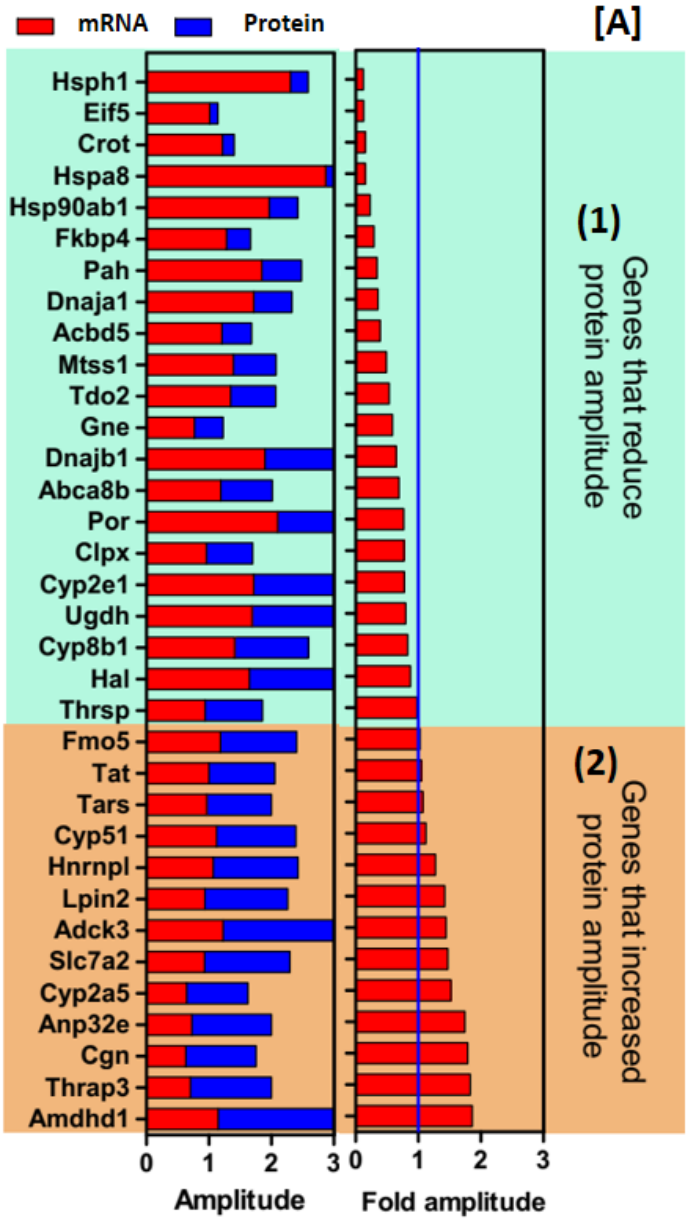
mRNA
Protein
[A]
Hsph1
Eif5
Crot
Hspa8
Hsp90ab1
Fkbp4
Pah
Dnaja1
Acbd5
Mtss1
Tdo2
Gne
Dnajb1
Abca8b
Por
Clpx
Cyp2e1
Ugdh
Cyp8b1
Hal
Thrsp
Fmo5
Tat
Tars
Cyp51
Hnrnpl
Lpin2
Adck3
Slc7a2
Cyp2a5
Anp32e
Cgn
Thrap3
Amdhd1
(1) Genes that reduce protein amplitude
(2) Genes that increased protein amplitude
0 1 2 3
Amplitude
0 1 2 3
Fold amplitude

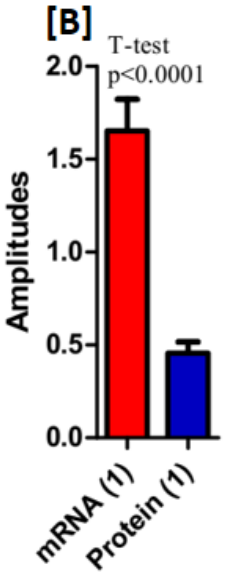
[B]
T-test
p<0.0001
Amplitudes
2.0
1.5
1.0
0.5
0.0
mRNA (1)
Protein (1)

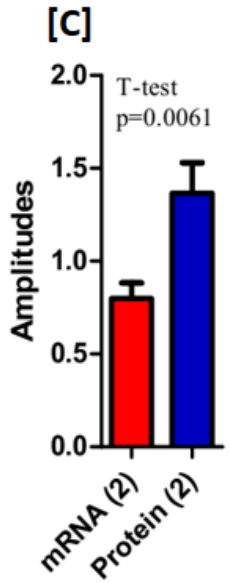
[C]
T-test
p=0.0061
Amplitudes
2.0
1.5
1.0
0.5
0.0
mRNA (2)
Protein (2)

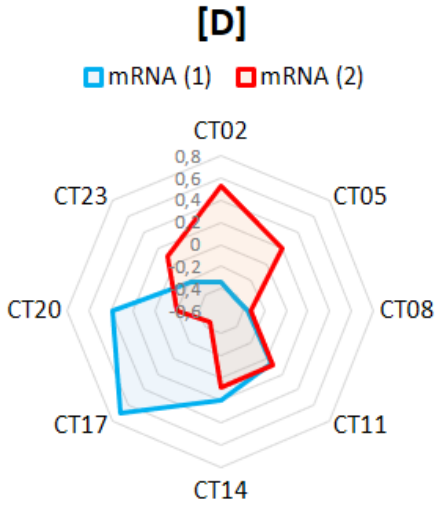
[D]
mRNA (1)
mRNA (2)
CT02
CT05
CT08
CT11
CT14
CT17
CT20
CT23

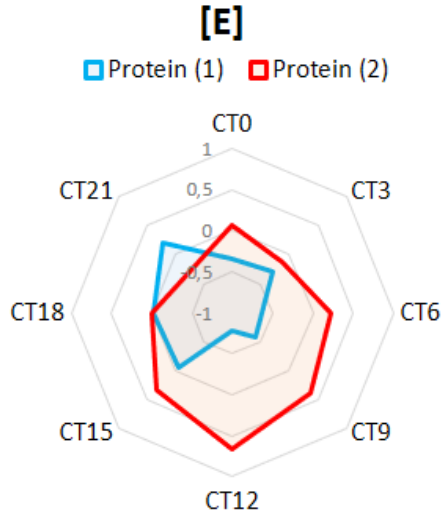
[E]
Protein (1)
Protein (2)
CT0
CT3
CT6
CT9
CT12
CT15
CT18
CT21


[F]
miRNA (1)
miRNA (2)
182
(48.9%)
33
(8.9%)
157
(42.2%)

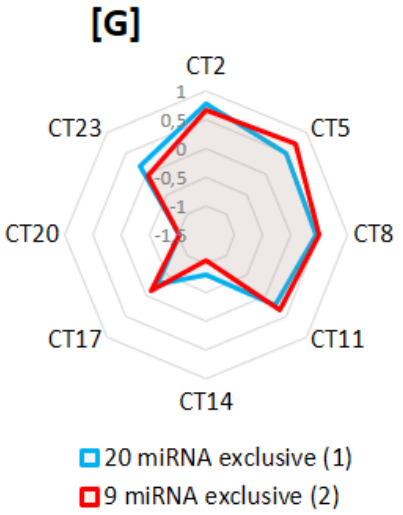
[G]
CT2
CT5
CT8
CT11
CT14
CT17
CT20
CT23
20 miRNA exclusive (1)
9 miRNA exclusive (2)

Figure 5 - Post-transcriptional changes in protein amplitudes and phases. [A] Set of genes with protein amplitude reduced or increased, relative to the corresponding mRNA. Fold change calculated relative to mRNA. The blue line corresponds to the reference value 1 (of the mRNA). Amplitude = Peak to trough ratio (P / T) or the ratio between maximum and minimum expression values. Different amplitudes (mRNA vs Protein) of genes that reduce [B] and increase [C] protein amplitudes. Phase differences between the proteins [D] and mRNA [E] of the different groups. [F] Number of miRNAs that target each set of genes. miRNAs have miRNA:mRNA interaction experimentally identified (Supplementary Table 1). In the radial plot the expression values were converted to Z-score to enable the visual comparison of rhythms of different intensities and amplitudes. The transcript expression data were obtained of RNA-seq (RNAm) assays from YOSHITANE et al., 2014, and the proteins from ROBLES et al. 2014 mass spectrometry assays.

In order to analyze the possible role of miRNAs in modulating the amplitudes of these genes, we used the ChemiRs tool (http://omics.biol.ntnu.edu.tw/) to identify miRNAs with validated interaction with mRNA of genes that alter amplitudes of their proteins. We identified 190 validated miRNAs for genes that increase amplitudes and 215 miRNAs reduce (Figure 5F and Supplementary Table 1). Interestingly, most of the identified miRNAs (91.13%) are group-specific (Figure 5F). From these group-specific miRNAs, 29 have circadian expression in YOSHITANE et al., 2014. 20 are cyclic miRNAs unique to the genes with reduction in protein amplitudes and 9 to the increase gene group. These miRNAs have no variation between their phase of oscillations (Figure 5G) and also no differences between amplitudes (data not shown).

Interestingly, miRNAs have different phase relationships with their mRNAs targets (Figure 6A), which may impact protein amplitudes (Figure 6B). miRNAs unique to genes with reduced protein amplitudes are in antiphase with target mRNAs (Figure 6D). The inverse is observed for the miRNAs of genes with high amplitudes (Figure 6B). The miRNAs and mRNAs of this group exhibit oscillation at a similar time (Figure 6D). The observed oscillations for mRNAs may also result from the action of post-transcriptional mechanisms, as the degradation induced by miRNAs. For this reason, we evaluated the temporal profiles of CTF and RNAPII activity in the promoters of the genes of both groups, in addition to the nascent transcription of their pre-mRNA (Figure 7). CTF have very similar DNA binding rates (Figure 7A). CLOCK-BMAL1, Ser5p and 8WG16 present small differences in DNA binding (Figure 7A-B), which does not explain the large phase divergences observed for pre-mRNAs (Figure 7B). Interestingly, similar to their mRNAs, the pre-mRNAs of the two groups have opposite expression phases (Figure 7B), show that the phase differences of mRNAs of genes that increase and reduce amplitudes may result from a non-core clock transcriptional modulator systems.

The analysis of the liver proteome under light-dark conditions also identifies proteins that in relation to the mRNA reduce the amplitudes [39]. This study demonstrates that only half of the cyclic proteins have rhythmic mRNA [39]. These proteins have phase delay in more than

6 hours in relation to the corresponding transcript [39]. In a free-running condition, Robles et al. 2014 demonstrates that 1/5 of the liver proteins are without rhythm in the mRNA and more than half are also delayed by more than 6h in relation to the mRNA [7]. Analysis of the distribution of proteins throughout the circadian cycle shows that 2/3 of the rhythm liver proteins present phase in subjective night (CT12 to CT24) and 1/3 on subjective day (CT0 to CT12) [7]. These divergences in the rhythms of mRNAs and proteins are also observed in other tissues, including SCN [40]. These findings show that several proteins are circadianally adjusted by post-transcriptional mechanisms.

By disruption of miRNA biogenesis, DU et al., 2014 identified that 30% of the transcriptome has phases and amplitudes adjusted by miRNAs [9]. Interestingly, in liver explants from *Dicer* knockout, the PER2:LUC gene reporter exhibit an a trend in elongation of the period in 41 minutes [9]. Chen et al. 2013 highlight miRNAs as an essential mechanism to generate time delay [8]. In contrast to observed by DU et al., 2014, in CHEN et al 2013, miRNA-deficient animals and cells dramatically shortened the period (by approximately 2 hs)[8]. In miRNA suppressed cells this period change is caused by the rapid translation of PER1-2 proteins [8].

A recent study, Yoo et al. 2017 associates miRNAs with the control of proteins amplitude by translation inhibition [41]. The study demonstrates that in different mammal tissues the absence of the 3'UTR (miRNA target sequence) enhanced amplitude (in 3x fold) and baseline level of PER2:LUC bioluminescence rhythms [41]. The absence of 3'UTR also affects the proteins of the feedback loop (BMAL1 and CRY1) increasing its amplitudes [41]. Importantly, animals without 3'UTR from *Per2* present an elongation of the freerunning periods and present different responses to environmental stimuli (temperature and luminosity)[41]. Yoo et al. 2017 also identify miR-24 as an important modulator of the PER2 protein amplitude [41]. Interestingly, increasing levels of miR-24 (through mimic assays) reduces the amplitude of PER2 [41]. Conversely, the decrease in miRNAs (by the inhibitor method) increases the amplitude of the PER2 clock gene [41]. The authors do not report which mature miR-24 (3p or 5p) target-3'UTR *Per2*. Here, we identified miR-24-3p with binding sites in mRNA of *Per2* (ChemiRs results: predicted in 7 of 10 algorithms and with experimental information in PubMed: 19748357). Analyzing RNA-seq and small RNA-seq data from Yoshitane et al. 2014, we identified that the mRNA of *Per2* and miR-24-3p presented circadian expression in mouse liver (Figure 8). Like the genes that reduce the amplitude in relation to their mRNAs (Figure 6A), the *Per2* transcript and miR-24-3p oscillate in opposite phases (Figure 8).

The findings of Yoo et al. 2017 corroborate our hypothesis of reducing protein amplitude by miRNAs that present phase opposite to target mRNAs (Figure 8). Interestingly, our analyzes demonstrate that the different adjustments (increase or decrease) on proteins amplitudes are dependent to the mRNAs oscillations. To our knowledge, this is the first analysis on the circadian function of miRNAs dependent on the transcription phase of the target gene and may help to better understand the role of miRNAs in circadian adjustment. However, further studies should be performed to validate these findings.

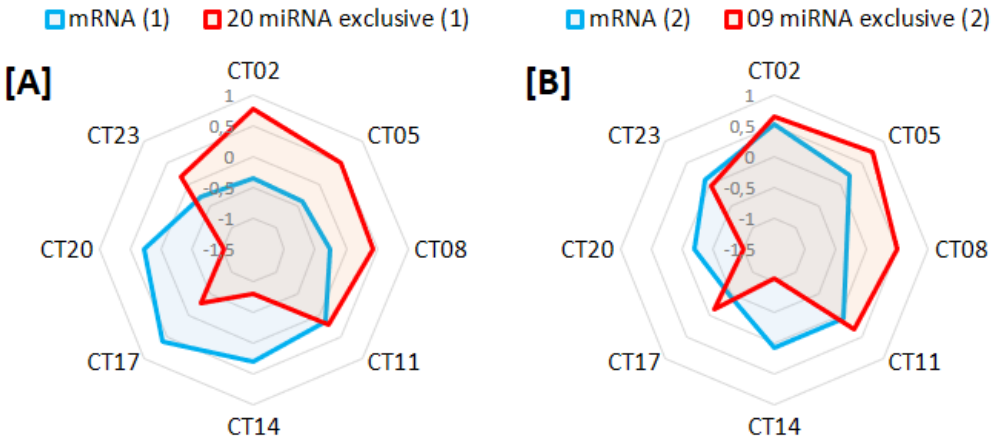

Figure 6- Different phase relations between miRNAs and mRNAs. [A-B] Set of miRNAs identified as modulators of genes with increase or reduction of protein amplitudes. Comparison between the expression phases of the miRNAs and target mRNAs of groups of genes that reduce [A] and amplify amplitudes [B]. The transcript expression data were obtained of RNA-seq (RNAm) and Small RNA-seq (miRNAs) assays from the same study (YOSHITANE et al., 2014).

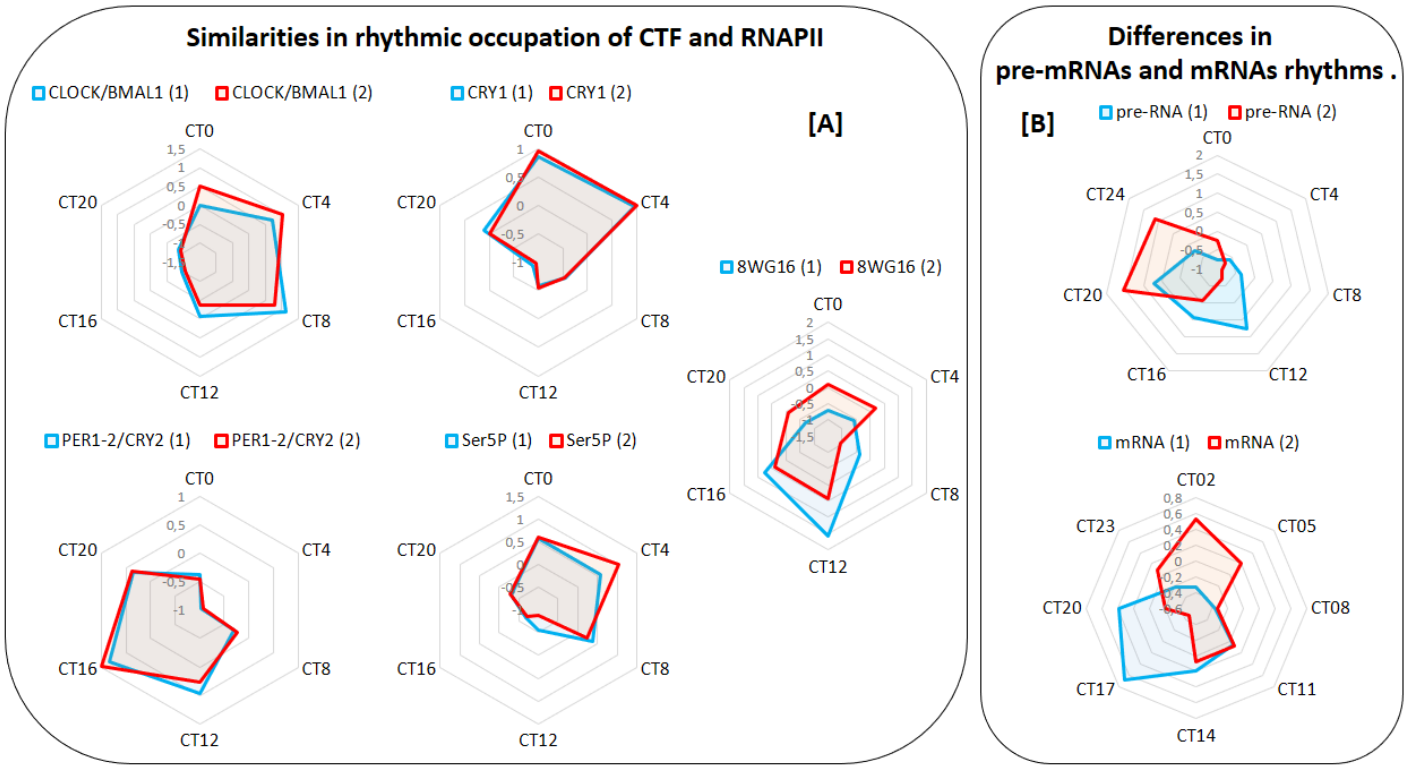

Figure 7- Genes with differences in protein amplitudes have similar transcriptional control and corresponding phases between their pre-mRNA and mRNA. [A-B] Circadian activity of CTF and RNAPII. [C] Rhythmic oscillation of pre-mRNAs and mRNAs. The oscillation profiles are shown in both radial and line graphics. Both rhythm occupancy data of FTC and oscillation of pre-mRNAs were obtained in [14]. The mRNA expression data were obtained from Seq RNA assays of YOSHITANE et al., 2014. Data were converted to Z-score to enable visual comparison of rhythms of different intensities and amplitudes.

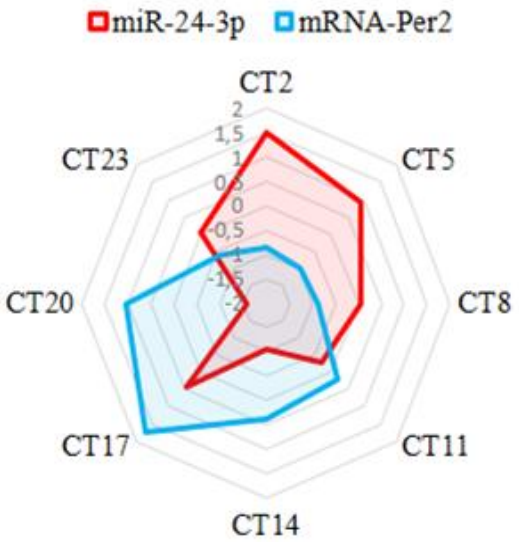

Figure 8 - As miRNAs that interact with mRNAs of genes that reduced protein amplitude, the miR-24 validated in Yoo, *et al.* 2017 also presents opposite phase to *Per2* mRNA. The data were converted to Z-score to enable the visual comparison of rhythms of different intensities and amplitudes. The transcript expression data were obtained of RNA-seq (mRNA) and Small RNA-seq (miRNAs) assays from the same study (YOSHITANE et al., 2014).

Conflict of interest statement

The author (s) declared no potential conflicts of interest with respect to the research, authorship, and/or publication of this article

Supplementary Figure:

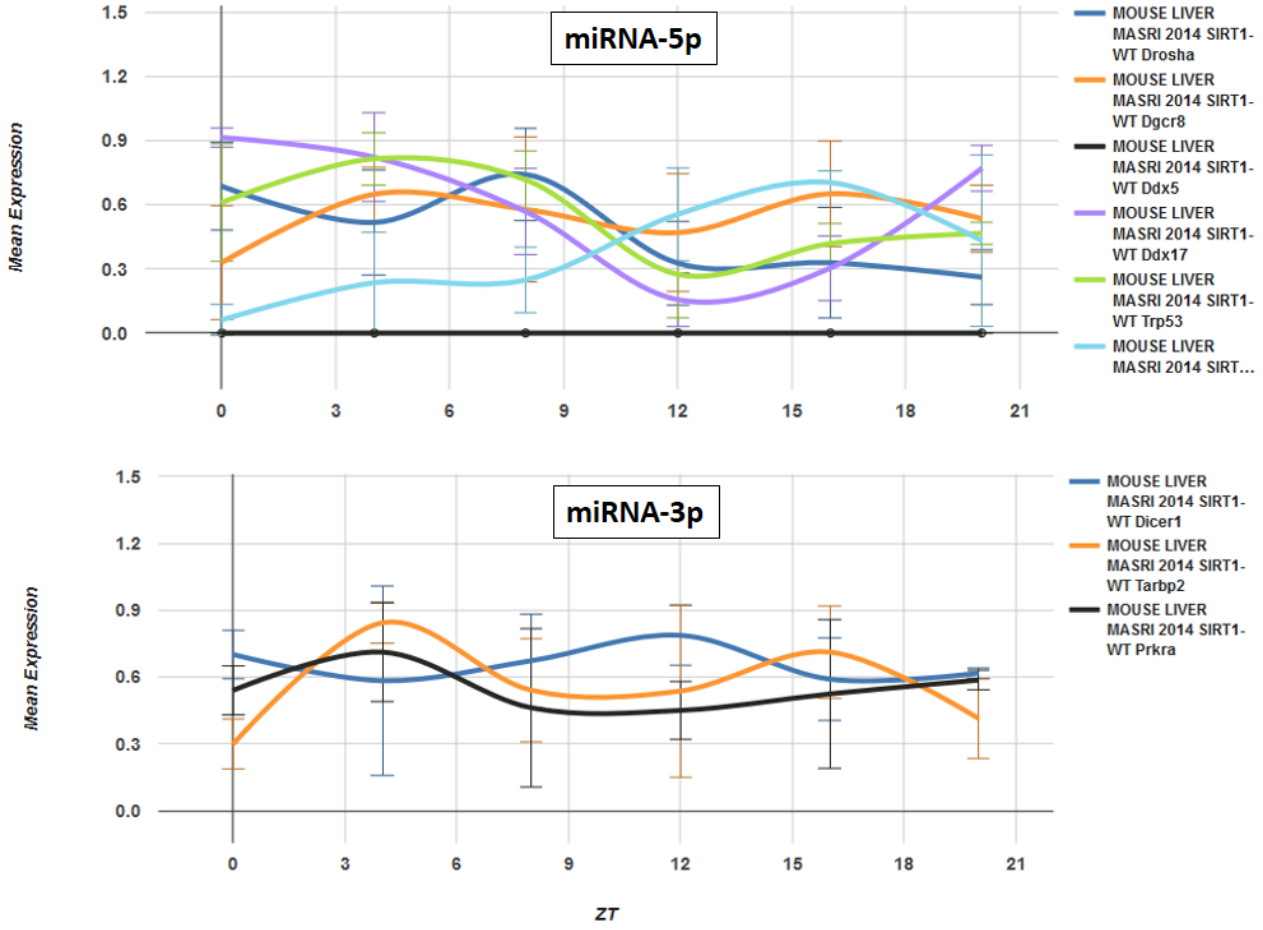

Supplementary Figure 1- Daily variations in the gene transcript expressions involved with miRNA-3p and miRNA-5p maturations. Source of data: CircadiOmics (http://circadiomics.ics.uci.edu/).

References

1. Hughes, M. E. *et al.* Guidelines for Genome-Scale Analysis of Biological Rhythms. *J. Biol. Rhythms* **32,** 380–393 (2017).

2. Bhargava, A., Herzel, H. & Ananthasubramaniam, B. Mining for novel candidate clock genes in the circadian regulatory network. *BMC Syst. Biol.* **9,** 1–14 (2015).

3. Brown, L. A. *et al.* Meta-analysis of transcriptomic datasets identifies genes enriched in the mammalian circadian pacemaker. *Nucleic Acids Res.* **45,** 9860–9873 (2017).

4. Pizarro, A., Hayer, K., Lahens, N. F. & Hogenesch, J. B. CircaDB: A database of mammalian circadian gene expression profiles. *Nucleic Acids Res.* **41,** 1009–1013 (2013).

5. Ceglia, N. *et al.* CircadiOmics : circadian omic web portal. *Nucleic Acids Res.* **46,** 1–6 (2018).

6. Mauvoisin, D. *et al.* Circadian clock-dependent and -independent rhythmic proteomes implement distinct diurnal functions in mouse liver. *Proc. Natl. Acad. Sci.* **111,** 167–172 (2014).

7. Robles, M. S., Cox, J. & Mann, M. In-Vivo Quantitative Proteomics Reveals a Key Contribution of Post-Transcriptional Mechanisms to the Circadian Regulation of Liver Metabolism. *PLoS Genet.* **10,** (2014).

8. Chen, R., Alessandro, M. D. & Lee, C. Article miRNAs Are Required for Generating a Time Delay Critical for the Circadian Oscillator. *Curr. Biol.* **23,** 1959–1968 (2013).

9. Du, N., Arpat, A. B., Matos, M. De & Gatfield, D. MicroRNAs shape circadian hepatic gene expression on a transcriptome-wide scale. 1–29 (2014). doi:10.7554/eLife.02510

10. Friedman, R. C., Farh, K. K. H., Burge, C. B. & Bartel, D. P. Most mammalian mRNAs are conserved targets of microRNAs. *Genome Res.* **19,** 92–105 (2009).

11. Zhang, R., Lahens, N. F., Ballance, H. I., Hughes, M. E. & Hogenesch, J. B. A circadian gene expression atlas in mammals: Implications for biology and medicine. *Proc. Natl. Acad. Sci.* **111,** 16219–16224 (2014).

12. Vollmers, C., Schmitz, R. J., Nathanson, J., Yeo, G. & Joseph, R. NIH Public Access. **16,** 833–845 (2013).

13. Yoshitane, H. *et al.* CLOCK-Controlled Polyphonic Regulation of Circadian Rhythms through Canonical and Noncanonical E-Boxes. *Mol. Cell. Biol.* **34,** 1776–1787 (2014).

14. Koike, N. *et al.* Transcriptional architecture and chromatin landscape of the core circadian clock in mammals. *Science (80-.).* **338,** 349–354 (2012).

15. Na, Y. J. *et al.* Comprehensive analysis of microRNA-mRNA co-expression in circadian rhythm. *Exp. Mol. Med.* **41,** 638–647 (2009).

16. Figueredo, D. D. S., Barbosa, M. R., Gitaí, D. L. G. & De Andrade, T. G. Predicted microRNAs for mammalian circadian rhythms. *J. Biol. Rhythms* **28,** 107–116 (2013).

17. Seok, H., Ham, J., Jang, E. & Chi, S. W. MicroRNA Target Recognition: Insights from Transcriptome-Wide Non-Canonical Interactions. *Mol. Cells* **39,** 375–381 (2016).

18. Zhang, Y., Xie, S. J., Xu, H. & Qu, L. H. CLIP: viewing the RNA world from an RNA-

protein interactome perspective. *Sci. China Life Sci.* **58,** 75–88 (2015).

19. Haecker, I. & Renne, R. HITS-CLIP and PAR-CLIP Advance Viral MiRNA Targetome Analysis. *Crit. Rev. Eukaryot. Gene Expr.* **24,** 101–116 (2014).

20. Hinske, L. C. hristia. *et al.* miRIAD-integrating microRNA inter- and intragenic data. *Database (Oxford).* **2014,** 1–9 (2014).

21. Su, E. C. *et al.* ChemiRs : a web application for microRNAs and chemicals. *BMC Bioinformatics* 1–10 (2016). doi:10.1186/s12859-016-1002-0

22. Vlachos, I. S. *et al.* DIANA-miRPath v3 . 0 : deciphering microRNA function with experimental support. **43,** 460–466 (2015).

23. Vlachos, I. S. *et al.* DIANA-TarBase v7.0: Indexing more than half a million experimentally supported miRNA:mRNA interactions. *Nucleic Acids Res.* **43,** D153–D159 (2015).

24. Li, S. & Zhang, L. Circadian Control of Global Transcription. *Biomed Res. Int.* **2015,** (2015).

25. Wang, H. *et al.* Oscillating primary transcripts harbor miRNAs with circadian functions. *Sci. Rep.* **6,** 1–13 (2016).

26. Ro, S., Park, C., Young, D., Sanders, K. M. & Yan, W. Tissue-dependent paired expression of miRNAs. **35,** 5944–5953 (2007).

27. Granados-López et al. Use of mature miRNA strand selection in miRNAs families in cervical cancer development. *Int. J. Mol. Sci.* **18,** (2017).

28. Meijer, H. A., Smith, E. M. & Bushell, M. Regulation of miRNA strand selection: follow the leader? *Biochem. Soc. Trans.* **42,** 1135–1140 (2014).

29. Suzuki, H. I. & Miyazono, K. Emerging complexity of microRNA generation cascades. *J. Biochem.* **149,** 15–25 (2011).

30. Davis-Dusenbery, B. N. & Hata, A. Mechanisms of control of microRNA biogenesis. *J. Biochem.* **148,** 381–392 (2010).

31. Yan, Y. *et al.* Dicer Expression Exhibits a Tissue-Specific Diurnal Pattern That Is Lost during Aging and in Diabetes. **8,** 1–11 (2013).

32. Régnier, M., Polizzi, A., Guillou, H. & Loiseau, N. Sphingolipid metabolism in non-

alcoholic fatty liver diseases. *Biochimie* (2018). doi:10.1016/j.biochi.2018.07.021

33. Tagaya, Y. & Gallo, R. C. The Exceptional Oncogenicity of. **8,** 8–11 (2017).

34. Moles, R., Nicot, C. & City, K. The Emerging Role of miRNAs in HTLV-1 Infection and ATLL Pathogenesis. 4047–4074 (2015). doi:10.3390/v7072805

35. Su, Q., Kumar, V., Sud, N. & Mahato, R. I. Role of MicroRNAs in the pathogenesis and treatment of progressive liver injury in NAFLD and liver fibrosis. *Adv. Drug Deliv. Rev.* (2018). doi:10.1016/j.addr.2018.01.009

36. Bernsmeier, C., Weisskopf, D. M., Pflueger, M. O. & Mosimann, J. Sleep Disruption and Daytime Sleepiness Correlating with Disease Severity and Insulin Resistance in Non-Alcoholic Fatty Liver Disease : A Comparison with Healthy Controls. 1–16 (2015). doi:10.1371/journal.pone.0143293

37. Kochan, D. Z. *et al.* Circadian disruption-induced microRNAome deregulation in rat mammary gland tissues. **2,** (2015).

38. Ha, M. & Kim, V. N. Regulation of microRNA biogenesis. *Nat. Rev. Mol. Cell Biol.* **15,** 509–524 (2014).

39. Mauvoisin, D. *et al.* Circadian clock-dependent and -independent rhythmic proteomes implement distinct diurnal functions in mouse liver. **111,** 167–172 (2014).

40. Deery, M. J. *et al.* Report Proteomic Analysis Reveals the Role of Synaptic Vesicle Cycling in Sustaining the Suprachiasmatic Circadian Clock. 2031–2036 (2009). doi:10.1016/j.cub.2009.10.024

41. Yoo, S.-H. *et al. Period2* 3′-UTR and microRNA-24 regulate circadian rhythms by repressing PERIOD2 protein accumulation. *Proc. Natl. Acad. Sci.* 201706611 (2017). doi:10.1073/pnas.1706611114

42 Umemura, Y. *et al.* Involvement of posttranscriptional regulation of *Clock* in the emergence of circadian clock oscillation during mouse development. *Proc. Natl. Acad. Sci.* 201703170 (2017). doi:10.1073/pnas.1703170114

43 Yan, Y. *et al.* Dicer Expression Exhibits a Tissue-Specific Diurnal Pattern That Is Lost during Aging and in Diabetes. **8,** 1–11 (2013).

ARTIGO 2: miR 29b modulates the circadian period in human cells.

Abstract

The inactivation of miRNA biogenesis confirmed the importance of miRNAs in the post transcriptional and translational control of circadian rhythms. However, only 11 miRNAs were validated as important for the amplitude or period adjustment. For this reason, the development of a method that efficiently identifies specific clock miRNAs is critical. In this study, we aimed to identify candidates miRNAs for the circadian timekeeper system through the systematization of data from circadian high-throughput experiments assay (HTA), miRNAs predicted targets and experimentally validated miRNA:mRNA interactions. In this study, we present 152 miRNAs to the clock system ranked through by score created by sum of different experimental evidences obtained from systematization of data. miR-29b-3p and miR-23b-3p are the most relevant miRNAs from list, with equal score (value: 22), and with circadian function confirmed in rhythm of human U2OS PER2:Luciferase (PER2:LUC) cells. Here, we demonstrate at first time that these two miRNAs importantly modulate the amplitude and period of endogenous rhythm. Increased levels of miR-29b-3p and miR-23b-3p by mimic approach reduce the amplitude of gene reporter PER2:LUC. miR-23b-3p lengthen the circadian period by 2.20h, a more significant effect than the two most famous miRNAs (miR-219a-1-3p and miR-132-3p), used herein as positive circadian controls. miR-29b-3p has an effect in period not seen before, a reduction of -2.93 h. Interestingly, this miRNA also induces changes in cellular morphology. miR-29b-3p and miR-23b-3p also reduce the amplitude of the PER2:LUC rhythm. The qPCR experiment show that miR-29b-3p alter the expression of 8 clock genes and *Tef*, an important clock-controlled transcription factor associated with output of the rhythmic signal. Of the 6 genes identified as miR-29b-3p targets (*Ter*, *Per1*, *Per2*, *Per3*, *Rora* and *Bhlhe40*), only *Bhlhe40* did not change their levels. The core clock genes with more significant effects are the paralogues genes *Per1*, *Per2* and *Per3*. *Per1-3* genes reduce expression by less than half (-0.51 ± 0.03, mean ± SD). The *Tef* gene was the most affected target, with the lowest expression reduction (-0.71). These qPCR results suggest that the circadian period shortening may result from the simultaneous reduction of the three Pers genes. And that *Tef* modulating by miR-29b-3p can affect the clock output. Furthermore, miR-29b-3p possesses exclusive targets that control important pathways for the global control of expression (chromatin organization and regulation of transcription by RNAPII) and pathways associated with cellular morphology (extracellular matrix and cell differentiation control). In this study, we present a promising strategy for the identification of clock miRNAs and show that the two top-candidate miRNAs (miR-29b-3p and miR-23b-3p) are relevant for the maintenance of the endogenous circadian period. In addition, we present new information about the miR-219a-1-3p and miR-132-3p, that also regulated the period of molecular rhythm.

Key words: Circadian, Clock genes, U2OS, Luciferase, miRNA, Amplitude, Period.

Introduction

In mammals, circadian rhythms are present in different tissues [1,2] and are adjusted by a small group of neurons from suprachiasmatic nucleus (SCN)[1,2]. SCN adjust their activity to the environment light, generating a signal that orchestrates the rhythms of the other regions of the body [1,2]. However, the NSQ is not fundamental to generate the rhythms of the clocks in peripheral tissues, only adjust them in relation to the environmental cues [3,4]. As SCN the different tissues present an autonomous rhythm, even when kept in cell culture, without systemic and environmental cues [5–7]. The autonomies of SCN and peripheral tissues result of the action of a common genetic system, the molecular clock, composed of a set of genes called clock genes[8]. The clock genes generates circadian rhythms in transcriptional level [9] and are present different organisms [10]. In mammals it has been demonstrated the clock genes possess robust circadian oscillation that in vivo and in different tissues [11,12]. The proteins from clock gene act as negative or positive circadian transcription factors (CTF) that interact in a feedback loop system and induces oscillation in the transcription of several genes, called clock-controlled genes (CCG)[13]. Although different genes are involded, this feedback loop system is common in different species and is important for the maintenance of cellular physiology because CCGs are associated with the rhythmic control of various biological processes[13].

Interestingly, studies have shown that many mRNA and protein oscillations are independent of CTF and that post-transcriptional/and translational regulation adjust rhythms in these genes[14–16]. Two Dicer Knockout confirm the importance of miRNAs in post-transcriptional and translational control of the rhythmic expression, including clock genes[16,17]. Because miRNAs affect 60% of the coding genes [18], it is possible that the Dicer Knockout model compromises basal cell pathways impacting the analyzes over a long time. In fact, Chen et al. 2013 reports that the mice die 1-5 weeks after Dicer Knockout [17]. It is possible that assays for the validation of individual miRNAs are also very informative. To date, few studies have identified miRNAs that modulate the period and amplitude of circadian rhythms [17,19–23]. miR-219, miR-142, miR-494 lengthens the circadian clock period, while miR-17, miR-24, miR-29a, miR-30a, miR-192, miR-194 and miR-155 reduce the period circadian [17,19–23]. miRbase presents 1978 mature miRNAs for mouse miRNA. However, the aforementioned circadian studies present only 11 (0.55% of 1978) miRNAs validated as important for the clock. The identification of clock miRNAs (miRNAs important for period adjustment, amplitude or maintenance of circadian rhythmicity) is critical for understanding the molecular timing machinery. For this, new studies are needed. A key point in the study of miRNAs is to identify

which of these small transcripts to test. Generally, the studies start from a list of target genes to identify candidate miRNAs by algorithm predictions [24]. Through bioinformatics, we have previously identified 69 clock candidates miRs equally predicted in 3 programs to control clock genes [24].

With a new approach, the present study aimed to identify miRNAs important for the clock by systematization of bioinformatics results (from FIGUEREDO et al., 2013), HTA and interactions miRNA: mRNA experimentally verified (from DIANA-TarBase v7.0). In this article we present a list of clock miRNAs candidates, with the two most relevant miRNAs validated in an important circadian study model (U2OS PER2:LUC).

Materials and methods

The systematization analysis of HTA experiments and identification of clock miRNAs

For the identification of candidate miRNAs, we performed the systematization analysis from 3 circadian studies of Chip-seq (KOIKE et al., 2012; WANG, H. et al., 2016b; YOSHITANE et al., 2014), 4 of RNA-seq [25–28], experimentally supported miRNA:mRNA interactions (from *DIANA-TarBase v7*.0)(VLACHOS et al., 2015), and a study of bioinformatics (FIGUEREDO et al., 2013). We generated a score for each identified miRNA, which results from the sum of: (1) confirmed circadian expression in different studies of RNA-seq, computing by study, for the host gene, pre-miRNA, or mature miRNA; (2) circadian modulation by different CTF (computing by transcription factor and per study); (3) number of predicted clock genes (computing the number of programs, in a total of 3 and also total of target genes); (4) total of validated clock genes (with extra punctuation for experimental information of direct interaction between miRNA: mRNA). In addition, we considered an extra score for clock genes equally predicted (in FIGUEREDO et al., 2013) and validated (in *DIANA-TarBase v7*.0). As targets, we selected 14 clock genes, which are: *Bhlhe40 Bhlhe41, Bmal1, Clock, Cry1, Cry2, Csnk1d, Csnk1e, Nr1d1, Nr1d2, Per1, Per2, Rora,* and *Rorb*. The identified miRNAs were ranked based on the total score. For us, the top list miRNAs were considered with greater relevance to the circadian system, and the two best candidates were selected for validation in U2OS cells.

U2OS PER2:LUC reporter

The U2OS Per2:Luciferase (Per2:Luc) reporter cell lines used in the study was developed by ZHANG et al., 2009 (ZHANG et al., 2009). The mirVana ™ miRNA Mimics system (Invitrogen, USA) was selected to increase the miRNAs cellular levels. mirVana ™

miRNA Mimics are small modified double stranded RNA molecules, designed to enable the functional analysis of miRNAs of interest after increasing their levels and activity. MirVana ™ miRNA Mimic Negative Control (or scramble) is a molecule chemically similar to mimic, however, with no known effects on different cell lines and human tissues. Scrambles are used as a negative control of transfection. U2OS cells were cultured in DMEM medium (Dulbecco's modified Eagle's medium) supplemented with 10% fetal bovine serum and the antibiotic dexamethasone (0.1uM, Sigma). Initially, 500 µl Opti-MEM and 3.75 µl mimics miRNA (15 nM) were mixed. An OPTI-MEM: Lipofectamine RNAiMAX solution was prepared in 15 mL conical tubes in the 500 ul: 7.5uL ratio, after mixing 4 mL of OPTI-MEM + 60 µL of Lipofectamine RNAiMAX. Invitrogen Lipofectamine RNAiMAX Transfection Reagent (Invitrogen) is a reagent that efficiently releases mimics in intracellular medium. Opti-MEM, on the other hand, allows the cells to be maintained under reduced serum conditions, which affect the efficiency of the lipofectamine transfection procedure. Better buffered than DMEM, Opti-MEM possesses a greater amount of HEPES and sodium bicarbonate, increasing the viability of the cells during transfection procedures. With the aid of a multi-channel pipette, 500 µL of the OPTI-MEM: Lipofectamine RNAiMAX blend were dispensed into the wells with diluted mimics (500 µL Opti-MEM). Opti-MEM allows cells to be maintained under reduced serum conditions, which affect the efficiency of the lipofectamine transfection procedure. Better buffered than DMEM, Opti-MEM possesses a greater amount of HEPES and sodium bicarbonate, increasing the viability of the cells during transfection procedures. With the multi-channel pipette, 500 µL of the OPTI-MEM: Lipofectamine RNAiMAX blend were dispensed into the wells with diluted mimics (500 µL Opti-MEM). In cell culture hood, the plates were incubated at room temperature for 20 minutes. Prior to their addition, the U2OS cells were washed in PBS and trypsinised. Thereafter, resuspended in 5 mL of DMEM (1X). 10 µL of cells in DMEM (1X) were used for counting the cells in hemocytometer, later diluted at 200,000 cells / mL. 750µl of the diluted cell solution were mixed to 500 µL of OPTI-MEM: Lipofectamine RNAiMAX: mimic. Finally, in 96-well plates, 250µL of the final solution (OPTI-MEM / Lipofectamine RNAiMAX / mimics / U2OS cells) were dispensed and incubated at 37 ° C / 24 hours. During this period cells were inspected and viability checked. One day after transfection, without disturbing the cells, the medium was vacuum aspirated. To detect the luminescence data from each well, 250ul of the U2OS Lumicycle medium (U2OSLM), formulated after mixing of 50mL Lumicycle media, 50ul of Forskolin and 100ul Luciferin, were added. The plates were sealed with optical adhesive, inserted into Lumicycle equipment

(Actimetrics, USA). The analysis of the activity rhythm of the Per2: Luc reporter gene in U2OS cells was performed with waveclock, an R function that reconstructs the modal frequencies of the luminescence data through a wavelet decomposition, which allows the calculation of the period and amplitude of oscillation (http://sgdp.iop.kcl.ac.uk/tprice/software.html).

Real-time PCR (qPCR)

Cells transfected with mimic and scramble were isolated using vacuum manifold and RNA extracted with Direct-zol RNA kit (Zymo research) follow manufacturer's protocol. RNA concentration was measured in NanoDrop (ThermoFisher) and 250 ng RNA were used for cDNA synthesis with qScript cDNA MasterMix (Quantabio). The cDNA was diluted (1:10) to the qPCR reactions. 11 clock genes (*Gapdh, Per1, Per2, Per3, Cry1, Cry2, Arntl, Arntl2, Tef, Rora, Rorc, Bhlhe40* e *Nr1d1*) were evaluated using the TaqMan system (Thermo Fisher) in QuantStudio Real-Time PCR (Thermo Fisher). The analyzes were done in triplicates (3 groups of cells / per mimic and scramble group) and in $2^{-\Delta\Delta \text{Cicle Threshold}}$. Reverse transcription reactions for cDNA synthesis were performed via miRscript RT II (Qiagen, catalog 218161). Concentrations of 531ng / uL, 524ng / uL, 371ng / uL, 361ng / uL and 773ng / uL were obtained for the samples 04hs, 10hs, 16hs and 22hs, respectively. With an average purity of 1.55 at 260nm/280nm.

Target genes identification, pathways and networks analysis.

We use the web application ChemiRs (http://omics.biol.ntnu.edu.tw/ChemiRs/)[29] to identify target genes to miRNAs tested in the functional assay (miR-29b-3p, miR-23b-3p, miR-132-3p and miR-219a-1-3p). In ChemiRs we considered only targets with miRNA-mRNA interaction reported in the literature (mostly non-circadian studies). The pathway analysis were performed with Metascape (metascape.org) (from a list of unique miR-29b-3p target genes). The network analyzes were performed on miRNet (network-based visual analysis of miRNAs and targets)[30] or in Metascape.

Statistical analyzes and graphical representations

The t-test was used to compare the mean of different groups, with $p < 0.05$. Graphpad Prism was used to generate graphs of qPCR expression data and U2OS PER2:LUC rhythm. Polar plot and radial graphs were generated in R functions. The Clock-miRNAs network illustration was made in miRNet and downloaded directly from the web portal.

Results and discussion

Identification of candidate miRNAs for control of mammalian clock genes

Considering the high numbers of mammalian miRNAs and their potential to regulate different targets, the identification of miRNAs modulators of clock genes (Clock microRNAs) may help to understand the complexity of the system and associated diseases.

miRNet networks analysis is based on miRNAs and targets with experimentally identified physical interaction (FAN et al., 2016). Using miRNet, we identified a network of different miRNAs and 12 clock genes (Figure 1). Interestingly, clock genes present clusters of unique miRNAs, with few shared miRNAs, suggesting synergistic (various miRNAs) and specific regulation (Figure 1). *Cry2*, *Per1* and *Rora* are highlighted by the high number of miRNA-interactions (Figure 1). It is possible that the combined binding of different miRNAs in the 3'UTR clock gene may differently adjust the oscillation of the clock mRNAs and proteins.

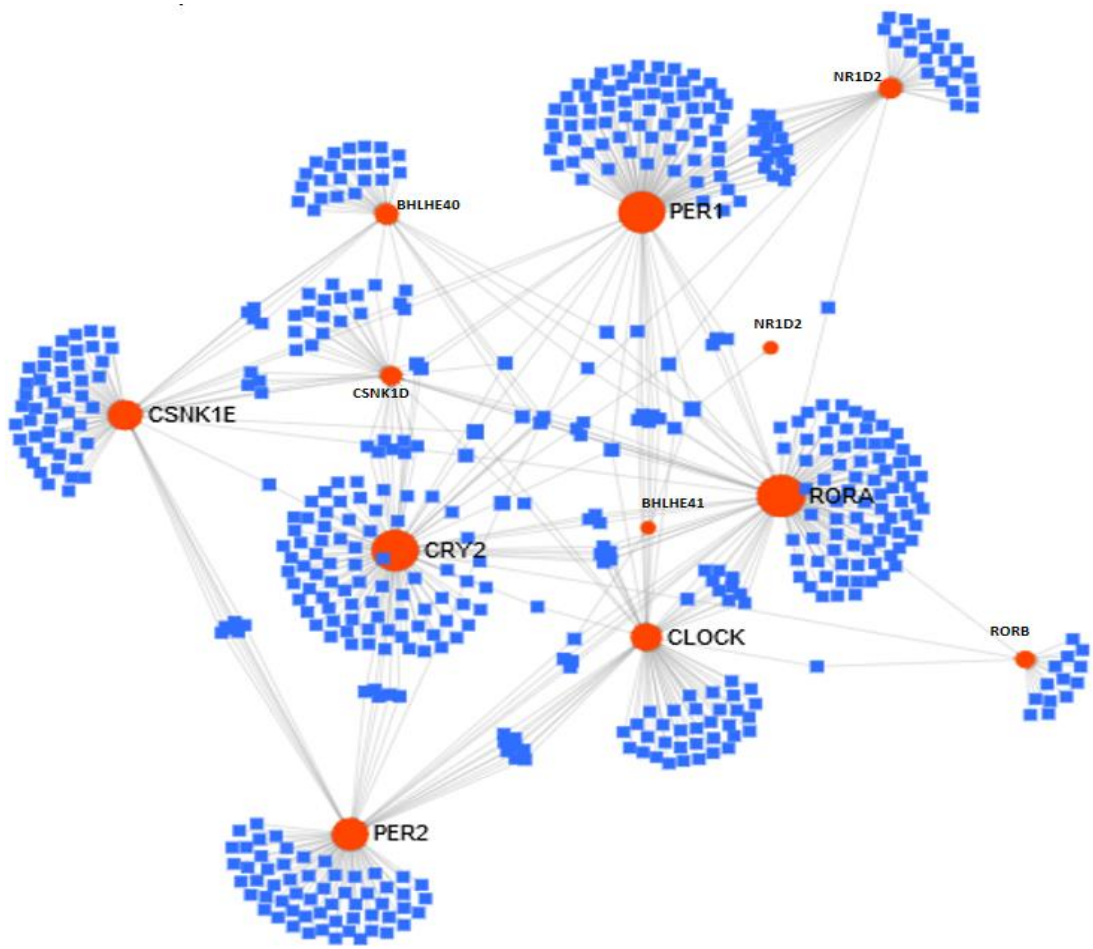

Figure 1 - Clock-miRNAs network. Each blue square corresponds to a miRNA experimentally identified in miRNet (www.mirnet.ca) and circles in oranges to the target clock genes. The lines at different points correspond to the miRNA-target interactions. Large circles have larger numbers of miRNAs-interactions.

In conjunction with prediction algorithms, validated miRNA:mRNA interaction potentiate the identification of genes important to the circadian system. Here, we systematized data from 3 circadian studies of Chip-seq [9,26,27], 4 of RNA-seq [25–28], a bioinformatics study [24] and interaction data obtained in DIANA Tarbase V.7[31]. For each identified miRNA was created a score that is the sum of circadian evidence (or experimental data): (1) confirmed circadian expression in different studies of RNA-seq, computing by study, for the host gene, pre-miRNA, or mature miRNA; (2) circadian modulation by different CTF (computing by transcription factor and per study); (3) number of predicted clock genes (computing the number of programs, in a total of 3 and also total the number of target genes); (4) total validated clock genes (with greater weight for experimental information of direct interaction between miRNA: mRNA). In addition, we considered an extra score for clock genes equally predicted and validated. As targets, we selected 14 clock genes, which are: *Bhlhe40 Bhlhe41, Bmal1, Clock, Cry1, Cry2, Csnk1d, Csnk1e, Nr1d1, Nr1d2, Per1, Per2, Rora* and *Rorb.*

With the result, we identified a list of 152 candidate miRNAs, with scores that ranged from 22 to 1 (Supplementary Table 1). The genes miR-23b, miR-29b-1, miR-340, miR-122, miR-27b, miR-26b, miR-101a, miR-30e, miR-181a-2, miR-30c, miR-24-1, miR-17, miR-30d, miR-29a, miR-let-7a-1, miR-30a, miR-21a, miR-103-2, miR-25 and miR-22 are the 20 miRNAs with the highest score (Supplementary Table 1). Of these, only 7 have any previous association with circadian rhythms. miR-23b and miR-29b-1 occupy the first position in the list, with the same score of 22 (Supplementary Table 1). miR-450b is the last one on the list, with a score of 0 (Supplementary Table 1). miR-23b and miR-29b-1 can be controlled by circadian system feedback loops, containing the same score of 15 for the Seq-Chip data (Supplementary Table 1). miR-23b oscillates in 4 studies of RNA-seq and miR-29b-1 in 2 (Supplementary Table 1). For miR-29b-1, the mature form miR-29b-3p has the 3'UTR of *Clock*, *Per1* and *Rora* as targets validated in Tarbase V.7, and *Per1* also predicted in 2 of the 3 algorithms used in Figueredo Dde S et al. 2013[24](Supplementary Table 1). On the other hand, the form 5p, miR-29b-1-5p, presents only 2 targets (*Clock* and *Nr1d2*) with interaction identified in DIANA Tarbase V.7 (Supplementary Table 1). For miR-23b, only miR-23b-3p exhibits binding sites in clock genes, more precisely in *Bhlhe41* and *Rora* (Supplementary Table 1). The latter is also predicted target, however in only one program (Supplementary Table 1).

The primary transcripts pri-mir-23b-27b-24-1 and pri-mir-29a-1-29b have circadian oscillation in mouse liver [32]. In assays performed at only one time in the circadian cycle and in human A549 lung carcinoma cells, Zhao et al. 2014 demonstrated that miR-29b-3p inhibits the

expression of the *Per1* gene at the level of mRNA and protein[33]. In pancreatic cells of mice miR-29b-3p presents daily variation in their expression [34]. miR-29b-3p binds directly to 3'UTR of *Per3*, reducing gene levels [34].

Although miR-29b-3p has previous association with circadian rhythms, functional mimic assays have been performed in only one moment [33,34] and do not demonstrate the impact of miRNA on rhythm control circadian. Zhang et al. 2009 demonstrated that the *in vitro* model of human osteosarcoma (U2OS) cells, knock-in for the Luciferase (LUC) reporter gene in the terminal region of *Per2* gene (PER2: LUC), enables detailed analysis of the effect caused by the change of the expression of candidate genes in molecular biological clock system [35]. Importantly, U2OS PER2:LUC maintains the circadian rhythm for several days, allows the control of cyclical environmental cues and data collection with a greater frequency (shorter time interval), which makes it possible to analyze the periods and amplitudes of the rhythms[35]. Thus, in order to evaluate the relevance of the miRNAs to the circadian system, we tested miR-23b-3p and miR-29b-3p in the same model used in Zhang et al 2009. As a method of functional interference, we used the mimic system, which when transfected with U2OS PER2:LUC cells increases miRNA levels, which enhances its function. To test the efficiency of our miRNA selection strategy, we also evaluated miR-450b-5p, which ranks last on our list, with a score of 0. As circadian positive controls, we selected miR-219a-1-3p and miR- 132-3p [23]. miR-219a-1-3p and miR-132-3p adjust, *in vivo*, the period and entrainment of circadian rhythms, respectively [23]. These miRNAs also exhibit circadian expression in suprachiasmatic nuclei of mice in their pre-miRNAs and mature miRNAs [23].

As expected, miR-450b-5p does not present differences in its rhythm parameters, with a period of 23.25 ± 0.47h, very similar to the controls (Figure 2). On the other hand, miR-219a-1-3p and miR-132-3p alter the oscillation of reporter PER2:LUC (Figure 3). As observed in the analysis on rhythm of mice rest activity [23], at the molecular level, miR-219a-1-3p also changes the circadian period (increase of + 1.75h, mean/standard deviation of: 26.45 ± 0.17 h) (Figure 3A-B). However, in vivo assays Cheng et al 2007 use antagomirs, a method opposite to that employed in our study [23]. On the contrary of mimics, antagomirs reduce the levels of miRNAs. However, both reduce the periods of the different rhythms. It is possible that these effects result from the different cell types and models evaluated, mouse NSQ [23] and U2OS PER2:LUC (Figure 3), and/or the tested rhythm, behavioral[23] and molecular (Figure 3). In fact, results obtained in different study models (*in vivo* x *in vitro*) have been discussed [35]. Although at a lower magnitude than miR-219a-1-3p, miR-132-3p also lengthens the endogenous cell period

(+ 1.06h, 25.76 ± 0.05h) (Figure 3A-B). Before, at behavioral level, miR-132-3p does not change the rest activity period [23]. Here, we present the first evidence of the adjustment of the molecular period by miR-132-3p.

Increasing levels of our two candidate miRNAs generate stronger period changes than those observed for miR-132-3p and miR-219a-1-3p (Figure 3A). miR-23b-3p, elongated the period by almost 27h (+ 2.20h, 26.90 ± 0.24h)(Figure 3A-B), a more significant effect than miR-219a-1-3p and miR-132-3p, with previously confirmed action in vivo [23]. miR-29b-3p shows the largest change in period, a reduction of almost 3h (-2.93h, 21.77 ± 0.11h)(Figure 3A-B). In relation to the scramble, miR-29b-3p, miR-23b-3p and miR-219a-1-3p also reduce the reporter gene amplitude (Figure 3B), especially miR-219a-1-3p, with lower amplitude, 3.24 times less than the amplitude observed in the scramble group (Figure 3C). Interestingly, in addition to altering the circadian rhythm, miR-29b-3p mimic transfection induces differentiation of cell morphology from epithelial (polygonal cubes, organized and compressed) to fibroblast-like cells (elongated and less organized) (data not shown). Many studies already associate miR-29b-3p with the control of cell differentiation [36,37]. For example, miR-29b-3p promotes differentiation of embryonic stem cells into neural tube epithelial cells [36].

Together, the results show the relevance of miR-29b-3p and miR-23b-3p to the circadian system, corroborating our strategy of gene identification based on systematization of data from *high-throughput* experiments (Supplementary Table 1). In addition, our results provide new information regarding the function of miR-219a-1-3p and miR-132-3, which also adjusts period and amplitude of human (U2OS cells) circadian rhythms at molecular level (Figure 3A).

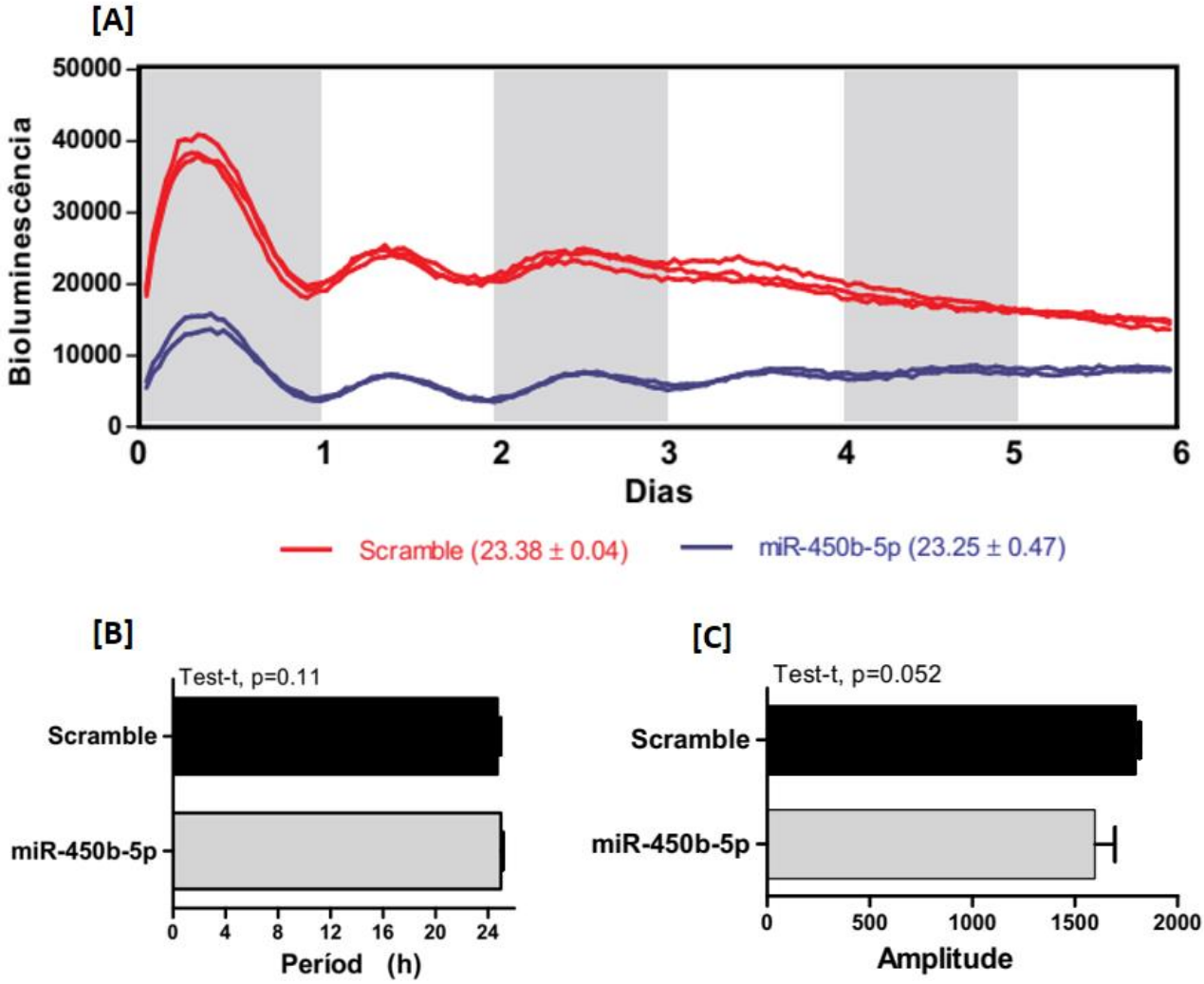

Figure 2. The negative controls (Scramble e miR-450b-5p) do not alter the circadian rhythm of Per2: Luciferase in U2OS cells. [A] Per2: Luciferase luminescence oscillation after transfection of miR-450b-5p mimic and scramble mimic. The values in parentheses are the mean ± standard deviation. Analysis of the period [B] and amplitude [C] calculated in waveclock. (h): hour.

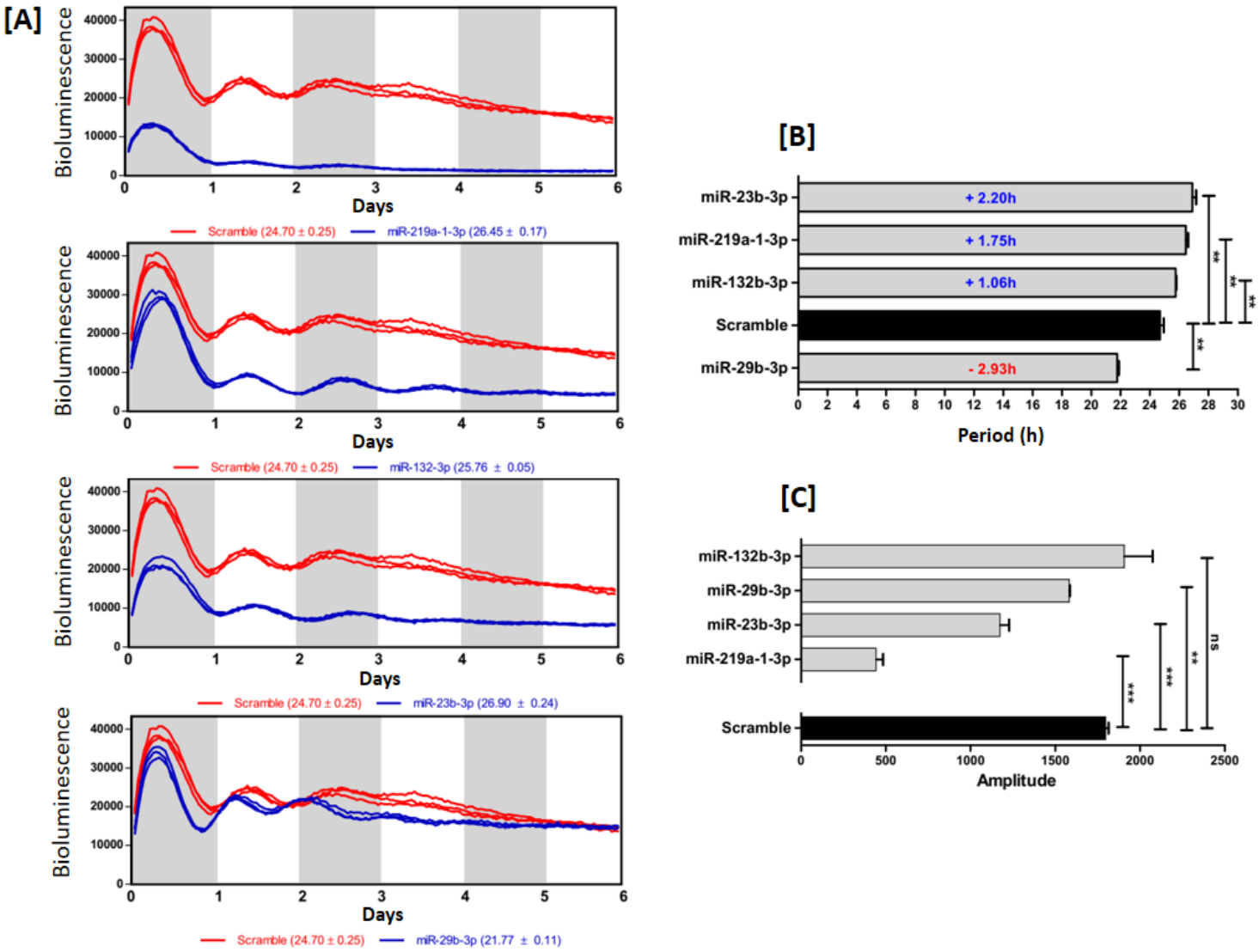

Figure 3. miR-29b-3p and miR-23b-3p alter the circadian rhythm of Per2: Luciferase in U2OS cells. [A] Per2: Luciferase luminescence oscillation after mimics and scramble transfection. The values in parentheses are the mean ± standard deviation. Analysis of the period [B] and amplitude [C] calculated in waveclock. The values inside the bars inform the changes of the periods in hours. T-test, ** p <0.001; *** p <0.0001; ns (p> 0.05).

miR-29b-3p alters the clock genes expression

The findings make the observed result for miR-29b-3p even more interesting. For this reason, in an attempt to understand the rare reduction of the period obtained after increasing levels of miR-29b-3p, we focused our efforts on the analysis of clock genes and pathways modulated by this miRNA.

Few miRNAs were validated as amplitudes and circadian period modulators[17,19–23]. And the number of coding genes that reduce the circadian period (n = 87) is much smaller than those that increase (n = 203) (see Table S1 of ZHANG, E. E. et al., 2009). Interestingly, Dicer-deficient cells (no miRNAs) exhibited a shorter period (by ~ 2 hrs). And here, the analysis of a

single miRNA (miR-29b-3p) reduces dramatically the period by almost 3h (period: 21.77h) (Figure 3). Periods smaller than 22h were rarely identified in genome-wide RNAi Screen in U2OS cells, even for clock genes and high doses of siRNA[35]. Only two assay had periods < 21.77h[35]. Knockouts of clock genes *Per3, Per1* and *Per2* shorten the circadian period by approximately 0.5, 1.0 and 1.5 h, respectively[383940]. Chen et al. 2013 and Nagel et al. 2009 suggest that the shortening period was generated by the action of miRNAs in the modulation of *Period* gene family [17,20]. Three different studies validated miR-29b-3p as a modulator of *Per1*, *Per2* and *Per3* genes, in human, zebrafish and rat, respectively[33,34,41]. It is possible that the alteration of the period caused by miR-29b-3p might result from reduced clock genes, especially *Period* gene family. To amplify the miR-29b-3p analyzes, we performed new target study with 10 prediction algorithms (from ChemiRs) to better identify clock genes modulated by miR-29b-3p and we sum the results of prediction with different experimental information to highlight more relevant target genes (Figure 4A).

Here, in addition to *Per1*, *Per2* and *Per3*, validated by Zhao et al. 2014, Hung et al. 2016 and Jacovetti et al. 2017[33,34,41], we identified the clock genes, *Clock, Arntl, Rora* and *Bhlhe40* with 3'UTRs targets for miR-29b-3p (Figure 4A). We have also identified the *Tef* gene as the target of miR-29b-3p (Figure 4A). *Tef* is a transcription factor responsible for circadian signal output by the control of CCGs[43]. miR-29b-3p may have greater relevance for the modulation of the *Period* family and *Rora*, target genes with greater evidence of miR-29b-3p control (Figure 4A). In addition, the *Per1* and *Per3* genes have highly conserved target sequences (Figure 4B). Thus, these 8 genes can be post-transcriptionally modulated by miR-29b-3p.

To test the effect of miR-29b-3p on modulating the expression of transcripts from set clock genes (total of 11 genes), we performed qPCR assays on RNA samples isolated from U2OS cells transfected with mimic miR-29b-3p or with the scramble (Figure 5). 7 genes reduced expression after increasing miRNA (Figure 5A), only two increased their levels (Figure 5C). *Bhlhe40* and *Arntl* remained unchanged (Figure 5B). The fold variation in relation to the scramble was from 0.29 to 1.29 (Figure 5D). 5 genes (*Arntl2, Tef, Per2, Per1, Nr1d1* and *Per3*) had their levels reduced to half or more than half, and only 2 (*Cry1* and *Cry2*) increased above 1.25 (Figure 5D). Of the affected clock genes, 5 genes act on the inhibition of circadian transcription (*Per1, Per2, Per3, Cry1* and *Cry2*) and two on activation (*Arnt2* and *Nr1d1*). Of these, 4 are not predicted (*Arntl2, Nr1d1, Cry1* and *Cry2*) (Figure 4A). The 3'UTRs of the 3 genes *Per1*, *Per2* and *Per3* have miR-29b-3p binding sites and are among the genes with the greatest reduction in expression (Figure 4D). As mentioned previously, *Per1*, *Per2* and *Per3*

were validated as targets of miR-29b-3p [33,34,41]. It is possible that the observed effect on the system (set of affected genes) results from changes in the expression of some targets. Baggs et al. 2009 demonstrated examples of compensatory mechanisms in which, after the knockdown of a specific gene, other elements of the clock elevate expression in an attempt to balance the system, maintaining the function and robustness of the circadian rhythm [42]. Here, the 3 paralogs genes (*Per1*, *Per2* e *Per3*) have their levels concomitantly reduced and in equal proportion (Figure 5D). It is possible that the observed increases in *Cry1* and *Cry2*, also in the same proportion (Figure 5D), may correspond to a compensatory event after the action of miR-29b-3p on the 3'UTRs of the *Per1-3* genes [42]. In fact, *Cry1* and *Cry2* showed increase of their levels after the *Per1* knockdown [42]. In addition, the reverse seems to be true, since the double reduction of *Cry1* and *Cry2*, in vitro (knockdown) or in vivo (double knockout mice, $Cry1^{-/-}Cry2^{-/-}$) induces increased levels of *Per1*, *Per2* and *Per3* [42]. Although lacking the expression studied in this assay, our *in silico* assays also identify Clock gene 3'UTR-sequences as the target of miR-29b-3p. The reduction of *Clock* levels via miR-29b-3p would explain the effects observed on *Nr1d1* and *Arntl2* (Figure 5D), since *Clock* knockdown triggers the reduction of the expression of the two genes [42]. Finally, the changes detected in the other 2 genes, *Tef*, an important clock-controlled transcription factor for circadian signal output by modulation of CCGs [43], and *Rora* (member of a secondary loop) may occur both of the action of the miRNA in their mRNAs, and/or by the propagation of signal after the perturbation caused in *Clock*, *Per1*, *Per2* and *Per3*.

[A]

Identification of miR-29b-3p:mRNAs interactions predicted and validated

	Arntl2	*Tef*	*Per2*	*Per1*	*Per3*	*Nr1d1*	*Rora*	*Arntl*	*Bhlhe40*	*Cry1*	*Cry2*	*Clock*
ChemiR	0	2	5	6	7	---	3	1	2	---	---	---
	---	---	---	PubMed:24578160	---	---	---	---	---	---	---	---
DIANA-TarBase v7.0	---	---	---	PubMed:25083871	PubMed:23597149,25083871	---	PubMed: 22100165, 22927820,24374217,23142080,23597149	---	---	---	---	PubMed: 25083871
Figueredo et al. 2013	---	---	---	2	---	---	---	---	---	---	---	---
Circadian literature	---	---	PubMed:27846817	PubMed:24578160	PubMed:28674733	---	---	---	---	---	---	---
Sum of informations	**0**	**2**	**6**	**11**	**10**	**0**	**8**	**1**	**2**	**0**	**0**	**1**

ChemiRs: total of prediction algorithms and PubMed miRNA:mRNA validated interaction; **DIANA-TarBase v7.0:** PubMed miRNA:mRNA validated interaction;
Figueredo et al. 2013: total of prediction algorithms; **Circadian literature:** total of circadian studies

[B]

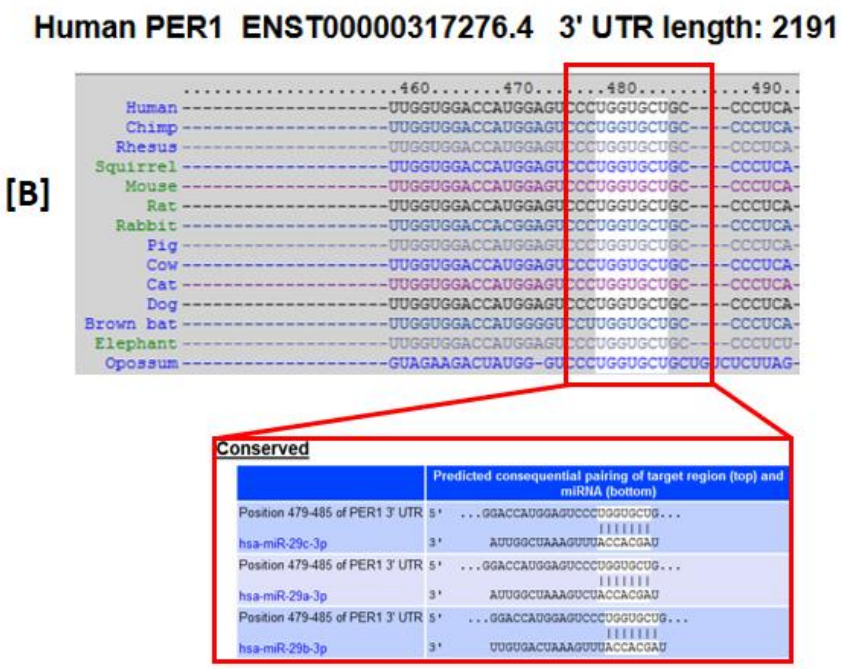

[C]

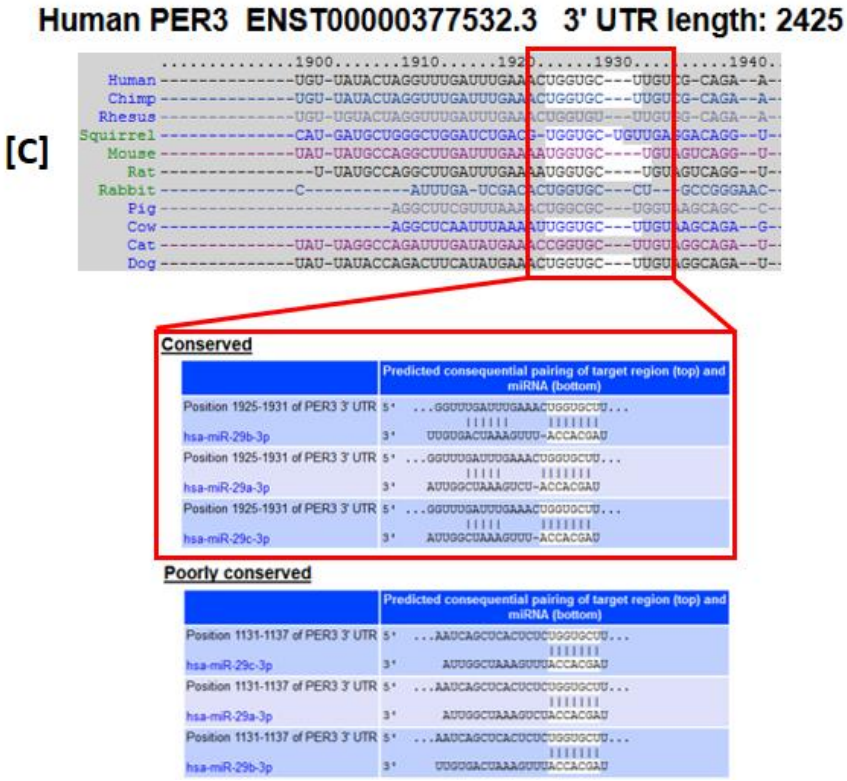

Figure 4. miR-29b-3p targets identified in 10 prediction algorithms and miRNA:mRNA interactions data bases or circadian studies. [A] Presentation of all results, which when added highlight the relevance of miR-29b-3p per target. miR-29 family target sites conserved in different species, for 3'UTR of *Per1* [B] and [c] *Per3*. Data obtained in the TargetScanHuman 7.2 algorithm.

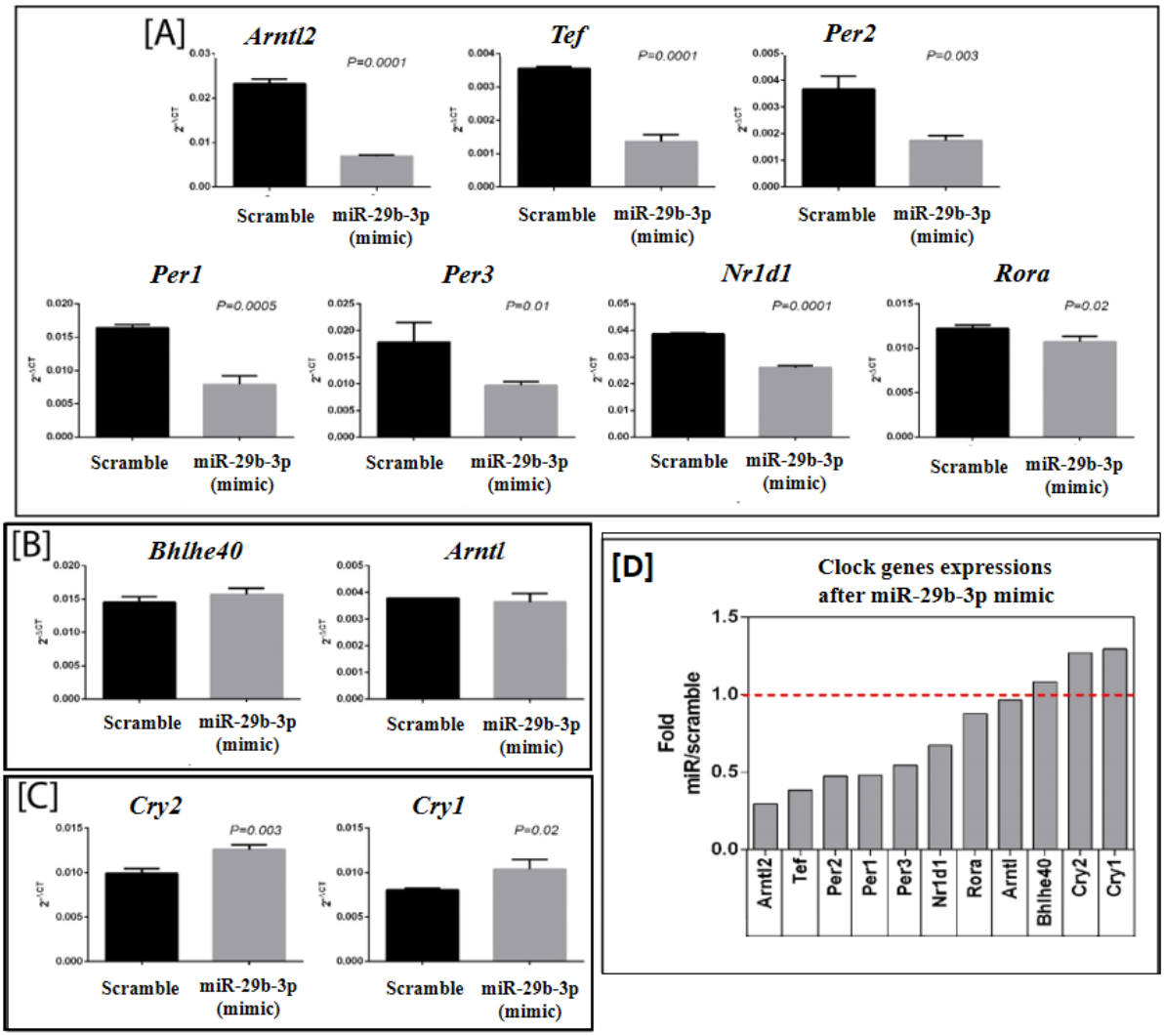

Figure 5. Increased miR-29b-3p levels alter the expression of 9 clock genes. [A] Genes clock with reduced, [B] unchanged and with [C] increased in expression after miR-29b-3p mimic. T-test, p <0.05. [D] Fold change relative to scramble (reference, value = 1, red line). Genes sorted by effect on expression, levels of the lowest transcripts (*Arntl2*) to the highest (*Cry1*). The analyzes were done in triplicates (3 groups of cells/per mimic and scramble group). The qPCR data were normalized with the housekeeping gene GAPDH in $2^{-\Delta\Delta Ct}$ calculations.

Exclusive target genes of miR-29b-3p are associated with inhibition of transcription, chromatin alterations and cell differentiation.

From 10 prediction algorithms and experimental information about miRNA:mRNA interaction (from ChemiRs web tool) we identify 313 target genes for miR-23b-3p, 244 for miR-132b-3p, 225 for miR-29b-3p and 51 for miR- 219a-1-3p (Supplementary Table 1)(Figure 6A). Interestingly, when comparing the targets of the 4 different miRNAs, only 25 are shared, demonstrating miRNA-specific regulation (Figure 6A). In mouse liver, 40 (18.95%) of the 211 unique targets of miR-29b-3p have circadian oscillation at mRNA level (from Yoshinate et al 2014). Of these, only 12 genes also present rhythmic pre-mRNA (from Koike et al 2012), suggesting that 70.3% (n = 28) of miR-29b-3p mRNAs targets have circadian expression induced by cyclic post-transcriptional mechanisms.

To understand the results obtained in the functional assays of miR-29b-3p, the 211 unique target genes were used to identify affected pathways. Twenty pathways were identified, with the organization of the extracellular matrix being the most representative (Figure 6 and 7). Interestingly, genes associated with the negative regulation pathway of cellular differentiation (total: 26 genes) are targets of miR-29b-3p (Figure 6 and 7), corroborating with the observation of alterations in the morphology of U2OS cells after addition of miR-29b-3p mimic (data not shown). We highlight two pathways associated with chromatin organization (28 genes) and negative regulation of transcription by RNAPII (31 genes) (Figure 6 and 7), with rhythmicity previously described[9] and associated with global transcript control. It is possible that the reduction of PER2:LUC period after miR-29b-3p mimic may result from changes in the transcriptional structure.

In addition, network study shows interaction between the products of the genes of these two groups (chromatin organization and regulation of transcription) with elements of extracellular matrix disassembly (7 genes) and response to oxygen levels (Figure 7). In turn, genes responding to oxygen levels are associated with cell differentiation genes (Figure 7). Interestingly, the response to oxygen levels (GO: 0070482) is defined by Gene Ontology (www.geneontology.org) as any process that results in a change in the state or activity of a cell or an organism (in terms of movement, secretion, enzyme production, gene expression, etc.) as a result of a stimulus that reflects the presence, absence or concentration of oxygen. Thus, we believe that the stimulation, or the increase of miR-19b-3p levels with the mimic system, induces the alterations of fibroblast-like epithelial cells and the activity (PER2: LUC rhythm) of U2OS cells. The changes may also be potentiated by possible changes in the rhythm of the chromatin, the RNAPII and 9 altered clock genes (Figure 5).

The results presented in this study demonstrate the analysis of data available in HTA may help chronobiologists in identifying new clock genes, including clock miRNAs. Unfortunately, in many countries HTA approaches are still costly, especially in studies that require the combination of methods (Chip-seq, RNA-seq, Hits-Clip and mass spectrometry, for example) and many samples/times (as circadian experiments). Liver has a greater number of HTA studies because is one of the most commonly mouse organs used in chronobiological science, given its ease collection, good sample yield and rhythmicity. Although the rhythms possess specific tissue variations, aspects or basic phenomena are maintained in many cells, such as the system of molecular loops. Our systematization of mouse liver HTA data enabled the identification of a list of 152 candidate miRNAs, with significant validation two top-two

candidates in human cells. These two miRNAs had a significant effect on circadian period adjustment, with a rare reduction presented by miR-29b-3p, that may result from circadian modulation of basic transcriptional pathways and *Period* family. miR-29b-3p modulates expression of clock genes and at the same time can be transcriptionally controlled by CTF(Figure 8). The miRNA may also adjust the output rhythms by direct control of CCGs (involved with chromatin, cell differentiation, others) or by modulation of CFTs that induce transcription of CCGs, such as *Tef* (Figure 8). Future studies are needed to confirm these findings and better understand the role of miR-29b-3p in cell and animals timing.

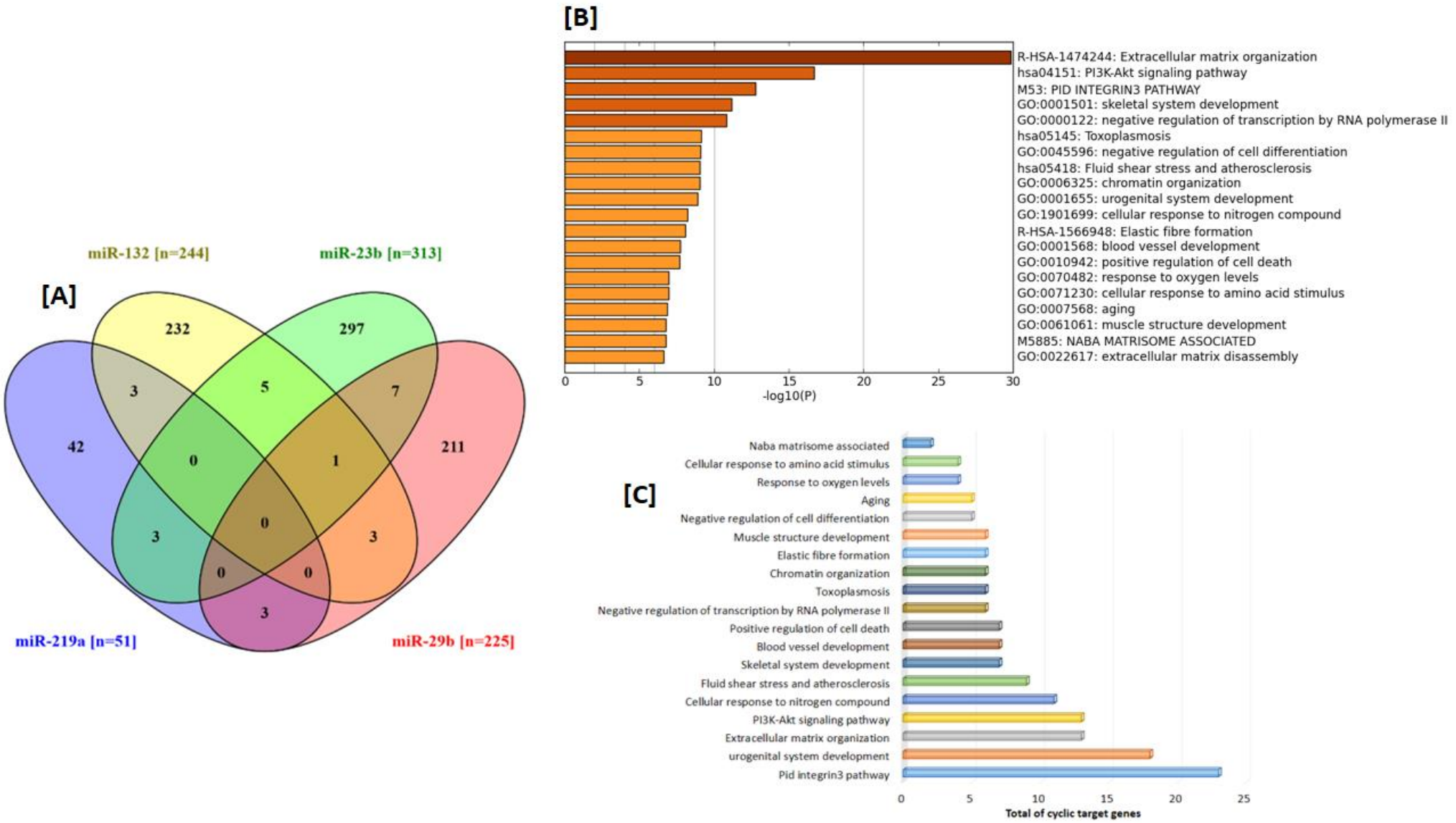

Figure 6. miR-29b-3p has exclusives targets associated with transcriptome control. [A] Comparison of target genes identified for the 4 circadian miRNAs. [B] Heat map of enriched pathways for the 211 unique targets of miR-29b-3p, colored by p-values. Analyzes made in Metascape (metascape.org). [C] Number of cyclic targets per pathway.

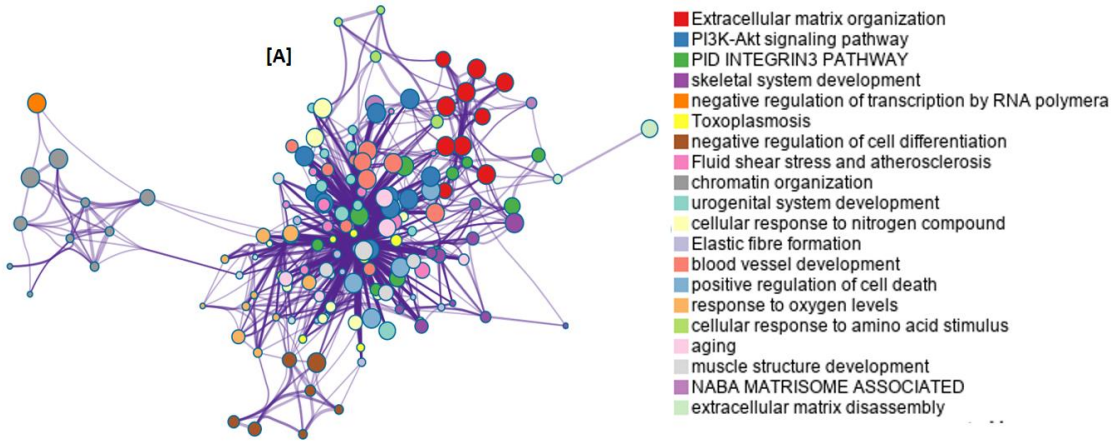

Figure 7. Network of enriched pathways for exclusives targets of miR-29b-3p. Groups that share the same cluster are closer to each other. Analyzes made in Metascape (metascape.org).

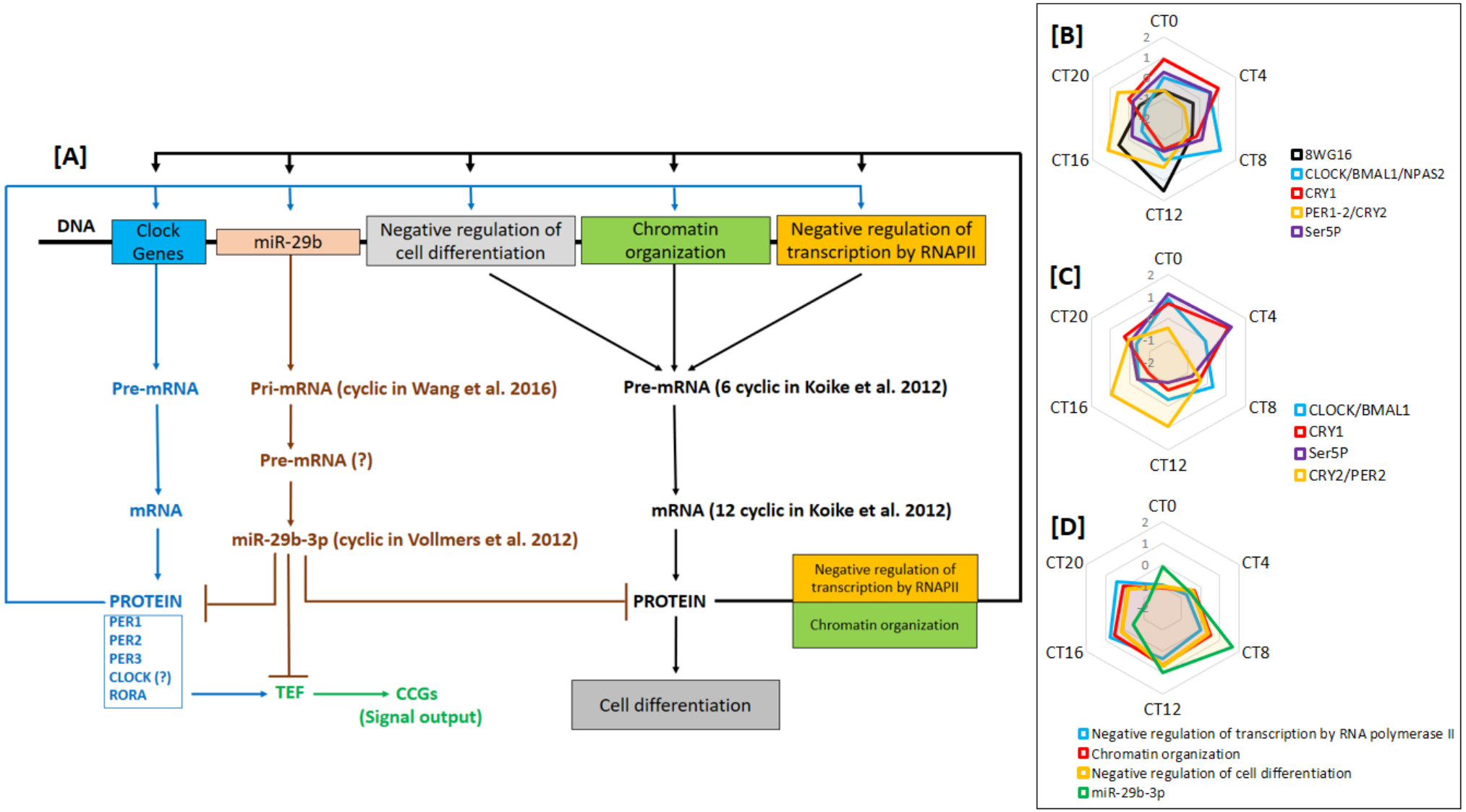

Figure 8. miR-29b-3p and the clock feedback loop system. [A] Hypothesis of the role of miR-29b-3p in the circadian system. [B] Chip-seq (from Koike et. al 2012) for 3 pathways modulated by miRNA and for [C] miR-29b-3p. [D] RNA-seq and small RNA-seq data (from Yoshitene et al 2014) for 3 pathways modulated by miRNA and for miR-29b-3p, respectively [Figura do próprio autor, 2018].

Conflict of interest statement

The author(s) declared no potential conflicts of interest with respect to the research, authorship, and/or publication of this article.

References

1. Hastings, M. H., Maywood, E. S. & Brancaccio, M. Generation of circadian rhythms in the suprachiasmatic nucleus. *Nat. Rev. Neurosci.* 1 (2018). doi:10.1038/s41583-018-0026-z
2. Pilorz, V., Helfrich-Förster, C. & Oster, H. The role of the circadian clock system in physiology. *Pflugers Arch. Eur. J. Physiol.* **470,** 227–239 (2018).
3. Husse, J., Leliavski, A., Tsang, A. H., Oster, H. & Eichele, G. The light-dark cycle controls peripheral rhythmicity in mice with a genetically ablated suprachiasmatic nucleus clock. *FASEB J.* **28,** 4950–4960 (2014).
4. Izumo, M. *et al.* Differential effects of light and feeding on circadian organization of peripheral clocks in a forebrain Bmal1 mutant. *Elife* **3,** 1–27 (2014).
5. Welsh, D. K., Takahashi, J. S. & Kay, S. A. Suprachiasmatic Nucleus: Cell Autonomy and Network Properties. *Annu. Rev. Physiol.* **72,** 551–577 (2010).
6. Ruan, G. X., Allen, G. C., Yamazaki, S. & McMahon, D. G. An autonomous circadian clock in the inner mouse retina regulated by dopamine and GABA. *PLoS Biol.* **6,** 2248–2265 (2008).
7. Moore, S. R. *et al.* Robust circadian rhythms in organoid cultures from PERIOD2::LUCIFERASE mouse small intestine. *Dis. Model. Mech.* **7,** 1123–1130 (2014).
8. Schibler, U. *et al.* Clock-Talk: Interactions between central and peripheral circadian oscillators in mammals. *Cold Spring Harb. Symp. Quant. Biol.* **80,** 223–232 (2016).
9. Koike, N. *et al.* Transcriptional architecture and chromatin landscape of the core circadian clock in mammals. *Science (80-.).* **338,** 349–354 (2012).
10. Mendoza-Viveros, L. *et al.* Molecular modulators of the circadian clock: lessons from flies and mice. *Cell. Mol. Life Sci.* **74,** 1035–1059 (2017).
11. Hamada, T. *et al.* In vivo imaging of clock gene expression in multiple tissues of freely moving mice. *Nat. Commun.* **7,** 1–13 (2016).
12. Saini, C. *et al.* Real-time recording of circadian liver gene expression in freely moving mice reveals the phase-setting behavior of hepatocyte clocks. *Genes Dev.* **27,** 1526–1536 (2013).

13. Chaix, A., Zarrinpar, A. & Panda, S. The circadian coordination of cell biology. *J. Cell Biol.* **215,** 15–25 (2016).
14. Robles, M. S., Cox, J. & Mann, M. In-Vivo Quantitative Proteomics Reveals a Key Contribution of Post-Transcriptional Mechanisms to the Circadian Regulation of Liver Metabolism. *PLoS Genet.* **10,** (2014).
15. Mauvoisin, D. *et al.* Circadian clock-dependent and -independent rhythmic proteomes implement distinct diurnal functions in mouse liver. *Proc. Natl. Acad. Sci.* **111,** 167–172 (2014).
16. Du, N., Arpat, A. B., Matos, M. De & Gatfield, D. MicroRNAs shape circadian hepatic gene expression on a transcriptome-wide scale. 1–29 (2014). doi:10.7554/eLife.02510
17. Chen, R., Alessandro, M. D. & Lee, C. Article miRNAs Are Required for Generating a Time Delay Critical for the Circadian Oscillator. *Curr. Biol.* **23,** 1959–1968 (2013).
18. Friedman, R. C., Farh, K. K. H., Burge, C. B. & Bartel, D. P. Most mammalian mRNAs are conserved targets of microRNAs. *Genome Res.* **19,** 92–105 (2009).
19. Smith, S. S., Dole, N. S., Franceschetti, T., Hrdlicka, H. C. & Delany, A. M. MicroRNA-433 dampens glucocorticoid receptor signaling, impacting circadian rhythm and osteoblastic gene expression. *J. Biol. Chem.* **291,** 21717–21728 (2016).
20. Nagel, R., Clijsters, L. & Agami, R. The miRNA-192/194 cluster regulates the Period gene family and the circadian clock. *FEBS J.* **276,** 5447–5455 (2009).
21. Curtis, A. M. *et al.* Circadian control of innate immunity in macrophages by miR-155 targeting *Bmal1*. *Proc. Natl. Acad. Sci.* **112,** 7231–7236 (2015).
22. Gao, Q., Zhou, L., Yang, S. Y. & Cao, J. M. A novel role of microRNA 17-5p in the modulation of circadian rhythm. *Sci. Rep.* **6,** 1–12 (2016).
23. Cheng, H. Y. M. *et al.* microRNA Modulation of Circadian-Clock Period and Entrainment. *Neuron* **54,** 813–829 (2007).
24. c, D. D. S., Barbosa, M. R., Gitaí, D. L. G. & De Andrade, T. G. Predicted microRNAs for mammalian circadian rhythms. *J. Biol. Rhythms* **28,** 107–116 (2013).
25. Fang, B. *et al.* Circadian enhancers coordinate multiple phases of rhythmic gene transcription in vivo. *Cell* **159,** 1140–1152 (2014).
26. Wang, H. *et al.* Oscillating primary transcripts harbor miRNAs with circadian functions. *Sci. Rep.* **6,** 1–13 (2016).
27. Yoshitane, H. *et al.* CLOCK-Controlled Polyphonic Regulation of Circadian Rhythms through Canonical and Noncanonical E-Boxes. *Mol. Cell. Biol.* **34,** 1776–1787 (2014).

28. Vollmers, C., Schmitz, R. J., Nathanson, J., Yeo, G. & Joseph, R. NIH Public Access. **16,** 833–845 (2013).
29. Su, E. C. *et al.* ChemiRs : a web application for microRNAs and chemicals. *BMC Bioinformatics* 1–10 (2016). doi:10.1186/s12859-016-1002-0
30. Fan, Y. *et al.* miRNet - dissecting miRNA-target interactions and functional associations through network-based visual analysis. *Nucleic Acids Res.* **44,** W135–W141 (2016).
31. Vlachos, I. S. *et al.* DIANA-TarBase v7.0: Indexing more than half a million experimentally supported miRNA:mRNA interactions. *Nucleic Acids Res.* **43,** D153–D159 (2015).
32. Wang, H. *et al.* Oscillating primary transcripts harbor miRNAs with circadian functions. *Sci. Rep.* **6,** 1–13 (2016).
33. Zhao, X. *et al.* MiR-29a / b / c regulate human circadian gene hPER1 expression by targeting its 3 0 UTR. **46,** 1–5 (2014).
34. Jacovetti, C. *et al.* MicroRNAs modulate core-clock gene expression in pancreatic islets during early postnatal life in rats. *Diabetologia* **60,** 2011–2020 (2017).
35. Zhang, E. E. *et al.* A Genome-wide RNAi Screen for Modifiers of the Circadian Clock in Human Cells. *Cell* **139,** 199–210 (2009).
36. Xi, J. *et al.* Mir-29b Mediates the Neural Tube versus Neural Crest Fate Decision during Embryonic Stem Cell Neural Differentiation. *Stem Cell Reports* **9,** 571–586 (2017).
37. Jauhari, A., Singh, T. & Yadav, S. Expression of miR-145 and Its Target Proteins Are Regulated by miR-29b in Differentiated Neurons. *Mol. Neurobiol.* 1–13 (2018). doi:10.1007/s12035-018-1009-9
38. Shearman, L. P., Jin, X., Lee, C., Reppert, S. M. & Weaver, D. R. Targeted Disruption of the mPer3 Gene : Subtle Effects on Circadian Clock Function. **20,** 6269–6275 (2000).
39. Fig, D. The mPer2 gene encodes a functional component of the mammalian circadian clock. **400,** 169–173 (1999).
40. Zheng, B. *et al.* Nonredundant Roles of the mPer1 and mPer2 Genes in the Mammalian Circadian Clock. **105,** 683–694 (2001).
41. Hung, I., Hsiao, Y., Sun, H. S., Chen, T. & Lee, S. MicroRNAs regulate gene plasticity during cold shock in zebrafish larvae. *BMC Genomics* 1–18 (2016). doi:10.1186/s12864-016-3239-4
42. Baggs, J. E. *et al.* Network features of the mammalian circadian clock. *PLoS Biol.* **7,** 0563–0575 (2009).

43. Katarzyna Bozek. Regulation of Clock-Controlled Genes in Mammals. *PLoS One* **101,** 1435–1439 (2009).

ARTIGO 3

CHRONOBIOLOGY INTERNATIONAL
https://doi.org/10.1080/07420528.2017.1410168

Usual normalization strategies for gene expression studies impair the detection and analysis of circadian patterns

Diego de Siqueira Figueredo[a], Mayara Rodrigues Barbosa[a], Daniel Gomes Coimbra[a,c], José Luiz Araújo dos Santos[a], Ellyda Fernanda Lopes Costa[a], Bruna Del Vechio Koike[a], Magna Suzana Alexandre Moreira[b], and Tiago Gomes de Andrade[a,c,*]

[a]Laboratory of Molecular Chronobiology, Federal University of Alagoas (UFAL), Arapiraca, Alagoas, Brazil; [b]Laboratory of Pharmacology and Immunity, Federal University of Alagoas (UFAL), Maceió, Alagoas, Brazil; [c]Faculty of Medicine, Federal University of Alagoas (UFAL), Maceió, Alagoas, Brazil

ABSTRACT

Recent studies have shown that transcriptomes from different tissues present circadian oscillations. Therefore, the endogenous variation of total RNA should be considered as a potential bias in circadian studies of gene expression. However, normalization strategies generally include the equalization of total RNA concentration between samples prior to cDNA synthesis. Moreover, endogenous housekeeping genes (HKGs) frequently used for data normalization may exhibit circadian variation and distort experimental results if not detected or considered. In this study, we controlled experimental conditions from the amount of initial brain tissue samples through extraction steps, cDNA synthesis, and quantitative real time PCR (qPCR) to demonstrate a circadian oscillation of total RNA concentration. We also identified that the normalization of the RNA's yield affected the rhythmic profiles of different genes, including *Per1-2* and *Bmal1*. Five widely used HKGs (*Actb, Eif2a, Gapdh, Hprt1*, and *B2m*) also presented rhythmic variations not detected by geNorm algorithm. In addition, the analysis of exogenous microRNAs (Cel-miR-54 and Cel-miR-39) spiked during RNA extraction suggests that the yield was affected by total RNA concentration, which may impact circadian studies of small RNAs. The results indicate that the approach of tissue normalization without total RNA equalization prior to cDNA synthesis can avoid bias from endogenous broad variations in transcript levels. Also, the circadian analysis of $2^{-\text{Cycle threshold (Ct)}}$ data, without HKGs, may be an alternative for chronobiological studies under controlled experimental conditions.

KEYWORDS

Circadian; microRNAs; bias; spike-in; normalization; housekeeping genes

Introduction

Circadian rhythms are biological processes that oscillate around a 24-h period. In mammals, they are present in various tissues under a cellular autonomous control (Buhr and Takahashi, 2013; Mohawk et al., 2013). At the molecular level, these rhythms are regulated by a set of genes, named clock genes. The clock genes products (RNAs and proteins) present a circadian expression and/or activity in different cell types, modulating a variety of biological processes through the regulation of clock control genes (Korenčič et al., 2014).

RNA polymerases (Pols), Pol-I (Neubert and Rautenberg, 1976), Pol-II (Koike et al., 2013; Neubert and Rautenberg, 1976) and recently, Pol-III (Mange et al., 2017), the key enzymes involved in eukaryotic transcription, were reported with a circadian activity. Accordingly, different classes of transcripts, such as mRNA, microRNAs, lncRNAs, lincRNAs, anti-senseRNAs and precursor 45S ribosomal RNA (45S rRNA), show oscillating levels in a global scale (Vollmers et al., 2013; Yoshitane et al., 2014; Zhang et al., 2014)

Therefore, it is presumable that the total RNA yield from tissue extracts can be affected by the endogenous rhythms of different RNA molecules resulting in concentrations with detectable circadian oscillations. However, the majority of the protocols used for gene expression analysis recommend the normalization of RNA concentrations between samples. As previously reported, this

CONTACT Tiago Gomes de Andrade deandrade.tiago@gmail.com
*Current Address: [3]Faculty of Medicine, Federal University of Alagoas (UFAL), Maceió, Alagoas, Brazil.
Color versions of one or more of the figures in the article can be found online at www.tandfonline.com/icbi.
Supplemental data for this article can be access on the publisher's website.

strategy does not consider differences in the constitution of total RNA or other transcriptional variations (Coate and Doyle, 2015; Lovén et al., 2012). rRNAs, for example, have a circadian transcriptional rhythm (Jouffe et al., 2013) and are the most abundant molecules in total RNA extracts from eukaryotic cells, representing approximately 80% of all transcripts (Kobayashi, 2011). Consequently, these molecules contribute significantly to the measured concentrations of total RNA samples. Similarly, rhythmic synthesis of other transcripts should be considered as potential bias.

Another standard choice for gene expression analysis is the use of endogenous HKGs for data normalization. Taking into account the temporal variation of the transcriptome in different tissues, it is possible that genes previously considered constitutive have circadian expression of their transcripts instead. Nevertheless, although extremely relevant, this type of analysis is barely used in the chronobiology field, and the choice of a HKG is generally made without a prior validation. In fact, the few studies performed to investigate the temporal stability of HKGs reported variation in several genes (Cleal et al., 2014; de Siqueira Figueredo et al., 2015; Dong et al., 2011; Kamphuis et al., 2005; Kosir et al., 2010; Marcolino-Gomes et al., 2015; Matsumura et al., 2014), including the widely used *Gapdh* and *Actb* (Kamphuis et al., 2005; Matsumura et al., 2014).

As alternatives, non-circadian studies previously reported different approaches for the control of experimental variations, such as the use of the same amount of cells or tissue for RNA extraction with control of the experimental procedures (extraction, cDNA synthesis and qPCR) (Adamski et al., 2014; Li et al., 2013; Spiekermann et al., 2015) or the use of exogenous RNAs (spike-ins) as a substitute of HKGs for data normalization (Bower et al., 2007; Li et al., 2013). In this work, we aimed to analyze: (1) the circadian variation in total RNA concentrations obtained from normalized brain tissue samples; (2) the expression stability of six commonly used HKGs (*Actb, Gapdh, B2m, Hprt1, Rpl13a, Eif2a*) based on circadian statistical approaches; (3) the use of spike-ins during extraction steps for data normalization.

Material and methods

Animals

C57BL/6 mice of 8–12 weeks (n = 24) were initially adapted in 12:12 light dark cycle (LD). For the analysis of endogenous rhythms, the animals were submitted to a free-running condition (constant darkness — DD) for two days. Striatum and brain stem were obtained every four circadian times (CTs) (four animals per group). Subsequently, another batch of animals (n = 24) was maintained in a 12:12 LD condition in order to collect striatum and mPFC (medial prefrontal cortex) every four Zeitgeber times (ZTs) (four animals per group). The study was approved by the Committee on Ethics of Federal University of Alagoas (CEUA56/2015).

Tissue normalization, RNA isolation, and quantification

The tissues were isolated by the same researcher to minimize possible methodological differences using protocols described by Spijker (Ka Wan, 2011). After tissue dissection, 1.5 mL micro-tubes containing 750 µL of TRIzol® LS Reagent (Thermofisher, USA) were tared to zero. Then, the tissue samples were weighed directly into 1.5 mL micro-tubes containing 750 µL of TRIzol® LS Reagent (Thermofisher, USA), and the corresponding concentrations (ng/µL) were calculated. The samples were dissolved using a 5 mL syringe and, subsequently, normalized (diluted) to the sample with the lowest concentration value, by compensating Trizol volumes. For the other extraction steps, a fixed volume of Trizol with the same tissue concentration was used. RNA extraction was performed using equal pipetting volumes thereafter in each step of the Trizol protocol, which was adapted to guarantee the homogeneity of the samples throughout the procedure: (1) using the same volume of chloroform, glycogen (20 µg/L), isopropanol and ethanol, 75%; (2) transferring the same volume of the aqueous phase to a new tube; (3) diluting RNA in the same volume of RNase-free water (50 µL). In brain stem, two exogenous RNA molecules (RNA spike-ins)

were added in the Trizol reagent at the same concentration (0.26 fmol) before RNA isolation procedure. We selected two *Caenorhabditis elegans* microRNA mimic molecules (Cel-miR-39 and Cel-miR-54) purchased from Qiagen Company, Germany (IDs: 219610 and 219600). These small transcripts are commonly used as spike-ins, which can be easily detected by qPCR and do not show homology in mammals. Cel-miR-54-3p was added before tissue homogenization, and Cel-miR-39-3p was added right after this procedure, during tissue normalization. The total RNA concentration was quantified in triplicates for each sample in BioPhotometer plus spectrophotometer (Eppendorf, USA).

cDNA synthesis

Two approaches were used for cDNA synthesis: Group 1 (G1) using the same volume of total RNA samples (0.75 µL) and Group 2 (G2) normalizing RNA for the same concentration (500 ng/sample). Reactions were performed with miScript Reverse Transcription Kit (Qiagen, Germany) according to manufacturer's protocol, in a final volume of 20 µL. All cDNA samples were diluted (1:10) in RNase free water.

Quantitative real-time PCR

We selected six commonly used HKGs (*Actb, Gapdh, Ppib, Hprt1, Rplp1*, and *Eif2a*) and the circadian genes *Bmal1, Clock, Per1, and Per2* for validation. qPCR reactions were performed using StepOne Plus (Applied Biosystems, USA) with 0.35 µL of each primer (3.5 µM), 5 µL of SYBR® Select Master Mix (Thermofisher, USA), 2.15 µL of nuclease-free water (Amresco, USA) and 2.5 µL of cDNA. The cycling conditions were in StepOnePlus™ Fast Mode. All qPCR reactions were performed in duplicates as technical replicates. Only reactions with standard deviation (SD) of 0.5 Ct between replicates were considered in the study. For efficiency tests of primer pairs, the pooled cDNA was diluted five times (1:2; 1:4; 1:8; 1:16; and 1:32). The efficiency value was determined by the StepOne Software v2.3 (Applied Biosystems, USA). Only primers with PCR efficiency between 90% and 110% and with a single melting curve were considered for experiments.

The primers were designed based on Gene Runner 5.0.58 version beta and Oligo Explorer version 1.4 beta or obtained from previous studies (Kosir et al., 2010) (Table 1). Sequence alignments were performed using blast (http://blast.ncbi.nlm.nih.gov/Blast.cgi) to ascertain the primers specificity. miScript PCR System (Qiagen, Germany) was used for the analysis of spike-ins levels, with 2 µL

Table 1. Primer sequences, amplicon length, and PCR efficiency values.

Gene		*Primer sequence (5′ – 3′)	Amplicon length (bp)	PCR efficiency (%)
Actb	***F:***	CTTCCTCCCTGGAGAAGAGC	124	94.0
	R:	ATGCCACAGGATTCCATACC		
Gapdh	***F:***	CCAATGTGTCCGTCGTGGATCT	239	92.4
	R:	GTTGAAGTCGCAGGAGACAACC		
Hprt1	***F:***	TCCTCCTCAGACCGCTTTT	90	94.3
	R:	CCTGGTTCATCATCGCTAATC		
Ppib	***F:***	GGAGATGGCACAGGAGGAAA	73	90.6
	R:	CCGTAGTGCTTCAGTTTGAAGTTCT		
Eif2a	***F:***	CAACGTGGCAGCCTTACA	74	110.0
	R:	TTTCATGTCATAAAGTTGTAGGTTAGG		
Rplp1	***F:***	GCATCTACTCCGCCCTCA	58	95.8
	R:	ATCTTATCCTCCGTGACCGT		
Bmal1	***F:***	CCACAGGATAAGAGGGTCATCG	65	97.3
	R:	GCGTACTTGTGATGTTCAGCG		
Clock	***F:***	AGGAGGGAAAGTGCTCTGTTGTAG	106	108.9
	R:	GCCACCACAGCAGTTCTTACAG		
Per1	***F:***	CTTGATGTGACGGCGTGTG	92	96.4
	R:	CCCAATCCATCCAGTTCTGAG		
Per2	***F:***	CATATCTTCTACCGTCTCTAGCTCG	71	95.1
	R:	GCTACAGCAGCACCATCGTG		

*Primers sequences for *Actb, Gapdh, Hprt1, Ppib, Eif2a (19), and Rplp1* (25) were obtained from previous studies. Primers for clock genes were designed herein.

of miScript Primer Assays (ID: 218300), 10 µL of 2x QuantiTect SYBR Green PCR Master Mix, 2 µL of 10x miScript Universal primer, and 4 µL of RNase-free water. The cycling conditions were 95°C/15 min for initial activation of HotStartTaq DNA Polymerase, 94°C/15 sec for denaturation, 55°C/30 sec for annealing, and 70°C/30 sec for extension in a total of 40 cycles.

Data analysis

Cosinor and Fourier, two specific methods for biological rhythms analysis (Refinetti et al., 2007), were used to investigate oscillatory patterns in gene expression. We considered both Ct (Cycle threshold) data converted into absolute values (10^{10})x 2^{-Ct} (or 2^{-Ct}), as previously reported (Kamphuis et al., 2005) and normalized data ($2^{-\Delta\Delta Ct}$; ΔΔCt: {Ct [Gene of interest] - Ct $[HKG]_{Sample\text{-}A}$} - {Ct [Gene of interest] - Ct $[HKG]_{Reference\ sample\ or\ calibrator}$}) with different HKGs. In the intra-group analyzes, to evidence alterations in the amplitudes and temporal profiles, both 2^{-Ct} and $2^{-\Delta\Delta Ct}$ data were converted to fold change in relation to the nadir (circadian time group with the lowest expression set to the reference value = 1). This calculation enables the adjustment of scales and the comparison between the data from G1 and G2 or different HKGs normalization. In both 2^{-Ct} and $2^{-\Delta\Delta Ct}$, the CT group with the lowest expression value was used as calibrator sample. To analyze the effect of normalization with *Ppib* in G1 (vs 2^{-Ct}), the fold change was calculated in relation to the CT00 (calibrator, also set to 1), allowing comparison of the CT16 data from two conditions (in this case, 2^{-Ct} and $2^{-\Delta\Delta Ct\ [normalized\ with\ Ppib]}$). In some analyzes, the data were converted to Z-score in order to allow phase relationship comparisons between gene expression or spike-in levels data (both 2^{-Ct} scale) and total RNA oscillation data (which present another measurement scale: ng/µL). For this, the individual expression data (X) were converted to Z-score (Z) based on the values of the standard deviation (SD) and the mean (M) of all data: Z = (X – M)/SD. One way ANOVA (with the Bonferroni's correction) and t-test (Sidak-Bonferroni's correction) were used to compare different time points and analysis. geNorm was used as a complementary analysis for the study of HKGs. This program was designed to identify the most stable control genes based on the expression pattern of a gene group (Vandesompele et al., 2002).

The graphics and calculations were performed using the GraphPad Prism 6, IBM SPSS 20, Cosinor (http://www.circadian.org/softwar.html) and CircWave V1.4 (http://www.euclock.org/results/item/circ-wave.html) software. In the Cosinor program, rhythm parameters (robustness, amplitudes, and acrophases) were calculated using the cosinor regression method adjusted for a fixed 24-h period. The Cosinor program generates unique rhythm's parameters values for the adjusted waveform obtained from the means of animal groups data (n = 4/CTs). The acrophase calculation and the cross-correlation test were used to analyze the phase relationships of the genes under different conditions. The IBM SPSS 20 program was used to calculate the cross correlation test, with $p < 0.05$. In the same way, the peak-to-trough ratio (P/T) was performed as a complement to the amplitude analysis. The P/T was calculated by: [peak]/[trough]. Peak = Mean of CT or ZT group with highest expression, or total RNA concentration. Trough = Mean of CT or ZT group with lower expression, or total RNA concentration. The fitted cosine waves presented in all figures were generated in the Circwave program (from Fourier analyses also), adjusted to a fixed 24 h period.

Results

Total RNA extracted from normalized tissue samples presents rhythmic variation

We evaluated the concentration of RNA samples collected from brain tissues across six different circadian times (CT) or zeitgeber times (ZT). Tissue samples concentrations were normalized before RNA extraction. Initially, striatum and brain stem were obtained from animals in free-running. Both structures presented circadian variation in total RNA concentrations, with acrophases occurring at CT16 and CT17, respectively (Figure 1). Afterward, we measured RNA concentrations from striatum and mPFC obtained from animals under 12:12 LD. Striatum also presented daily variation in total RNA concentration in this

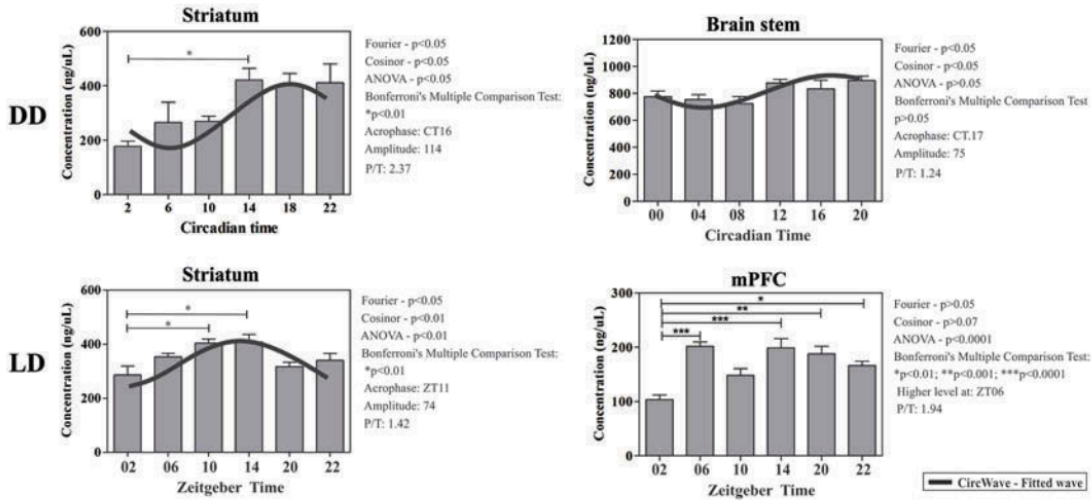

Figure 1. Circadian and daily variation of total RNA concentration in different brain tissues. Analyses performed with three statistical methods are shown: Cosinor and Fourier for rhythm detection; ANOVA with Bonferroni's multiple comparison test for analysis of differences between groups (circadian times-CTs or Zeitgeber Times-ZTs). Dark lines represent the fitted curves (from CircWave program). The data are presented in mean ± SD. Each group (ZT or CT) consists of a total of four biological replicates (mice).

condition, whose acrophase occurs at ZT11 (Figure 1). Although mPFC data did not fit to a cosine-wave (Fourier and Cosinor, $p > 0.05$), a significantly lower RNA concentration was identified at CT02 (ANOVA, $p = 0.0001$) (Figure 1).

Normalization of total RNA concentrations affects the circadian expression of clock genes

We performed gene expression analyses from brain stem samples collected at six different times. Brain stem was selected because it presented both circadian rhythm and a higher yield in total RNA concentration, allowing different normalization approaches. To investigate the bias concerning the RNA normalization in circadian experiments, we compared the expression of four clock genes (*Clock, Bmal1*, and *Per1-2*) in two groups: Group-1 (G1) cDNA synthesis from a fixed volume (0.75 ul) of total RNA of each sample; Group-2 (G2) cDNA synthesis from the same total RNA concentration (500 ng/sample). In G1, Cosinor and Fourier analyses of 2^{-Ct} data showed a circadian variation of *Per1, Per2*, and *Bmal1* (Table 2). In G2, only *Per2* and *Bmal1* presented rhythmic expression (Table 2). In both groups (G1 and G2), *Clock* mRNA showed a constitutive expression (Table 2).

Table 2. Summary of the circadian analysis with 2^{-Ct}, *Ppib* normalization and the best geNorm combination.

	Without HKG		HKG with variation in a single CT		Best HKGs combination	
	2^{-Ct}		*Ppib*		*Eif2a/Actb*	*Rplp1/Hprt1*
	G1	G2	G1	G2	G1	G2
	Acrophase (amplitude)	Acrophase (amplitude)	Acrophase (amplitude)	Acrophase (amplitude)	Acrophase (amplitude)	Acrophase (amplitude)
Clock genes						
Clock	n/s	n/s	n/s	n/s	00.84 (0.354)	n/s
Bmal1	03.90 (0.411)	02.77 (0.673)	02.88 (0.276)	02.61 (0.622)	01.81 (0.761)	02.32 (1.112)
Per1	14.06 (1.700)	n/s	14.92 (1.677)	n/s	15.40 (1.314)	n/s
Per2	15.21 (1.215)	13.75 (0.511)	16.02 (1.728)	15.27 (0.598)	16.58 (1.288)	n/s
HKGs						
Gapdh	12.50 (0.440)	11.67 (0.453)	4	n/s	n/s	n/s
Actb	10.93 (0.275)	11.00 (0.492)	4	n/s		n/s
Eif2a	10.71 (0.323)	10.49 (0.364)	4	n/s		n/s
Hprt1	13.16 (0.743)	11.62 (0.541)	4	13.51 (0.363)	15.24 (0.480)	
Rplp1	12.89 (0.188)	n/s	4	n/s	n/s	
Ppib	n/s	n/s	4	—	00.83 (0.338)	02.13 (0.305)
Total cyclic genes	***8***	***6***	***8***	***3***	***6***	***2***

G1 - cDNA from the same RNA volume; **G2** - cDNA from the same RNA concentration. n/s – *p > 0,05* in Fourier and Cosinor. Amplitudes and acrophases were calculated from fold change normalized data. **Nadir** = calibrator.

The normalization of total RNA concentration altered the amplitudes and P/T of clock genes expression, and differentially affected genes that were in phase or anti-phase, relative to total RNA rhythm (Figure 2 and Supplementary Figure S1). As shown, *Bmal1* and *Per1-2* are in anti-phase and in-phase in relation to total RNA, respectively (Figure 2A and Supplementary Figure S1). The use of a fixed RNA concentration increases the amplitude calculated by Cosinor method and P/T of *Bmal1* (P/T = 1.76 in G1, P/T = 3.05 in G2) expression, decreases P/T of *Per1* (P/T = 4.42 in G1; P/T = 3.5 in G2) and both amplitude and P/T of *Per2* (P/T = 3.39 in G1; P/T 2.15 in G2) (Figure 2B and 2C). The differences in fold change are close to that observed for the RNA concentration (P/T = 1.2). *Per1* and *Per2* presented a reduction (G1-G2 fold difference) in P/T of 0.92 and 1.14, respectively. *Bmal1* presented an increase (G2-G1 fold difference) of 1.29 after total RNA normalization. In addition, the robustness of the rhythm was reduced in G2, in particular for *Per2* (a decrease of 46.5%) (Figure 2C). The impact of RNA normalization is more evident, however, for *Per1* in which it becomes arrhythmic, without a detectable oscillation in the Cosinor or Fourier methods. Furthermore, similar to *Per2, Per1* levels were reduced after RNA normalization (Figure 2B). The descriptive analysis of the acrophases for *Bmal1* and *Per2* revealed small differences after adjustment of RNA concentration, 1.1 to *Bmal1*, and 1.5 to *Per2* (Figure 2C). However, the cross-correlation analysis did not detect statistical differences in the clock genes phases (Supplementary Figure S2).

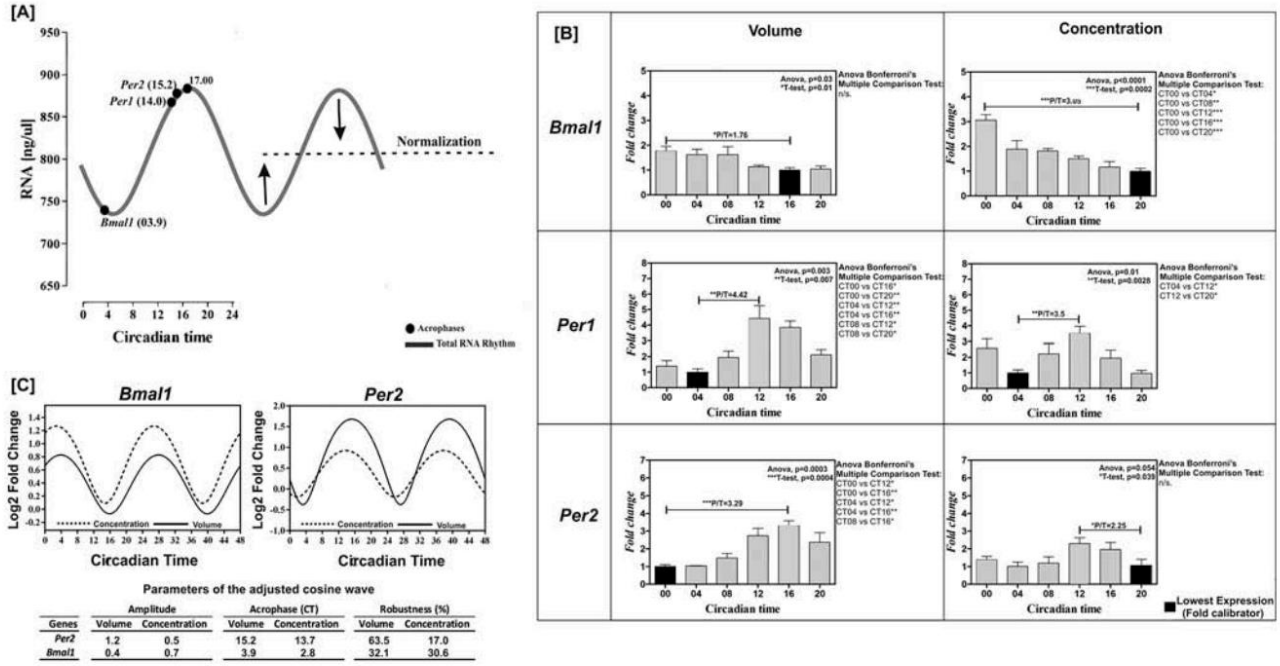

Figure 2. Comparative analysis of *Per1-2* and *Bmal1* expression profiles using two normalization strategies (G1 and G2). (A) The rhythm of total brain stem RNA (fitted curve), clock genes acrophases (black circles), and normalization to the same concentration strategy (dotted line and arrows) used in cDNA synthesis. (B) Intra-group analysis. ANOVA with Bonferroni's correction was used to compare all CTs. T-test was used for the study of only two groups: The CTs corresponding to peak and trough (P/T). The horizontal lines with asterisks show the t-test results and P/T value. Data are presented in mean ± SD, and the black bars are the group with the lowest expression (nadir) used as the fold change calibrator (in 2^{-Ct}). Each group (Circadian Time) consists of a total of four biological replicates (mice). (C) Comparative analysis of clock genes expression profiles that are rhythmic in G1 and G2 according to Cosinor regression methods. The lines show the fitted cosine wave of 2^{-Ct} (from G1). The waves were obtained from the same animal group data presented in Figure B and were double-plotted to facilitate the visualization. Wave data are presented as the fold change in log scale. The table shows the cosine wave parameters for the two conditions. The rhythm robustness was computed as the percentage of variance accounted for by the rhythm and is displayed as a percentage. *Per-1* lost its rhythmicity after RNA normalization and for this reason was not included in the wave analysis. $p < 0.05$ was considered significant for all statistical tests. PCR reactions were performed with two technical replicates.

Circadian analysis identified temporal variation of candidate HKGs

The commonly used statistical methods for circadian rhythms Cosinor and Fourier were selected to analyze the expression profile of candidate HKGs. In G1, all HKGs exhibited circadian expression in 2^{-Ct} data, except *Ppib* that demonstrated no significant circadian variation (Table 2). A complementary analysis with t-test revealed a downregulation of *Ppib* in CT20 compared to CT00, with a 1.46 P/T (Supplementary Figure S3). In G2, in addition to *Ppib*, no variations were detected in *Rplp1* expression (Table 2). In this group, the t-test showed a downregulation of *Rplp1* in CT04 (CT04 vs CT08, p = 0.038; CT04 vs CT12, p = 0.039). As observed for clock genes, the expression profiles of HKGs were affected after normalization of RNA concentration (Table 2). The acrophases of the four HKGs reveal small phase shift values after RNA adjustment (Table 2). However, similar to that observed for the clock genes, the cross-correlation analysis did not detect statistical differences in phases (Supplementary Figure S4).

We also evaluated the expression stability of candidate HKGs according to geNorm program, the main algorithm used for this purpose. In G1, HKGs presented expression stability with M values varying between 0.61 (*Hprt1*) and 0.36 (*Eif2a* and *Actb*) (Supplementary Figure S5A). According to these analyses, *Eif2a* and *Actb* were the most stable genes and *Hprt1* the most unstable considering the G1 group (Supplementary Figure S5A). In G2, the M values varied between 0.44 (*Ppib*) and 0.00 (*Rplp1* and *Hprt1*) (Supplementary Figure S5B). In this group, *Rplp1* and *Hprt1* were the most stable genes and *Ppib* the most unstable (Supplementary Figure S5B). In all cases, the geNorm program calculated acceptable stability index (below the 1.5 cut-off), indicating oscillating transcripts as stable HKGs (Supplementary Figure S5).

Inconsistencies in qPCR results from normalization with HKGs and spike-ins

Table 2 summarizes the results from normalizations with the best geNorm combinations. For comparison purposes, the 2^{-Ct} data are also presented (Table 2). In general, the equalization of RNA concentrations reduces the detection of circadian variation in gene expression normalized to HKGs (Table 2). The normalization with *Ppib* presented (in G1) more genes with circadian variation (Table 2). Interestingly, 2^{-Ct} analyses in G1 resulted in a wider detection of circadian variations (8 genes), including the clock genes *Per1-2* and *Bmal1* (Table 2). However, when the best HKGs combination (from G1) suggested by the geNorm ranking (*Eif2a*/*Actb)* was considered, it was observed that only six genes presented circadian variation, including *Clock* (Table 2). The combination *Rplp1*/*Hprt1* (from G2) detects oscillation in only two genes, *Bmal1* and *Ppib* (Table 2). Using *Rplp1*/*Hprt1* as normalizer, circadian variations were not detected in the clock genes *Per1* and *Per2* (Table 2).

In G2, *Bmal1* presented circadian variation in all normalizations (individual HKGs and geNorm combinations). However, in G2 *Per1* had no oscillation detected in all different normalizations, and *Per2* presented rhythmic expression only when normalized with *Ppib*. For this reason, we used the data obtained in G1 for the comparison of the expression profiles after different normalizations. Data for *Ppib* and the best geNorm combination are shown in Table 2 (normalization data for other single HKGs are not shown herein).

Figure 3A shows different profiles for *Per1-2* and *Bmal1* depending on the analytical strategy used in G1. In comparison to the non-normalized data (2^{-Ct}), clock genes presented alterations in the circadian oscillation profile (Figure 3A) with variations in their amplitudes and P/T (Figure 3B). Also for acrophases, a larger dispersion was observed: 14.42 to 17.34 CT for *Per1*; 15.94 to 17.68 CTs for *Per2*; and 0.60 to 3.20 CT for *Bmal1* (Figure 3B), with phase shifts larger than 3 CTs (Figure 3B). However, the cross-correlation analysis detected phase variation (of time lag 1) only in *Per2* after normalization with Cel-miR-54 (Supplementary Figure S6).

In 2^{-Ct}, *Hprt1* (acrophase: CT13.16) presented a phase closer to *Per1-2*. When *Per1-2* is normalized with *Hprt1*, they do not show circadian variation in their expression (Supplementary Figure S7). Although *Ppib* did not present a profile adjustable

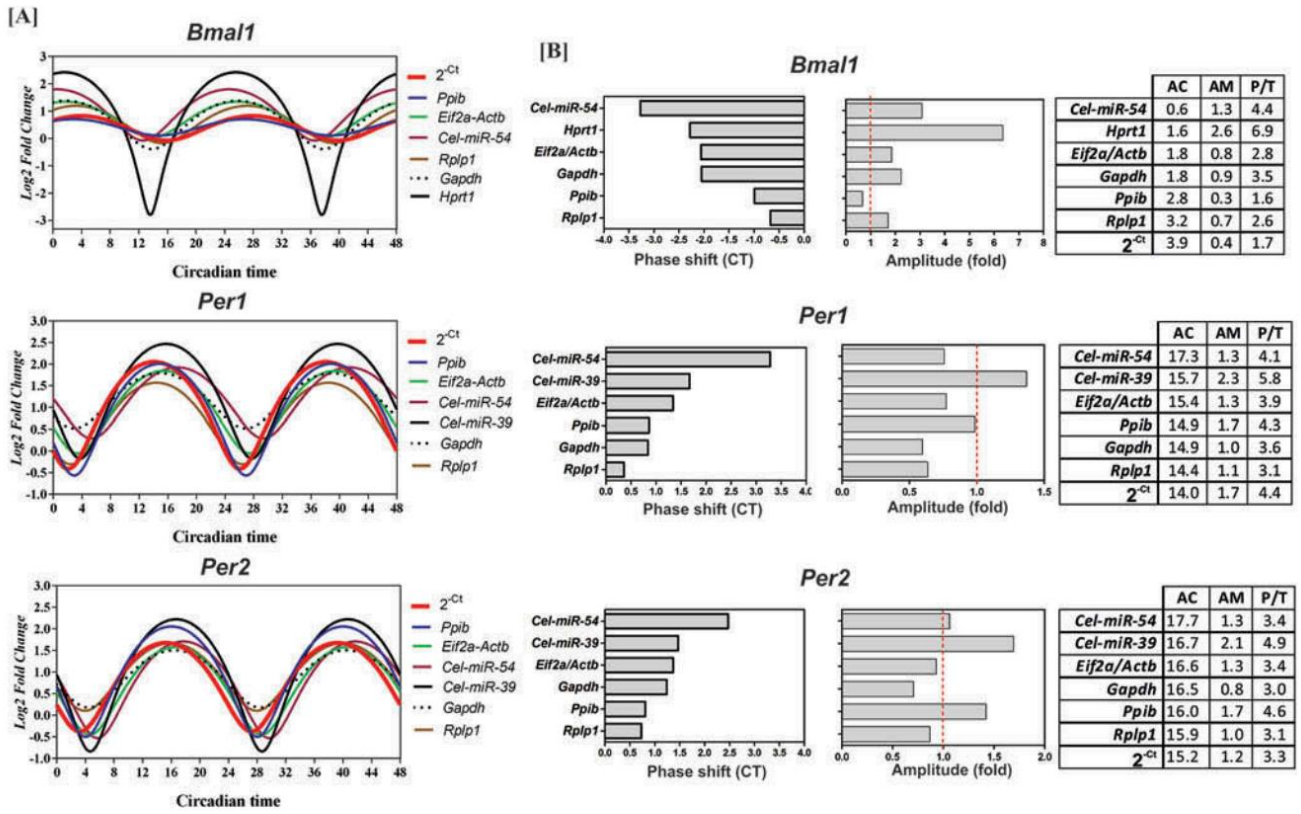

Bmal1	AC	AM	P/T
Cel-miR-54	0.6	1.3	4.4
Hprt1	1.6	2.6	6.9
Eif2a/Actb	1.8	0.8	2.8
Gapdh	1.8	0.9	3.5
Ppib	2.8	0.3	1.6
Rplp1	3.2	0.7	2.6
2^{-Ct}	3.9	0.4	1.7

Per1	AC	AM	P/T
Cel-miR-54	17.3	1.3	4.1
Cel-miR-39	15.7	2.3	5.8
Eif2a/Actb	15.4	1.3	3.9
Ppib	14.9	1.7	4.3
Gapdh	14.9	1.0	3.6
Rplp1	14.4	1.1	3.1
2^{-Ct}	14.0	1.7	4.4

Per2	AC	AM	P/T
Cel-miR-54	17.7	1.3	3.4
Cel-miR-39	16.7	2.1	4.9
Eif2a/Actb	16.6	1.3	3.4
Gapdh	16.5	0.8	3.0
Ppib	16.0	1.7	4.6
Rplp1	15.9	1.0	3.1
2^{-Ct}	15.2	1.2	3.3

Figure 3. Comparative analysis of the expression profile of *Per1-2* and *Bmal1* after normalization with oscillating HKGs and spike-ins. Expression data were obtained with cDNA from the same volume of RNA sample (G1). *Eif2a/Actb* was considered (by geNorm) the best combination for G1. (A) Comparison of the cosine expression profile (from CircWave program). The lines show the fitted cosine wave. The waves were double-plotted to facilitate the analysis. Wave data (from $2^{-\Delta\Delta Ct}$, with different HKG normalizations or 2^{-Ct}) are presented as the fold change in log scale. The sample (CT group) with the lowest expression was used as calibrator. In the *Bmal1* plot, the normalization with Cel-miR-39 is absent because no rhythmic variation was detected. The same occurs for normalizations with *Hprt1* in *Per1* and *Per2* graphs. (B) Analysis of the phases, amplitudes, and P/T of expression after the different normalizations. The waves, acrophases, and amplitude were obtained with the cosine method from group analysis (4 animals for each CT). The phase shift and amplitude (fold) were calculated in relation to 2^{-Ct} method. $p < 0.05$ was considered significant for statistical test. PCR reactions were performed with two technical replicates. AC: Acrophase; AM: Amplitude; P/T: peak-to-trough ratio.

to a cosine wave, t-test analysis revealed a reduced level of *Ppib* in CT20 (Supplementary Figure S3).

To analyze the effects of expression instability on a single CT (the CT20), we compared the oscillation profile of genes that showed circadian variation in G1, and in both 2^{-Ct} and $2^{-\Delta\Delta Ct}$ (normalized with *Ppib*) (Figure 4). After normalization with *Ppib*, the genes *Gapdh, Actb* and *Hprt1* showed increased levels in CT20 (Figure 4).

Ppib had similar expression levels between CT16 and CT20 (Supplementary Figure S3). As observed in CT20, after normalization, *Bmal1* presented higher levels in CT16 (Figure 4). These differences resulted in small phase changes in gene expression of 0.8 to 2.4 CTs, such as the phase-delay observed for *Per1, Per2, Eif2a, Gapdh, Actb, Rplp1*, and *Hprt1* and phase-advance for *Bmal1* (Figure 4). These differences, however, were not confirmed in cross-correlation test (Supplementary Figure S8).

We also selected two small exogenous RNAs (Cel-miR-39 and Cel-miR-54) as an alternative to HKGs for the normalization of expression data in circadian studies. Initially, we used 2^{-Ct} data from G1 to analyze the stability of spike-ins. Curiously, spike-ins presented differences in their levels that were fitted to cosine-waves (Supplementary Figure S9). Cel-miR-54 showed an acrophase in CT10.2 and Cel-miR-39 in CT6.8, both in anti-phase to the total RNA rhythm (Supplementary Figure S9). Cel-miR-39 amplitude (0.84) is slightly lower than that of Cel-miR-54 (amplitude; 0.96). As demonstrated in Figure 3, in G1 the use of spike-ins altered the circadian profile of clock

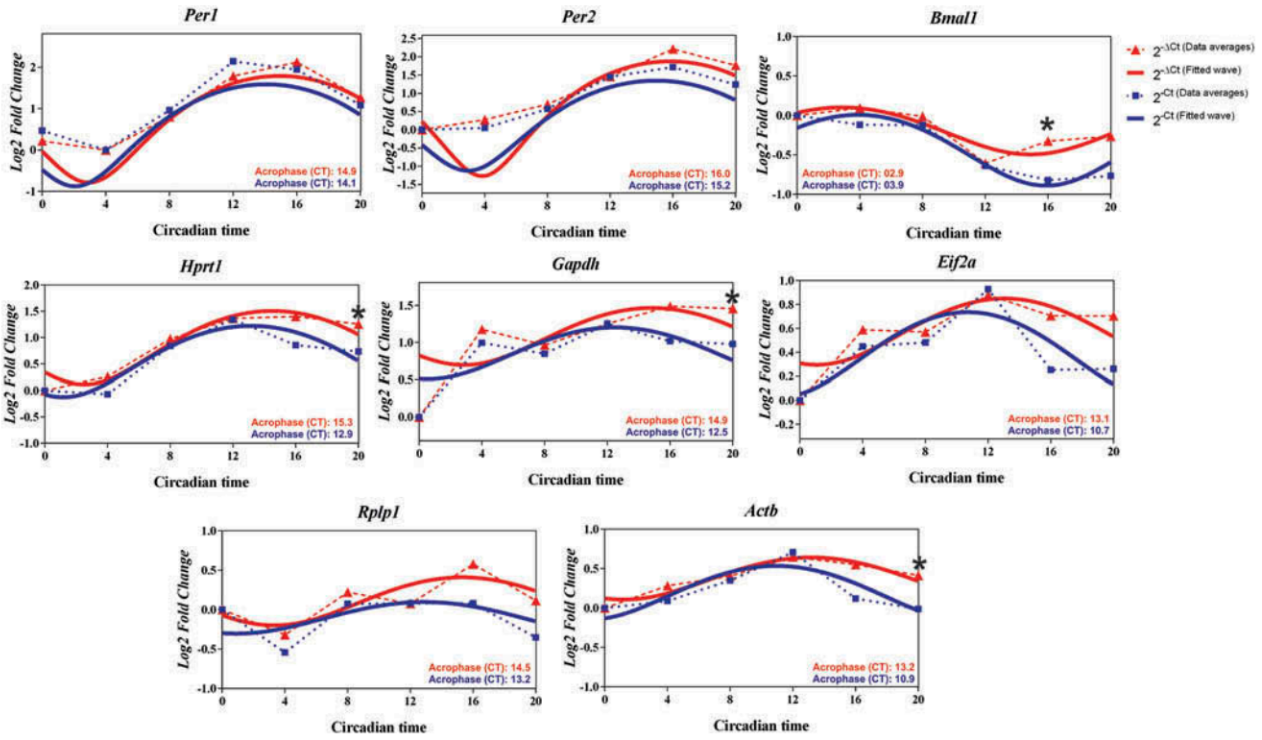

Figure 4. Comparative analysis of gene expression profiles after normalization with *Ppib*. *T-test* with Sidak-Bonferroni's correction was used to comparison of CT groups from $2^{-\Delta\Delta Ct}$ and 2^{-Ct},*p < 0.05. Closed lines show the fitted cosine wave (from CircWave program). Fitted waves were single-plotted together with the average of the raw data (dashed lines). In all cases, *Ppib* was used as HKG (in $2^{-\Delta\Delta Ct}$). Each group (CT) consists of a total of four biological replicates. CT00 was used as the calibrator. Wave data are presented as the fold change in log scale. qPCR reactions were performed with two technical replicates.

genes, particularly *Bmal1*, which loss its rhythm after normalization with Cel-miR-39 and *Per2*, which changes its phase in 1 CT after Cel-miR-54 normalization (detected in the in cross-correlation analysis; cross-correlation Function = 0.84; time lag in CT = 1) (Figure 3A and Supplementary figure S6).

In addition, when *Bmal1* was normalized with Cel-miR-54 in G1, it presented higher amplitude (3.1 times higher than in 2^{-Ct}) and P/T ratio (P/T = 4.41; 2.5 times higher than in 2^{-Ct}) (Figure 3B). On the other hand, *Per1-2* showed higher increases in their amplitudes and P/T after normalization with Cel-miR-39 (Figure 3B). The adjustment of RNA concentration (in G2) also affected the results after spike-ins normalizations (Supplementary Table 3). In G1, eight rhythmic genes were detected after Cel-miR-39 normalizations (*Clock, Per1-2, Actb, Gapdh, Hprt, Eif2a*, and *Rplp1*) and seven after Cel-miR-54 normalizations (*Clock, Per1-2, Gapdh, Hprt1, Ppib*, and *Bmal1*) (Supplementary Table 3). After normalization with Cel-miR-54, only *Bmal1* shows oscillation under both conditions (G1 and G2), but with a reduction of robustness (31.2% to 19.6%) and a small alteration of acrophase (in 0.5 CT), not detected by cross-correlation test (Supplementary Figure S10 and Supplementary Table 3).

Discussion

Total RNA normalization and the use of HKGs are the gold standard strategies used to minimize experimental variations in gene expression analysis. However, these traditional approaches are based on the assumption that control and experimental cells have a similar amount of total RNA and thus must be normalized to input RNA (Bustin et al., 2010). This leads to erroneous conclusions, where RNA concentrations differ between experimental and control cells (Li et al., 2013; Lovén et al., 2012; Rahl et al., 2011) or when candidate HKGs expression are affected by the condition being investigated (Kosir et al., 2010).

For these reasons, distinct studies emphasize the need for caution in interpreting genome-wide expression data, particularly in experiments involving global changes in transcription (Coate and Doyle, 2015; Li et al., 2013; Lovén et al., 2012), which include temporal variations in the composition and amount of RNA at different tissues (Zhang et al., 2014). Indeed, as demonstrated in our results and discussed herein, the combination of the aforementioned strategies impaired the rhythm detection of the majority of the genes analyzed.

Alternatives for gene expression normalization, such as adjusting the amount of biological material used for RNA extraction, were previously proposed (Adamski et al., 2014; Li et al., 2013; Lovén et al., 2012). In this work, we demonstrated a circadian rhythm and daily variations of total RNA concentrations in brain extracts normalized by the amount of input tissue. As observed for other rhythms, the phases shift depending on the light-dark condition, as shown for striatum. Usually, the RNA concentrations from different dissection times are normalized prior to conversion into cDNA. As the rhythmic variation is biological, we hypothesized that the normalization of RNA concentrations may introduces bias, such as: (1) amplitude reduction, if the gene of interest is in phase with the rhythm of total RNA concentration; (2) amplitude increase if the gene of interest is in anti-phase to the total RNA concentration rhythm; (3) induction of a rhythm if the gene of interest is constitutive. (4) rhythm loss for genes with low amplitudes.

As expected, the results demonstrate that RNA normalization affects the cyclic gene expression pattern in a phase-dependent manner. *Per1* and *Per2* have acrophases closer to the rhythm of total RNA concentration and presented a reduction in P/T of 0.92 and 1.14, respectively. However, the anti-phase gene *Bmal1* showed an increased fold difference of 1.29. As expected, the variations in these three genes were close to the P/T of 1.2 (of total RNA in G1), which suggests that the magnitude of this interference is related to the fold change in total RNA. In our analysis, the highest P/T observed for RNA concentration was 2.37 for striatum. For genes with intermediate phases between nadir and acrophase, the fold change would not reproduce the exact ratio for total RNA normalization, since the effect for each time point would be different. Therefore, the relative increment and reduction in each time point will depend on the rhythmic profile of the target gene compared to total RNA.

Although the visual inspection of the data suggests small changes in the phases of some genes, the cross-correlation analysis did not confirm the differences observed. We believe that the 4-h sampling could have limited the precise analysis of phases by the cross-correlation test or the acrophase estimation by Cosinor method.

Considering that these effects may alter the expression of distinct transcripts, it is possible that the number and the profile of oscillating genes could be significantly divergent than that presented until now. In fact, several disparities were observed between circadian studies (Doherty and Kay, 2010; Yoshitane et al., 2014). The comparison of the results from five studies using *Drosophila* head revealed few overlaps in the specific transcripts identified, in which only seven genes (1%) were cyclical in all studies (Boothroyd and Young, 2008; Doherty and Kay, 2010). In mouse liver transcriptome, Yoshitane et al. identified that only 268 genes (23.8%) of 1126 transcripts were also circadianly transcribed in two other studies (Yoshitane et al., 2014). These studies followed the manufacturer's recommendations for normalization of RNA samples used in RNA-Seq libraries (Koike et al., 2013; Menet et al., 2012; Yoshitane et al., 2014).

HKGs are supposedly constitutively expressed genes (Vandesompele et al., 2002) across distinct conditions, allowing data normalization for potential experimental variations during extraction and amplification procedures. In chronobiological studies, these genes should not vary in time. However, to the best of our knowledge, there are few studies concerning temporal variation in the expression of HKGs (Cleal et al., 2014; de Siqueira Figueredo et al., 2015; Dong et al., 2011; Kamphuis et al., 2005; Kosir et al., 2010; Marcolino-Gomes et al., 2015; Matsumura et al., 2014), despite the evidences in the literature showing that this analysis may be critical for obtaining consistent results: circadian rhythms control a variety of basic cellular process in which these HKGs are

involved (Chaix et al., 2016), and some widely used HKGs have been shown to present a circadian variation in gene expression (Kamphuis et al., 2005; Matsumura et al., 2014). Generally, genes are chosen as HKGs without prior analysis of their circadian profile.

Herein, we investigated the expression stability of six candidate HKGs in mouse brain stem using specific methods for the analysis of circadian variations and compared the results obtained with geNorm approach. Kamphuis et al. used ANOVA analysis of 2^{-Ct} data to investigate the circadian stability of candidate HKGs (Kamphuis et al., 2005). Dong et al. (2011) used Fourier analysis and gene expression time-series across Hella cell cycle to predict HKGs (Dong et al., 2011). Similarly, we applied Cosinor and Fourier analyses of 2^{-Ct} data to identify rhythms in the expression of these genes. The results demonstrate that only *Ppib* does not have a circadian oscillation profile fitted to a cosine wave. However, *Ppib* presented a decrease in its expression in CT20, and this variation was detectable only in a point-to-point analysis. Also, *Ppib* is circadianly expressed in mouse liver and distal colon according to CircaDB database (http://circadb.hogeneschlab.org) (Pizarro et al., 2013), indicating that this gene cannot be used as universal HKG for circadian studies. As expected, the use of HKGs that exhibit circadian oscillations impacted the rhythmic profile of the target genes, even if the variation of the HKG is evidenced only in one CT.

Interestingly, these temporal variations in HKGs were not detected by geNorm, a widely used method aiming to help in accurate normalization of qPCR data, including some circadian studies (Cleal et al., 2014; de Siqueira Figueredo et al., 2015; Kamphuis et al., 2005; Kosir et al., 2010; Marcolino-Gomes et al., 2015). geNorm proposers considered that the ratio of two ideal HKGs is identical in all samples and experimental conditions (Vandesompele et al., 2002). For each HKG, the pair wise variation with all genes is determined, and the expression stability index (or M index) is defined as the average of pairwise variation of a gene with all HKGs (Vandesompele et al., 2002). Then, geNorm excludes genes with higher M values, recalculating new indices for the remaining HKGs (Vandesompele et al., 2002). At the end, the program ranks the candidate HKGs according to an acceptable stability index ($M < 1.5$). However, geNorm was not developed specifically to investigate circadian variation in gene expression. In fact, by the pairwise variation principle, it is possible that two genes could be considered highly stable if their temporal expression pattern is similar. Equivalently, in the finfish, following 4 weeks of nutritional fasting, geNorm software erroneously suggested *ef1-α*, *rpl8*, and *ubq* as the most stable HKGs, whereas these genes simply exhibit similar patterns in response to fasting condition (de Santis et al., 2011).

Furthermore, the circadian variation in gene expression is tissue specific (Korenčič et al., 2014), and hence, a certain stable HKG in one particular tissue could oscillate its transcript levels in others. Thus, the stability analysis should be done for different tissues and experimental conditions, which is expensive and time consuming, making the study of HKGs virtually impracticable. Indeed, it was reported that qPCR can be used without endogenous controls if the technical procedure is performed under controlled conditions (Adamski et al., 2014; Spiekermann et al., 2015).

The insertion of exogenous RNA molecules (spike-ins) during the extraction steps has been described as an alternative used to replace HKGs (Bower et al., 2007; Coate and Doyle, 2015). Spike-ins allow the identification of variations in the quantity and RNA composition, which would not be possible with HKGs or in normalized input RNA (Li et al., 2013; van de Peppel et al., 2003).

In this work, during the RNA isolation procedure, we used the same amount of brain tissue and an equal concentration of spike-ins as surrogates for the control of experimental variations in circadian studies. We demonstrated, however, that spike-ins were not a good alternative for the normalization of expression data in both G1 and G2. For example, *Clock* gene (constitutive in 2^{-Ct}) presented a rhythmic expression in G1 after spike-in normalization. In G2, they reduced the number of cyclic genes to only *Bmal1*. Interestingly, these spike-ins exhibited oscillations at their levels and in opposite phases to the total RNA rhythm. Previous reports have shown that microRNA recovery is influenced by the amount of RNA input (El-Khoury et al., 2016). In this case, it is

possible that the rhythm of total RNA interfered in the isolation efficiency of spike-ins, generating an oscillatory profile. Considering this potential interference, researchers should be cautious in interpreting circadian variations of small RNAs depending on the experimental procedures adopted.

We used Trizol method for total RNA extraction, which may have introduced bias in the spike-in (microRNA) analysis (El-Khoury et al., 2016). Although it is the most widely used method for RNA isolation (Duy et al., 2015; Mraz et al., 2009), Trizol presents lower RNA yield and purity, in comparison to microRNA isolation kits, which may have also affected qPCR efficiency (El-Khoury et al., 2016). However, potential variances in cDNA synthesis and qPCR efficiencies due to variations in total RNA were not evaluated in this study. Additionally, we did not explore distinct RNA fractions to evaluate potential rhythmicity or experimental interference. Other extraction procedures could be considered in future studies.

Soft tissues such as brain are easier to homogenize compared to other solid tissues, which may have facilitated the normalization procedure proposed herein. Hence, the strategy must be evaluated in other conditions. For delicate tissues or cell suspensions, however, normalizing the initial amount of biological material should be preferable in circadian studies, according to our findings.

The samples were prepared in conditions that would allow the detection of the natural rhythm of brain transcriptome. In fact, we identified oscillations in the total RNA concentrations, as well as in target genes. However, we did not control other inherent issues such as circadian variation in cell volume, which is partially a result from the increased number of transcripts and other molecules, but also a potential bias of this study.

In a recent and elegant study, Sinturel et al. demonstrated diurnal oscillations in liver cell size accompanied by changes in RNA and protein levels (Sinturel et al., 2017). These findings support the idea of new methodological approaches that consider the natural temporal variation in biological samples, such as cellular volumes and transcriptome oscillations, two rhythms that may be interconnected, according to the evidences reported by Sinturel et al. (Sinturel et al., 2017). These efforts are necessary and can minimize the divergences observed between studies.

Our study presents a possible strategy for the analysis of circadian data based on the normalization of tissue sample input, the control of RNA extraction conditions, and the use of statistical methods for rhythmic phenomena. Normalization of total RNA extracts introduces bias that can have a critical impact in the interpretation of circadian rhythms, especially for genes with low amplitude. Besides, under controlled conditions, 2^{-Ct} data and Cosinor/Fourier or other rhythmic analysis are options to the lack of consistent HKGs for circadian researches.

Based on the results, it is recommended that the natural temporal variation in the transcriptome should be accounted in the experimental designs aiming to investigate circadian changes in gene expression since the isolation of the starting biological material and throughout the whole experimental protocols. Further replicating studies performed in other tissues and conditions would be valuable to consolidate this approach.

Declaration of interest

There are no conflicts of interest.

References

Adamski MG, Gumann P, Baird AE. 2014. A method for quantitative analysis of standard and high-throughput qPCR expression data based on input sample quantity. PLoS One. 9. doi:10.1371/journal.pone.0103917.

Boothroyd CE, Young MW. 2008. The in(put)s and out(put)s of the Drosophila circadian clock. Ann N Y Acad Sci. 1129:350–57. doi:10.1196/annals.1417.006.

Bower NI, Moser RJ, Hill JR, Lehnert SA. 2007. Universal reference method for real-time PCR gene expression analysis of preimplantation embryos. Biotechniques. 42:199–206. doi:10.2144/000112314.

Buhr ED, Takahashi JS. 2013. Molecular components of the mammalian circadian clock. Handb Exp Pharmacol. 217:3–27. doi:10.1007/978-3-642-25950-0-1.

Bustin SA, Beaulieu J-F, Huggett J, Jaggi R, Kibenge FSB, Olsvik PA, Penning LC, Toegel S. 2010. MIQE précis: Practical implementation of minimum standard guidelines for fluorescence-based quantitative real-time PCR experiments. BMC Mol Biol. 11:74. doi:10.1186/1471-2199-11-74.

Chaix A, Zarrinpar A, Panda S. 2016. The circadian coordination of cell biology. J Cell Biol. 215:15–25. doi:10.1083/jcb.201603076.

Cleal JK, Shepherd JN, Shearer JL, Bruce KD, Cagampang FR. 2014. Sensitivity of housekeeping genes in the suprachiasmatic nucleus of the mouse brain to diet and the daily light-dark cycle. Brain Res. 1575:72–77. doi:10.1016/j.brainres.2014.05.031.

Coate JE, Doyle JJ. 2015. Variation in transcriptome size: Are we getting the message? Chromosoma. 124:27–43. doi:10.1007/s00412-014-0496-3.

de Santis C, Smith-Keune C, Jerry DR. 2011. Normalizing RT-qPCR data: Are we getting the right answers? An appraisal of normalization approaches and internal reference genes from a case study in the finfish lates calcarifer. Mar Biotechnol (NY). 13:170–80. doi:10.1007/s10126-010-9277-z.

de Siqueira Figueredo D, Gita?? DLG, De Andrade TG. 2015. Daily variations in the expression of miR-16 and miR-181a in human leukocytes. Blood Cells Mol Dis. 54:364–68. doi:10.1016/j.bcmd.2015.01.004.

Doherty CJ, Kay SA. 2010. Circadian control of global gene expression patterns. Annu Rev Genet. 44:419–44. doi:10.1146/annurev-genet-102209-163432.

Dong B, Zhang P, Chen X, Liu L, Wang Y, He S, Chen R. 2011. Predicting housekeeping genes based on fourier analysis. PLoS One. 6:1–11. doi:10.1371/journal.pone.0021012.

Duy J, Koehler JW, Honko AN, Minogue TD. 2015. Optimized microRNA purification from TRIzol-treated plasma. BMC Genomics. 16:95. doi:10.1186/s12864-015-1299-5.

El-Khoury V, Pierson S, Kaoma T, Bernardin F, Berchem G. 2016. Assessing cellular and circulating miRNA recovery: The impact of the RNA isolation method and the quantity of input material. Sci Rep. 6:19529. doi:10.1038/srep19529.

Jouffe C, Cretenet G, Symul L, Martin E, Atger F, Naef F, Gachon F. 2013. The circadian clock coordinates ribosome biogenesis. PLoS Biol. 11:e1001455. doi:10.1371/journal.pbio.1001455.

Kamphuis W, Cailotto C, Dijk F, Bergen A, Buijs RM. 2005. Circadian expression of clock genes and clock-controlled genes in the rat retina. Biochem Biophys Res Commun. 330:18–26. doi:10.1016/j.bbrc.2005.02.118.

Kobayashi T. 2011. Regulation of ribosomal RNA gene copy number and its role in modulating genome integrity and evolutionary adaptability in yeast. Cell Mol Life Sci. 68:1395–403. doi:10.1007/s00018-010-0613-2.

Koike N, Yoo S, Huang H, Kumar V, Lee C, Kim K, Takahashi JS. 2013. NIH Public Access. 338:349–54. doi:10.1126/science.1226339.Transcriptional.

Korenčič A, Košir R, Bordyugov G, Lehmann R, Rozman D, Herzel H. 2014. Timing of circadian genes in mammalian tissues. Sci Rep. 4:5782. doi:10.1038/srep05782.

Kosir R, Acimovic J, Golicnik M, Perse M, Majdic G, Fink M, Rozman D. 2010. Determination of reference genes for circadian studies in different tissues and mouse strains. BMC Mol Biol. 11:60. doi:10.1186/1471-2199-11-60.

Li Y, Wang H, Muffat J, Cheng AW, Orlando DA, Lovén J, Kwok SM, Feldman DA, Bateup HS, Gao Q, et al. 2013. Global transcriptional and translational repression in human-embryonic- stem-cell-derived rett syndrome neurons. Cell Stem Cell. 13:446–58. doi:10.1016/j.stem.2013.09.001.

Lovén J, Orlando DA, Sigova AA, Lin CY, Rahl PB, Burge CB, Levens DL, Lee TI, Young RA. 2012. Revisiting global gene expression analysis. Cell. 151:476–82. doi:10.1016/j.cell.2012.10.012.

Mange F, Praz V, Migliavacca E, Willis IM, Schütz F, Hernandez N. 2017. Diurnal regulation of RNA polymerase III transcription is under the control of both the feeding-fasting response and the circadian clock. Genome Res. gr.217521.116. 27:973–84. doi:10.1101/gr.217521.116.

Marcolino-Gomes J, Rodrigues FA, Fuganti-Pagliarini R, Nakayama TJ, Reis RR, Farias JRB, Harmon FG, Molinari HBC, Molinari MDC, Nepomuceno A. 2015. Transcriptome-wide identification of reference genes for expression analysis of soybean responses to drought stress along the day. PLoS One. 10:1–16. doi:10.1371/journal.pone.0139051.

Matsumura R, Okamoto A, Node K, Akashi M. 2014. Compensation for intracellular environment in expression levels of mammalian circadian clock genes. Sci Rep. 4:4032. doi:10.1038/srep04032.

Menet JS, Rodriguez J, Abruzzi KC, Rosbash M. 2012. Nascent-Seq reveals novel features of mouse circadian transcriptional regulation. Elife. 2012:1–25. doi:10.7554/eLife.00011.

Mohawk JA, Green CB, Takahashi JS. 2013. Central and peripheral circadian clocks in mammal. Annu Rev Neurosci. 445–62. doi:10.1146/annurev-neuro-060909-153128.CENTRAL.

Mraz M, Malinova K, Mayer J, Pospisilova S. 2009. MicroRNA isolation and stability in stored RNA samples. Biochem Biophys Res Commun. 390:1–4. doi:10.1016/j.bbrc.2009.09.061.

Neubert D, Rautenberg M. 1976. Circadian fluctuations in the activity of DNA-dependent RNA polymerases I and II in the nuclei isolated from mouse tissues and the significance for pharmacological and toxicological studies on transcription. Arch Toxicol. 36:217–34. doi:10.1007/BF00340530.

Pizarro A, Hayer K, Lahens NF, Hogenesch JB. 2013. CircaDB: A database of mammalian circadian gene expression profiles. Nucleic Acids Res. 41:D1009–1013. doi:10.1093/nar/gks1161.

Rahl PB, Paranal RM, Burge CB, Bradner JE, Lin CY, Love J. 2011. Transcriptional amplification in tumor cells with elevated c-Myc. Cell. 151:56–67. doi:10.1016/j.cell.2012.08.026.

Refinetti R, Lissen GC, Halberg F. 2007. Procedures for numerical analysis of circadian rhythms. Biological Rhythm Research. doi:10.1080/09291010600903692.

Sinturel F, Gerber A, Mauvoisin D, Green CB, Sinturel F, Gerber A, Mauvoisin D, Wang J, Gatfield D, Stubblefield JJ. 2017. Diurnal oscillations in liver mass and cell size accompany ribosome assembly cycles article diurnal

oscillations in liver mass and cell size accompany ribosome assembly cycles. Cell. 651–63. doi:10.1016/j.cell.2017.04.015.

Spiekermann M, Dieckmann K, Balks T. 2015. Is relative quantification dispensable for the measurement of micro-rnas as serum biomarkers in germ cell tumors? Anticancer Res. 122:0–4.

Ka Wan L. 2011. Neuroproteomics. In: Spijker S, editor. Chapter 2 dissection of rodent brain regions. Vol. 57. Springer Protocols. p. 13–26.

van de Peppel J, Kemmeren P, van Bakel H, Radonjic M, van Leenen D, Holstege FCP. 2003. Monitoring global messenger RNA changes in externally controlled microarray experiments. EMBO Rep. 4:387–93. doi:10.1038/sj.embor.embor798.

Vandesompele J, De Preter K, Pattyn F, Poppe B, van Roy N, De Paepe A, Speleman F. 2002. Accurate normalization of real-time quantitative RT-PCR data by geometric averaging of multiple internal control genes. Genome Biol. 3. RESEARCH0034. doi:10.1186/gb-2002-3-7-research0034.

Vollmers C, Schmitz RJ, Nathanson J, Yeo G, Joseph R. 2013. NIH Public Access. 16:833–45. doi:10.1016/j.cmet.2012.11.004.Circadian.

Yoshitane H, Ozaki H, Terajima H, Du NH, Suzuki Y, Fujimori T, Kosaka N, Shimba S, Sugano S, Takagi T, et al. 2014. CLOCK-controlled polyphonic regulations of circadian rhythms through canonical and non-canonical E-boxes. Mol Cell Biol. 34. MCB.01465-13. 1776–87. doi:10.1128/MCB.01465-13.

Zhang R, Lahens NF, Ballance HI, Hughes ME, Hogenesch JB. 2014. A circadian gene expression atlas in mammals: Implications for biology and medicine. Proc Natl Acad Sci U S A. 111:16219–24. doi:10.1073/pnas.1408886111.

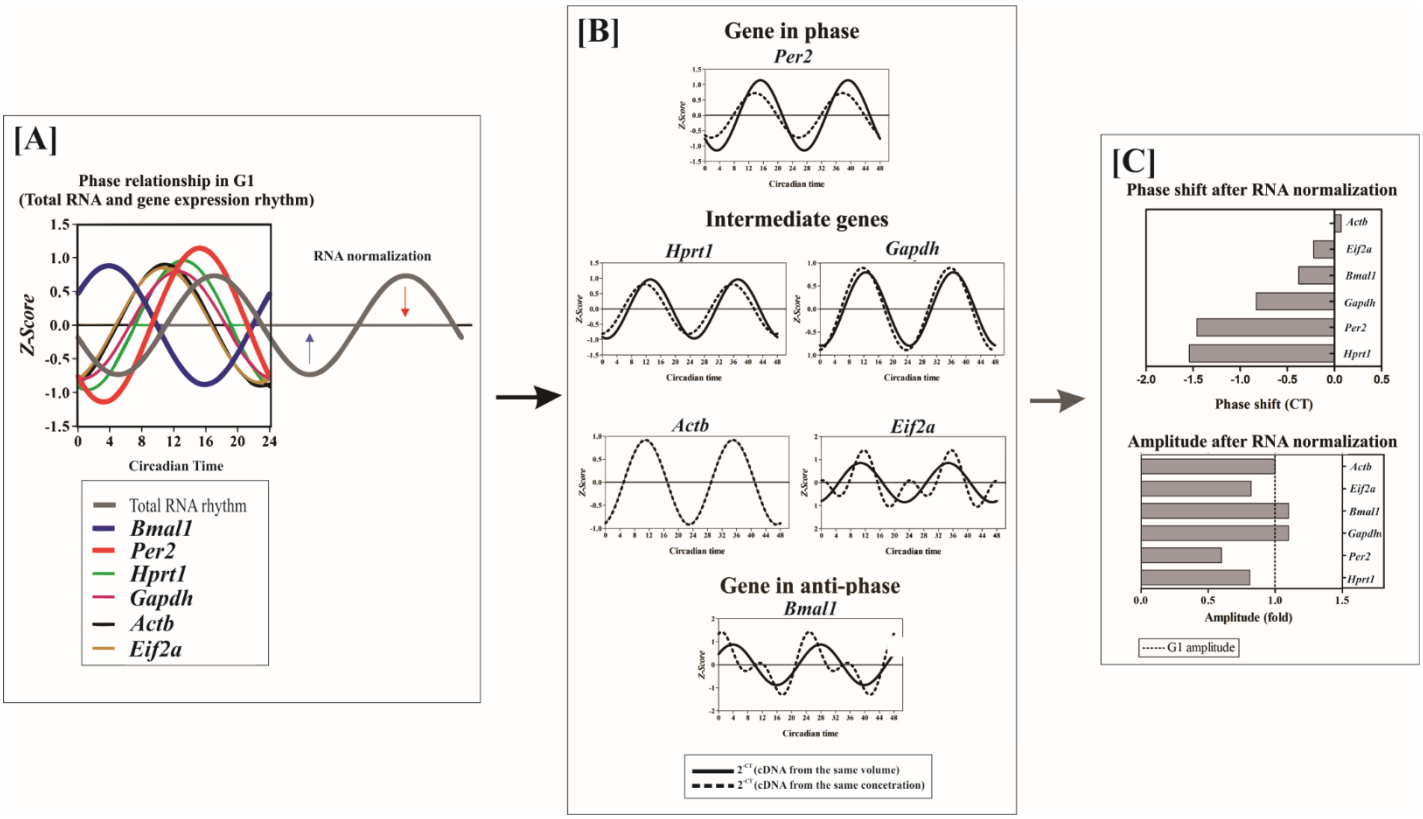

Supplementary Figure S1. The effect of total RNA normalization is phasedependent. (A) The fitted rhythms waves of the total brain stem RNA and gene expression is shown. RNA normalization for the same concentration before cDNA synthesis is represented as the horizontal line (which is also the mesor of the rhythm) and the arrows. (B) phase-dependent effect observed after the normalization procedure. (C) Phases shift and changes in amplitudes after RNA normalization.

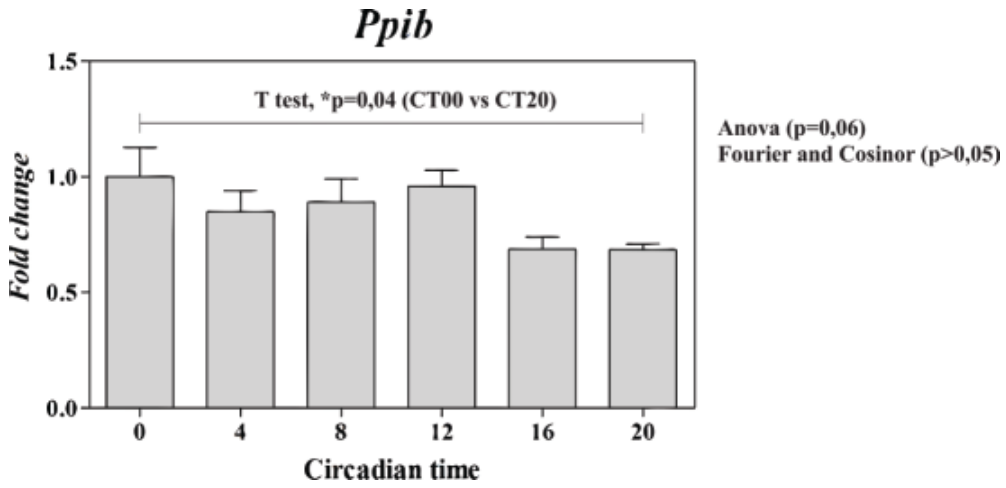

Supplementary Figure S2. Relative expression of *Ppib* across a circadian cycle. Bars correspond to the relative expression data (mean fold change and SD). The 00h sample was used as calibrator in fold change (2–Ct). $p < 0.05$ was considered significant for statistical test.

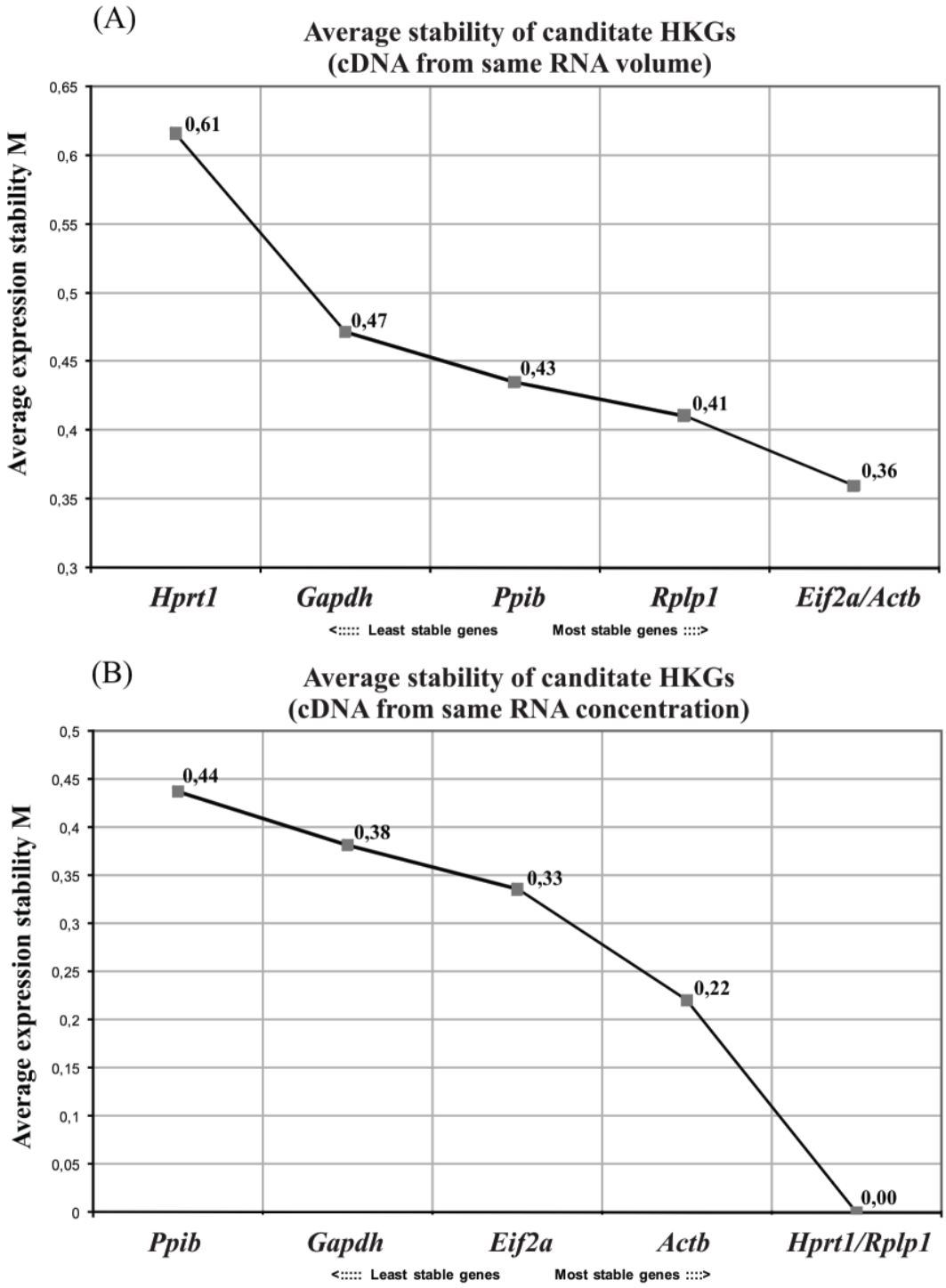

Supplementary Figure S3. geNorm stability analysis of reference genes in brain stem. The expression stability measures (M) of the six reference genes are presented. The x-axis from left to right indicates the ranking of the genes according to their expression stability; lower M values indicate higher expression stability. (A) analysis of cDNA from same RNA volume (B) analysis of cDNA from same RNA concentration.

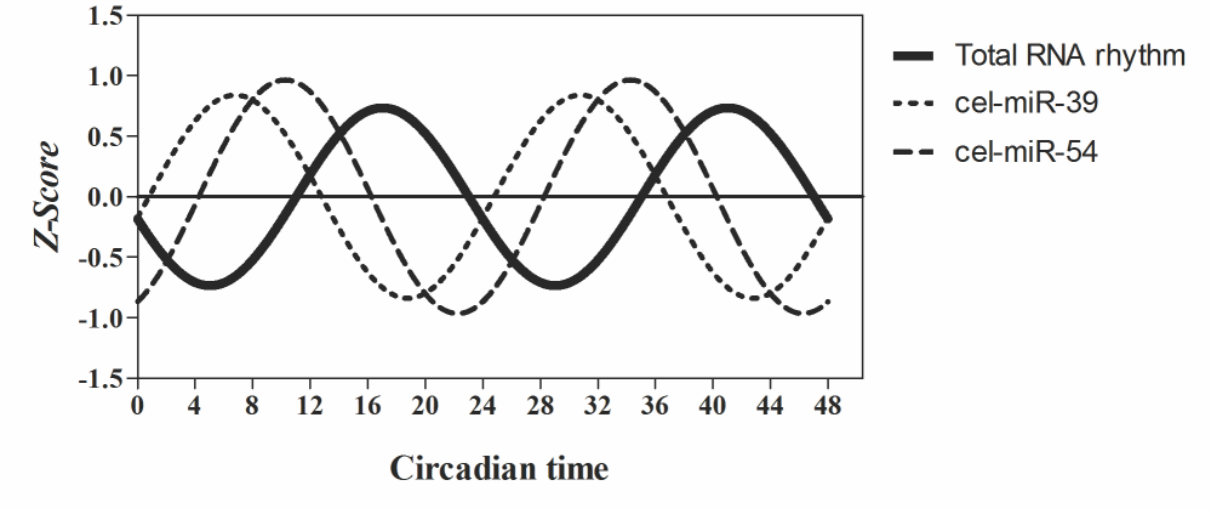

Supplementary Figure S4. Oscillations in spike-ins levels in cDNA from the same volume of RNA sample (G1). Lines show the fitted cosine wave of spike-ins and total RNA rhythm (from CircWave program). Waves were double-plotted to facilitate the analysis. For spike-ins, the 2–Ct data were converted into z-score. $p < 0.05$ was considered significant for statistical test.

4. CONSIDERAÇÕES FINAIS

Tendo como base os resultados encontrados nos diferentes artigos da tese, considera-se que:

Os miRNAs possuem transcrição induzida pela atividade rítmica das proteínas dos genes relógio e da RNAPII;

Os miRNAs possuem menor variação de fase que os RNAm, possivelmente em decorrência da ação de diferentes vias de maturação;

Os diferentes formas de maduras de miRNAs (-3p e -5p) possuem expressão diferencial, sugerindo diferenças em seus mecanismos pós-transcricionais de maturação;

miRNAs 3p e 5p possuem muitos alvos exclusivos, sendo os genes associados com o controle de ritmos circadianos preferencialmente modulados por miRNA-3p;

Que apenas 6 miRNAs dentre o conjunto analisado oscilam em ambos, miRNA-3p e miRNA-5p, indicando um mecanismo circadiano que seleciona uma das formas maduras;

Que os dois grupos de miRNAs que modulam genes que reduzem ou que aumentam a amplitude de suas proteínas (em relação ao RNAm) possuem a mesma fase de oscilação;

Que o ajuste das amplitudes das proteínas por miRNAs é dependente da fase do RNAm alvo;

Que a nossa análise de mineração de dados identificou 152 miRNAs candidatos ao controle do sistema molecular circadiano;

Que, dos 152 miRNAs, os dois de maior relevância, ou maior escore, miR-23b-3p e miR-29b-3p, possuem importante papel na manutenção da amplitude e do período dos ritmos circadianos;

Que o miR-29b-3p possui um efeito incomum para análises funcionais em um único gene, com redução do período de aproximadamente 3 horas;

Que o fenótipo observado pode resultar da ação inibitória do miR-29b-3p na expressão dos três genes relógio *Per1, Per2* e *Per3* e de genes associados com o controle global da transcrição (controle da RNAPII e alterações na estrutura de cromatina);

Que o ajuste da quantidade inicial de tecidos e o controle de condições experimentais, possibilitou demonstrar oscilação circadiana na concentração do RNA total de diferentes tecidos;

Que o ajuste do RNA para uma mesma concentração, durante a etapa de síntese de cDNA, afeta a expressão circadiana de diferentes genes, incluindo *Per1*, *Per2* e *Bmal1*;

Que o programa geNom não detectou variação na expressão de 5 HKGs (*Actb*, *Eif2a*, *Gapdh*, *Hprt1* e *B2m*), indicando que o programa pode não ser adequado para a análise de genes com ritmicidade;

Que os ensaios com *spike-ins* demonstram que o ajuste da concentração do RNA total compromete a análise de miRNAs;

Que o as análises com 2^{-Ct} podem ser uma alternativa para estudos cronobiológicos realizados em condições controladas.

5. REFERÊNCIAS DA INTRODUÇÃO GERAL

GUENTHNER, C. J.; LUITJE, M. E.; PYLE, L. A.; MOLYNEUX, P. C.; YU, J. K.; LI, A. S.; LEISE, T. L.; HARRINGTON, M. E. Circadian rhythms of PER2::LUC in individual primary mouse hepatocytes and cultures. **PLoS ONE**, v. 9, n. 2, 2014.

HAMADA, T.; SUTHERLAND, K.; ISHIKAWA, M.; MIYAMOTO, N.; HONMA, S.; SHIRATO, H.; HONMA, K. I. In vivo imaging of clock gene expression in multiple tissues of freely moving mice. **Nature Communications**, v. 7, n. May 2015, p. 1–13, 2016.

KASKOVA, Z. M.; TSARKOVA, A. S.; YAMPOLSKY, I. V. 1001 lights: Luciferins, luciferases, their mechanisms of action and applications in chemical analysis, biology and medicine. **Chemical Society Reviews**, v. 45, n. 21, p. 6048–6077, 2016.

MOORE, S. R.; PRUSZKA, J.; VALLANCE, J.; AIHARA, E.; MATSUURA, T.; MONTROSE, M. H.; SHROYER, N. F.; HONG, C. I. Robust circadian rhythms in organoid cultures from PERIOD2::LUCIFERASE mouse small intestine. **Disease Models & Mechanisms**, v. 7, n. 9, p. 1123–1130, 2014.

NELSON MARQUES; LUIZ MENNA-BARRETO. **Cronobiologia: Princípios e Aplicações**. 3.ed. ed. São Paulo: Edusp, 2003.

SAINI, C.; LIANI, A.; CURIE, T.; GOS, P.; KREPPEL, F.; EMMENEGGER, Y.; BONACINA, L.; WOLF, J. P.; POGET, Y. A.; FRANKEN, P.; SCHIBLER, U. Real-time recording of circadian liver gene expression in freely moving mice reveals the phase-setting behavior of hepatocyte clocks. **Genes and Development**, v. 27, n. 13, p. 1526–1536, 2013.

SEHGAL, A. **Molecular biology of circadian rhythms**. United States of America: [s.n.].

ZHANG, E. E. *et al.* A Genome-wide RNAi Screen for Modifiers of the Circadian Clock in Human Cells. **Cell**, v. 139, n. 1, p. 199–210, 2009.

BALAKRISHNAN, A.; STEARNS, A. T.; PARK, P. J.; DREYFUSS, J. M.; ASHLEY, S. W.; RHOADS, D. B.; TAVAKKOLIZADEH, A. MicroRNA mir-16 is anti-proliferative in enterocytes and exhibits diurnal rhythmicity in intestinal crypts. **Experimental Cell Research**, v. 316, n. 20, p. 3512–3521, 2010.

CHAIX, A.; ZARRINPAR, A.; PANDA, S. The circadian coordination of cell biology. **Journal of Cell Biology**, v. 215, n. 1, p. 15–25, 2016.

CHEN, R.; ALESSANDRO, M. D.; LEE, C. Article miRNAs Are Required for Generating a Time Delay Critical for the Circadian Oscillator. **Current Biology**, v. 23, n. 20, p. 1959–1968, 2013.

CHENG, H. Y. M.; PAPP, J. W.; VARLAMOVA, O.; DZIEMA, H.; RUSSELL, B.; CURFMAN, J. P.; NAKAZAWA, T.; SHIMIZU, K.; OKAMURA, H.; IMPEY, S.; OBRIETAN, K. microRNA Modulation of Circadian-Clock Period and Entrainment. **Neuron**, v. 54, n. 5, p. 813–829, 2007.

CURTIS, A. M. *et al.* Circadian control of innate immunity in macrophages by miR-155 targeting *Bmal1*. **Proceedings of the National Academy of Sciences**, v. 112, n. 23, p. 7231–7236, 2015.

DU, N.; ARPAT, A. B.; MATOS, M. DE; GATFIELD, D. MicroRNAs shape circadian hepatic gene expression on a transcriptome-wide scale. p. 1–29, 2014.

ERREN, T. C.; FALATURI, P.; MORFELD, P.; KNAUTH, P.; REITER, R. J.; PIEKARSKI, C. Shift Work and Cancer. **Deutsches Aerzteblatt Online**, p. 657–662, 2010.

FRIEDMAN, R. C.; FARH, K. K. H.; BURGE, C. B.; BARTEL, D. P. Most mammalian mRNAs are conserved targets of microRNAs. **Genome Research**, v. 19, n. 1, p. 92–105, 2009.

GAO, Q.; ZHOU, L.; YANG, S.; CAO, J. OPEN A novel role of microRNA 17-5p in the modulation of circadian rhythm. **Nature Publishing Group**, n. July, p. 1–12, 2016.

GAO, Q.; ZHOU, L.; YANG, S. Y.; CAO, J. M. A novel role of microRNA 17-5p in the modulation of circadian rhythm. **Scientific Reports**, v. 6, n. July, p. 1–12, 2016.

HA, M.; KIM, V. N. Regulation of microRNA biogenesis. **Nature Reviews Molecular Cell Biology**, v. 15, n. 8, p. 509–524, 2014.

HANSEN, K. F.; SAKAMOTO, K.; OBRIETAN, K. MicroRNAs: A potential interface between the circadian clock and human health. **Genome Medicine**, v. 3, n. 2, p. 1–8, 2011.

HASTINGS, M. H.; MAYWOOD, E. S.; BRANCACCIO, M. Generation of circadian rhythms in the suprachiasmatic nucleus. **Nature Reviews Neuroscience**, p. 1, 2018.

HONG, Z.; FENG, Z.; SAI, Z.; TAO, S. PER3, a novel target of miR-103, plays a suppressive role in colorectal cancer In vitro. **BMB Reports**, v. 47, n. 9, p. 500–505, 2014.

HUSSE, J.; LELIAVSKI, A.; TSANG, A. H.; OSTER, H.; EICHELE, G. The light-dark cycle controls peripheral rhythmicity in mice with a genetically ablated suprachiasmatic nucleus clock. **FASEB Journal**, v. 28, n. 11, p. 4950–4960, 2014.

IZUMO, M.; PEJCHAL, M.; SCHOOK, A. C.; LANGE, R. P.; WALISSER, J. A.; SATO, T. R.; WANG, X.; BRADFIELD, C. A.; TAKAHASHI, J. S. Differential effects of light and feeding on circadian organization of peripheral clocks in a forebrain Bmal1 mutant. **eLife**, v. 3, p. 1–27, 2014.

KOCHAN, D. Z.; ILNYTSKYY, Y.; GOLUBOV, A.; DEIBEL, S. H.; MCDONALD, J.; KOVALCHUK, O. Circadian disruption-induced microRNAome deregulation in rat mammary gland tissues. v. 2, n. 4, 2015.

KOIKE, N.; YOO, S. H.; HUANG, H. C.; KUMAR, V.; LEE, C.; KIM, T. K.; TAKAHASHI, J. S. Transcriptional architecture and chromatin landscape of the core circadian clock in mammals. **Science**, v. 338, n. 6105, p. 349–354, 2012.

MAUVOISIN, D.; WANG, J.; JOUFFE, C.; MARTIN, E.; ATGER, F.; WARIDEL, P.; QUADRONI, M.; GACHON, F.; NAEF, F. Circadian clock-dependent and -independent rhythmic proteomes implement distinct diurnal functions in mouse liver. **Proceedings of the National Academy of Sciences**, v. 111, n. 1, p. 167–172, 2014.

MENDOZA-VIVEROS, L.; BOUCHARD-CANNON, P.; HEGAZI, S.; CHENG, A. H.; PASTORE, S.; CHENG, H. Y. M. Molecular modulators of the circadian clock: lessons from flies and mice. **Cellular and Molecular Life Sciences**, v. 74, n. 6, p. 1035–1059, 2017.

MOORE, S. R.; PRUSZKA, J.; VALLANCE, J.; AIHARA, E.; MATSUURA, T.; MONTROSE, M. H.; SHROYER, N. F.; HONG, C. I. Robust circadian rhythms in organoid cultures from PERIOD2::LUCIFERASE mouse small intestine. **Disease Models & Mechanisms**, v. 7, n. 9, p. 1123–1130, 2014.

PILORZ, V.; HELFRICH-FÖRSTER, C.; OSTER, H. The role of the circadian clock system in physiology. **Pflugers Archiv European Journal of Physiology**, v. 470, n. 2, p. 227–239, 2018.

ROBLES, M. S.; COX, J.; MANN, M. In-Vivo Quantitative Proteomics Reveals a Key Contribution of Post-Transcriptional Mechanisms to the Circadian Regulation of Liver Metabolism. **PLoS Genetics**, v. 10, n. 1, 2014.

RUAN, G. X.; ALLEN, G. C.; YAMAZAKI, S.; MCMAHON, D. G. An autonomous circadian clock in the inner mouse retina regulated by dopamine and GABA. **PLoS Biology**, v. 6, n. 10, p. 2248–2265, 2008.

SAMULIN ERDEM, J.; NOTØ, H. Ø.; SKARE, Ø.; LIE, J. A. S.; PETERSEN-ØVERLEIR, M.; RESZKA, E.; PEPŁOŃSKA, B.; ZIENOLDDINY, S. Mechanisms of breast cancer risk in shift workers: Association of telomere shortening with the duration and intensity of night work. **Cancer Medicine**, 2017.

SCHIBLER, U. *et al.* Clock-Talk: Interactions between central and peripheral circadian oscillators in mammals. **Cold Spring Harbor Symposia on Quantitative Biology**, v. 80, p. 223–232, 2016.

SHI, F.; CHEN, X.; FU, A.; HANSEN, J.; STEVENS, R.; TJONNELAND, A.; VOGEL, U. B.; ZHENG, T.; ZHU, Y. Aberrant DNA methylation of miR-219 promoter in long-term night shiftworkers. **Environmental and molecular mutagenesis**, v. 54, n. 6, p. 406–13, jul. 2013.

SMITH, S. S.; DOLE, N. S.; FRANCESCHETTI, T.; HRDLICKA, H. C.; DELANY, A. M. MicroRNA-433 dampens glucocorticoid receptor signaling, impacting circadian rhythm and osteoblastic gene expression. **Journal of Biological Chemistry**, v. 291, n. 41, p. 21717–21728, 2016.

TAN, X.; ZHANG, P.; ZHOU, L.; YIN, B.; PAN, H.; PENG, X. Clock-controlled mir-142-3p can target its. **BMC Molecular Biology**, v. 13, n. 1, p. 1, 2012.

UMEMURA, Y.; KOIKE, N.; OHASHI, M.; TSUCHIYA, Y.; MENG, Q. J.; MINAMI, Y.; HARA, M.; HISATOMI, M.; YAGITA, K. Involvement of posttranscriptional regulation of *Clock* in the emergence of circadian clock oscillation during mouse development. **Proceedings of the National Academy of Sciences**, p. 201703170, 2017.

VOLLMERS, C.; SCHMITZ, R. J.; NATHANSON, J.; YEO, G.; JOSEPH, R. NIH Public Access. v. 16, n. 6, p. 833–845, 2013.

WELSH, D. K.; TAKAHASHI, J. S.; KAY, S. A. Suprachiasmatic Nucleus: Cell Autonomy and Network Properties. **Annual Review of Physiology**, v. 72, n. 1, p. 551–577, 2010.

YAN, Y.; SALAZAR, T. E.; II, J. M. D.; NGUYEN, D. V; CALZI, S. L.; BHATWADEKAR, A. D.; QI, X.; BUSIK, J. V; BOULTON, M. E.; GRANT, M. B. Dicer Expression Exhibits a Tissue-Specific Diurnal Pattern That Is Lost during Aging and in Diabetes. v. 8, n. 11, p. 1–11, 2013.

YOSHITANE, H. *et al.* CLOCK-Controlled Polyphonic Regulation of Circadian Rhythms through Canonical and Noncanonical E-Boxes. **Molecular and Cellular Biology**, v. 34, n. 10, p. 1776–1787, 2014.

ZHANG, R.; LAHENS, N. F.; BALLANCE, H. I.; HUGHES, M. E.; HOGENESCH, J. B. A circadian gene expression atlas in mammals: Implications for biology and medicine. **Proceedings of the National Academy of Sciences**, v. 111, n. 45, p. 16219–16224, 2014.